

**PHARMACOLOGICAL TARGETING OF FGFR SIGNALING TO  
INHIBIT BREAST CANCER RECURRENCE AND METASTASIS**

by

Saeed Salehin Akhand

**A Dissertation**

*Submitted to the Faculty of Purdue University*

*In Partial Fulfillment of the Requirements for the degree of*

**Doctor of Philosophy**



Department of Medicinal Chemistry and Molecular Pharmacology

West Lafayette, Indiana

May 2020

**THE PURDUE UNIVERSITY GRADUATE SCHOOL**  
**STATEMENT OF COMMITTEE APPROVAL**

**Dr. Michael Wendt, Chair**

Department of Medicinal Chemistry and Molecular Pharmacology

**Dr. Emily Dykhuizen**

Department of Medicinal Chemistry and molecular Pharmacology

**Dr. Chang-Deng Hu**

Department of Medicinal Chemistry and Molecular Pharmacology

**Dr. Timothy Ratliff**

Department of Comparative Pathobiology

**Approved by:**

Dr. Zhong-Yin Zhang

*Dedicated to my Mom, Ferdousi Islam, for her constant love and support  
And to my Dad, Nazrul Islam Akhand, who taught me how to dream big*

## ACKNOWLEDGMENTS

I would like to acknowledge and thank the people who have been a great influence and encouragement on my decision to pursue and undertake my studies in the field of Cancer biology and Immunology. Without these people, I fear that this journey would have been much harder.

First, I wish to thank my advisor, Dr. Michael K. Wendt, who accepted me into his laboratory, giving me this wonderful opportunity to grow as a scientist under his excellent mentorship. His constant encouragement, support, and advice were invaluable in this endeavor. The time I spent learning under Dr. Wendt was priceless beyond measure. I am confident that the training I have gained in his lab will allow me to accomplish greater success in the future.

I also want to thank the members of my committee, Dr. Emily Dykhuizen, Dr. Chang-Deng Hu, and Dr. Timothy Ratliff who have given valuable advice on the progress of my graduate work.

In addition to Dr. Wendt's support, within his laboratory, I found treasured and intelligent colleagues who were essential in helping me reach this academic goal. The input from the fellow grad students and postdocs and the support from my undergrad research trainees have been invaluable to my success as a graduate student. Last but not least, I want to thank the entire Department of Medicinal Chemistry and Molecular Pharmacology (MCMP) and Purdue University Interdisciplinary Life Science (PULSe) program who, gave me an excellent environment to study and work since I first arrived at Purdue University.

Finally, I wish to thank my family, who despite being across the world, have continued with their love and support. Special mention to my Mom, Emon and Shaon apa, Rumi bhai, Nabeeha, and Ishmam for being the biggest supporters in my life.

# TABLE OF CONTENTS

LIST OF FIGURES .....	8
LIST OF ABBREVIATIONS.....	15
ABSTRACT .....	16
CHAPTER 1. INTRODUCTION.....	18
1.1 Cancer dormancy .....	18
1.2 Breast cancer.....	20
1.3 Trastuzumab-emtansine (T-DM1) .....	21
1.4 Fibroblast growth factor receptors (FGFR).....	22
1.5 Epithelial to mesenchymal transition (EMT) .....	24
1.6 Tumor immune microenvironment.....	27
CHAPTER 2. FIBROBLAST GROWTH FACTOR RECEPTOR FACILITATES RECURRENCE OF MINIMAL RESIDUAL DISEASE FOLLOWING TRASTUZUMAB EMTANSINE THERAPY .....	30
2.1 Disclaimer.....	30
2.2 Introduction .....	30
2.3 Methods and materials .....	32
2.3.1 Cell cultures and reagents.....	32
2.3.2 Xenograft studies and drug treatments.....	32
2.3.3 Cell Biological assays .....	33
2.3.4 Immuno-assays .....	33
2.3.5 Kinomic analyses .....	33
2.3.6 Statistical analyses .....	34
2.4 Results .....	34
2.4.1 HER2 is diminished following recurrence of T-DM1 resistant minimal residual disease	34
2.4.2 In vitro establishment of T-DM1 resistant cells requires prior induction of epithelial- mesenchymal transition.....	35
2.4.3 FGFR1 is sufficient to reduce T-DM1 binding and efficacy.....	36

2.4.4	FGFR1 increases tumor recurrence following T-DM1-induced minimal residual disease	37
2.4.5	T-DM1 resistant cells are sensitive to covalent inhibition of FGFR	38
2.4.6	T-DM1 resistant tumors respond to systemic inhibition of FGFR	39
2.5	Figures	40
2.6	Conclusion	50
CHAPTER 3. THE SYSTEMICALLY DORMANT PHENOTYPE OF 4T07 BREAST CANCER CELLS IS MEDIATED BY THE IMMUNE SYSTEM.....		
		52
3.1	Disclaimer	52
3.2	Introduction	52
3.3	Methods and materials	53
3.3.1	Animal studies	53
3.3.2	Cell Line and reagents	53
3.3.3	Statistics	54
3.4	Results	54
3.4.1	4T07 cells are metastatic in immunodeficient mice	54
3.4.2	Primary tumor exposure prevents systemic tumor growth	54
3.4.3	CD8+ cells depletion promotes pulmonary outgrowth of systemically dormant 4T07 cells	55
3.5	Figures	56
3.6	Conclusion	61
CHAPTER 4. PHARMACOLOGICAL INHIBITION OF FGFR MODULATES THE METASTATIC IMMUNE MICROENVIRONMENT AND PROMOTES RESPONSE TO CHECKPOINT BLOCKADE .....		
		62
4.1	Disclaimer	62
4.2	Introduction	62
4.3	Methods and materials	63
4.3.1	Animal studies and drug dosing	63
4.3.2	Cell lines and reagents	63
4.3.3	Flow cytometry	64
4.3.4	Immunoassays	64

4.3.5	mRNA expression analyses .....	65
4.3.6	T-cell signaling and immune cell killing assays .....	65
4.3.7	Statistics.....	65
4.4	Results .....	66
4.4.1	Inhibition of metastatic tumor growth by FGFR targeted agents is enhanced by the immune system. ....	66
4.4.2	Inhibition of FGFR increases CD8+ cell in pulmonary tumors .....	66
4.4.3	FIIN4 treatment modulates immune suppressive populations in pulmonary tumors 67	
4.4.4	Combination of FIIN4 and immune-checkpoint-blockade therapy .....	67
4.5	Figures.....	69
4.6	Conclusion.....	75
CHAPTER 5. DISCUSSION AND FUTURE DIRECTIONS .....		77
5.1	Recurrence of minimal residual disease.....	77
5.2	Recurrence of immune mediated dormant tumors.....	80
5.3	A combination therapy to target metastatic tumors .....	82
5.4	Summary.....	87
REFERENCES .....		88
APPENDIX A. FGF2/CAR T CELLS.....		101

## LIST OF FIGURES

Figure 1.1 Cancer Dormancy and minimal residual disease. Cancer cells exit primary tumor sites even before the clinical detection of the local tumors. These disseminated tumors can maintain a dormant state and survive for months, years, or even decades. With the detection of the disease, patients undergo surgeries and therapeutic treatments leading to clinical remission. However, disseminated cells remain undetected and survive therapeutic treatments. Usually, there are three types of dormancy such as a) cellular dormancy b) vasculature mediated dormancy and c) immune-surveillance mediated dormancy. Various external stimuli and internal physiological factors can liberate these cells from dormancy and make them proliferative, ultimately results in the disease recurrence. Eventually, patients suffer from both local recurrences as well as systemic metastatic diseases. .... 19

Figure 1.2 Different therapeutic options for targeting FGFR signaling. Various options are available to target FGFR in different types of cancer. Current approaches to targets FGFR include selective and non-selective tyrosine kinase inhibitors and the monoclonal antibodies to block receptor function and sequester ligands. Different competitive and covalent inhibitors are also being developed that bind to the ATP-binding sites of the intracellular kinase domains of the receptors and prevent initiation of phosphorylation cascade of the FGFR signaling. Antibody therapies like FPA144, GP369, and MRGR18775 target the external domains of the kinase receptors. Additionally, Various engineered IgG are also being pursued to traps ligands that sequester the available ligands of the receptors and subsequent downregulation of the signaling. .... 23

Figure 1.3 Epithelial to mesenchymal transition. Growth factors, cytokines, and even different therapies can trigger EMT processes. The EMT program is orchestrated via upregulation of master regulators and subsequent modulation of transcription factors that result in several critical gene expression changes. Along the process, epithelial cells lose the expression of epithelial markers such as E-cadherin, EPCAM, claudins, cytokeratin, and upregulate the expression of mesenchymal markers such as vimentin, N-cadherin, fibronectin, and various MMPs. As a result of such drastic changes in gene expression, polarized epithelial cells lose their cell polarity, and adhesion rendered them with more migratory and invasive potentials ..... 26

Figure 1.4 The tumor microenvironment is a complex structure with vibrant cellular interactions. Cancer cells in the tumor lesions are surrounded by stromal fibroblasts, endothelial cells of blood vasculatures, and different types of immune cells. These multicellular structures are constantly interacting in paracrine and autocrine manners via various secreted growth factors, chemokines, and matrix proteins. Different types of immune cells play distinct roles leading to both metastasis promotion and cancer clearance. .... 28

Figure 2.1 HER2 is diminished following recurrence of T-DM1 resistant minimal residual disease. A Mice were inoculated with HME2 cells ( $2 \times 10^6$  cells/mouse) via the mammary fat pad and tumors were allowed to form for a period of 14 days. At this point mice were split into two cohorts (5 mice/group) and left untreated (no drug) or were treated with T-DM1 (9 mg/kg) at the indicated time points (arrows). Following complete regression of palpable tumors T-DM1 treatment was stopped. Recurrent tumors (3 mice) were again treated with T-DM1 (arrows). B Representative

bioluminescent images of tumor bearing mice before T-DM1 treatment (1° tumor), following T-DM1 treatment (MRD), and upon tumor recurrence. C Immunohistochemistry for HER2 expression in control and recurrent, T-DM1 resistant HME2 tumors. ....40

Figure 2.2 *In vitro* establishment of T-DM1 resistant cells requires prior induction of epithelial-mesenchymal transition. A HME2 cells were left untreated (parental) or were stimulated with TGF- $\beta$ 1 and allowed to recover (Post-TGF- $\beta$ ) as described in the materials and methods. These two cell populations were subsequently treated with T-DM1 (250 ng/ml) every three days for a period of 5 weeks. Representative wells were stained with crystal violet at the indicated time points to visualize viable cells. B Brightfield microscopy of crystal violet stained HME2 parental and post-TGF- $\beta$  cells following 3 weeks of continuous T-DM1 treatment. C The T-DM1 resistant (TDM1R) cells that survived 5 weeks of treatment were further expanded and cultured for a period of 4 weeks in the absence of T-DM1. These cells along with passage-matched parental HME2 cells were subjected 96 hour treatments with the indicated concentrations of T-DM1 and assayed for cell viability. Data are the mean  $\pm$ SE of three independent experiments resulting in the indicated P value. D Parental, post-TGF- $\beta$ , and TDM1R HME2 cells were stained with Alexafluor 647-labeled trastuzumab and antibody binding was quantified by flow cytometry. The percentage of cells in each quadrant with reference to forward scatter (FSC) is indicated. Also shown is the mean,  $\pm$ SD, percentages of low trastuzumab binding (Trastuzumab<sup>Low</sup>) cells of three independent experiments resulting in the indicated P values.....41

Figure 2.3 FGFR1 is sufficient to reduce T-DM1 efficacy. A Brightfield microscopy of HME2 parental, post-TGF- $\beta$ , and T-DM1 resistant (TDM1R) cells. B The cells described in panel A were analyzed by flow cytometry for cell surface expression of CD24 and CD44. The percentage of cells in each quadrant is indicated. C Whole cell lysates from HME2 parental, Post-TGF- $\beta$ , T-DM1 resistant (TDM1R), and HME2 cells constructed to stably express FGFR1 or GFP as a control were analyzed by immunoblot for expression of FGFR1, HER2, E-cadherin (Ecad), N-cadherin (Ncad), vimentin, and  $\beta$ -tubulin ( $\beta$ -Tub) served as a loading control. Data in panels B and C are representative of at least three separate analyses. D Expression values for FGFR1-4 were analyzed in the Long-HER data set. Data are the relative expression of individual patients that demonstrated long-term (Long-HER) or short-term (Poor-response) response to trastuzumab treatment, resulting in the indicated P values. E HME2 cells expressing FGFR1 or GFP as a control were treated with the indicated concentrations of T-DM1 for 96 hours at which point cell viability was quantified. Data are normalized to the untreated control cells and are the mean  $\pm$ SE of three independent experiments resulting in the indicated P value. F HME2 cells expressing FGFR1 or GFP as a control were incubated with Alexafluor 647-labeled trastuzumab and antibody binding was quantified by flow cytometry. Data are the mean fluorescence intensities, normalized to total HER2 levels as determined by immunoblot,  $\pm$ SD for three independent experiments resulting in the indicated P value. ....42

Figure 2.4 FGFR1 increases tumor recurrence following T-DM1-induced minimal residual disease. A Time line demarking the primary tumor growth period for HME2 cells constructed to express FGFR1 or GFP as a control. Cells were engrafted onto the mammary fat pad of female NRG mice (2x10<sup>6</sup> cells/mouse; n=5 mice per group). Tumor growth was monitored via digital caliper measurements at the indicated time points. T-DM1 treatment was initiated in each group when tumors reached an average of 1000 mm<sup>3</sup>, horizontal line. Representative bioluminescent images for each group are shown at the indicated time points. Days are in reference to tumor

engraftment (Day 0). B Time line demarking the T-DM1 treatment periods for each group. T-DM1 was administered via I.V. injections (9 mg/kg) at day 0 for HME2-GFP tumors and days 0,7 and 14 for HME2-FGFR1 tumors (arrows). Tumor regression was monitored via digital caliper measurements at the indicated time points. Representative bioluminescent images for each group are shown at the indicated time points. Days are in reference to initiation of T-DM1 treatment (Day 0) for each group. C Time line demarking the post-treatment observation period for each group. Once tumors regressed to a non-palpable state of minimal residual disease (MRD) mice were left untreated and monitored for tumor recurrence via digital caliper measurements. Representative bioluminescent images for each group are shown at the indicated time points. Days are in reference to achievement of MRD (Day 0) for each group. A representative HER2 IHC is shown for the recurrent tumors. Survival data in panel C were analyzed via a log rank test where tumor recurrence of >50 mm<sup>3</sup> was set as a criteria for disease progression. Data in panel A are the mean  $\pm$ SD of five mice per group resulting in the indicated P value. In panel B tumor size for each mouse is plotted individually. Data in panels A and B were analyzed via a two-way ANOVA. ....44

Figure 2.5 T-DM1 resistant cells are sensitive to covalent inhibition of FGFR. A HME2 parental and T-DM1 resistant (TDM1R) cells were treated with the indicated concentrations of lapatinib or FIIN4 for 2 hours. Cell lysates were subsequently assayed by immunoblot for phosphorylation of ERK1/2 and HER2,  $\beta$ -tubulin ( $\beta$ -Tub) served as a loading control. Data in panel A are representative of at least two independent experiments. B HME2 parental cells (parental) and TDM1R cells were plated in the presence of the indicated concentrations of lapatinib for 96 hours at which point cell viability was determined. C HME2 parental and TDM1R cells were plated in the presence of the indicated concentrations of afatinib for 96 hours at which point cell viability was determined. D HME2 parental and lapatinib resistant (LAPR) cells were plated in the presence of the indicated concentrations of T-DM1 for 96 hours at which point cell viability was determined. E HME2 parental and TDM1R cells were plated in the presence of the indicated concentrations of FIIN4 for 96 hours at which point cell viability was determined. Data in panels B-E are the mean  $\pm$ SE of at least three independent experiments resulting in the indicated P values. ....46

Figure 2.6 T-DM1 resistant tumors respond to systemic inhibition of FGFR. A Schematic representation of the *in vivo* derivation of T-DM1 resistant HME2 tumors. HME2 parental cells ( $2 \times 10^6$ ) were engrafted onto the mammary fat pad of an NSG mouse. This mouse was treated with T-DM1 until tumor regression was observed. Sections of the remaining tumor were directly transferred onto recipient mice. This was repeated twice until transferred tumors that no longer responded to T-DM1 therapy were identified. At this point sections of a T-DM1 resistant tumor were assessed by IHC for FGFR1 expression as compared to the originally engrafted HME2 tumors. Representative FGFR1 IHC staining is shown. B Bioluminescent imaging of mice bearing the T-DM1 resistant tumors described in panel A. These mice were left untreated (No Drug) or were treated with FIIN4 (100 mg/kg/q.o.d.). C Bioluminescent quantification of control and FIIN4-treated animals bearing T-DM1 resistant tumors. Data are normalized to the tumor luminescence values at the initiation of FIIN4 treatment (day 0). D Tumor size as determined by digital caliper measurements at the indicated time points during FIIN4 treatment. For panels C and D data are the mean  $\pm$ SE of five mice per group resulting in the indicated P-values. E Representative Ki67 and TUNEL staining of P3, T-DM1 resistant tumors from untreated and FIIN4 treated groups. Also shown are the mean  $\pm$ SD of TUNEL and Ki67 positive cells per high powered field (HPF), n=5, resulting in the indicated P values. ....48

Figure 2.7 Trastuzumab-resistant patient derived xenografts are sensitive to covalent inhibition of FGFR. A Schematic representation of the expansion protocol of HCI-012. Tumor bearing mice were split into two cohorts consisting of an untreated group and a group that was initially treated with T-DM1 (5 mg/kg) and then switched to FIIN4 (25 mg/kg/p.o.d). B PDX tumor bearing mice were treated as described in panel A and tumor size was measured by digital caliper measurements at the indicated time points. Closed arrows indicate T-DM1 treatments, open arrow indicates initiation of FIIN4 treatment. Data are the mean  $\pm$ SE of 5 mice per group resulting in the indicated p-value. C Representative histological sections of untreated HCI-012 tumors stained with antibodies for HER2 and FGFR1. D *Ex-vivo* HCI-012 tumor cells were grown for 20 days under 3D culture conditions in the presence or absence of the indicated compounds. Representative images are shown and cell viability was quantified by cell titer glow. Data are mean  $\pm$ SD of triplicate wells treated with the indicated compounds. ....49

Figure 3.1 4T07 cells are metastatic in immunodeficient mice. (A) Both immunodeficient(NU/NU) and immunocompetent(BALB/c) mice (n=5 mice per group) were engrafted with 4T07 cells (1x10<sup>6</sup>) via the mammary fat pad. Engraftment and primary tumor growth were monitored by bioluminescence at the indicated time points. (B and C) Fourteen days after engraftment the resulting primary lesions were surgically excised (B) and differences in tumor weight (n=5 mice per group) were analyzed via a paired T-test, resulting in the indicated P value. (D) These mice were subsequently monitored for pulmonary metastasis via bioluminescence imaging. The mean ( $\pm$ SE) bioluminescent values from each group taken at the indicated time points resulting in the indicated p values. (E) Bioluminescent images of representative mice from each group at the indicated timepoints. ....56

Figure 3.2 Primary tumor exposure prevents systemic tumor growth A) Schematic timeline of primary and systemic tumor engraftments. One group of mice (n=5) were engrafted with wild type 4T07 cells on the mammary fat pad. The primary tumors were grown for 14 days, surgically excised and mice were allowed to recover. These mice and primary tumor naïve littermates were subsequently challenged with firefly luciferase expressing 4T07 cells via the lateral tail vein and pulmonary tumor growth was quantified by bioluminescence. All time points are in reference to primary tumor engraftment (D0). (B) Excised wild type 4T07 primary tumors, 14 days after fat pad engraftment. (C) Bioluminescent images of three representative mice from the primary tumor naïve group and the group exposed to primary tumor formation. Images were taken immediately after tail vein injection (D41) to demonstrate equal pulmonary tumor cell challenge and 12 days later (D53). (D) The mean ( $\pm$ SE) bioluminescent values from each group taken at the indicated time points (n=5 mice per group) resulting in the indicated P value. Data are normalized to the challenge values obtained immediately following tail vein injection. (E) Survival analysis of primary tumor naïve mice and those exposed to primary tumor formation following pulmonary tumor challenge (n=5 mice per group).....57

Figure 3.3 Systemically-dormant 4T07 cells can undergo metastatic outgrowth upon depletion of CD8<sup>+</sup> cells. (A-C) ) Two groups of BALB/c mice were engrafted with 4T07 cells (5x10<sup>5</sup>) either via the fat pad or the tail vein. Mice were sacrificed at Day 14 and tissues were collected for flow cytometric analysis. In panels A and B, dot plots showing ancestry of the gated CD11b<sup>+</sup>CD8<sup>+</sup> cells in the indicated tissues. In panel C, the presence of CD8<sup>+</sup>CD11b<sup>+</sup> cells was quantified as a percent of CD8<sup>+</sup> cells in the indicated tissues (n=4 mice per group). (D) Schematic timeline detailing timing in which BALB/c mice (n=16 mice) were engrafted with 4T07 cells (1X10<sup>5</sup>) via the mammary fat pad. The primary tumors were grown for 4 weeks, surgically excised and mice

were subsequently treated with either IgG or  $\alpha$ CD8 antibodies (200  $\mu$ g) via intraperitoneal injections once every three days for the length of the experiment (n=8 mice per group). (E) Metastasis free survival analysis of IgG control mice (blue line) and CD8 depleted mice (red line) in days following the primary tumor removal (n=8 mice per group). The indicated p-value was calculated using a log rank test. (F) Bioluminescent images of representative mice at the 23 days after primary tumor removal. .... 59

Figure 4.1 Immune competent mice demonstrate prolonged antitumor effects following systemic inhibition of FGFR. (A) Timeline of the engraftment and treatment approaches. Firefly luciferase-expressing 4T07 cells (5x10<sup>5</sup>) were injected into the lateral tail vein of both BALB/c and NRG mice (n=10 mice each group) and cells were allowed to seed for two days. These mice were then treated with either DMSO or FIIN4 (100 mg/kg/po/qd) for 7 days. (B) The mean ( $\pm$ SE) pulmonary radiance values from each group was taken at the indicated time points (n=5 mice per group). Data are normalized to the load values obtained immediately following tail vein injection and were analyzed using a 2-way ANOVA. (C) Representative bioluminescent images of both BALB/c and NRG mice at Day 10 post tumor engraftment. (D) Survival analysis of indicated groups mice after stopping the treatment (n=5 mice per group). These data were analyzed using a log rank test.... 69

Figure 4.2 FIIN4 treatment leads to an elevated level of CD8+ cells in pulmonary tumors. (A, B and C) 4T07 cells (5x10<sup>5</sup>) were delivered to the lungs of BALB/c mice (n=20) via tail vein injection, and the mice were allowed to recover for two days. Mice were administered either DMSO or FIIN4 (25, 50 and 100 mg/kg/day) via oral gavage for 7 days. (n=5 mice per group). Following this treatment, mice were sacrificed and lungs were collected and fixed in paraformaldehyde for downstream histological analysis. (A) Representative images of pulmonary histological sections of each treatment group stained with H&E, or antibodies specific for CD8 or CD4. (B) Bioluminescent images of each group treatment group 10 days after pulmonary engraftment. (C) The mean ( $\pm$ SD) of CD8 and CD4 positive cells per high powered field (HPF), n=5. (D) Differential CXCL16 expression levels were obtained from the dataset GSE52452 in which MGHU3 were treated with the FGFR inhibitor PD173074. (E) RT-PCR analysis for CXCL16 obtained from 4T1 cells treated with 500 nM FIIN4 for 24 hours. (F) IHC analysis for CXCL16 in the control and FIIN4 treated (100 mg/kg/day) pulmonary tumors as described in panel A. (G) IHC analysis for CD8+ cells in control D2.A1 pulmonary tumors expressing a scrambled shRNA (shscram) and those depleted for FGFR1 expression (shFGFR1). .... 70

Figure 4.3 FIIN4 treatment modulates pulmonary immune populations in 4T07 tumor-bearing mice. Multicolor flow cytometry analyses were performed to measure the changes in various immune cell populations in the spleen and lungs of BALB/c mice bearing 4T07 pulmonary tumors following 7 days of systemic administration of FIIN4 (100 mg/kg,po,qd). (A and B) Representative dot plots and replicated quantification of myeloid-derived suppressor cells (MDSCs) identified as CD11b+Ly6chiLy6Glow populations and quantified as a frequency of live events in isolated lung and spleen tissues of each group. (C and D) Representative dot plots and replicated quantification of macrophages identified as CD11b+Ly6clowF4/80+ populations and quantified as a frequency of live events in the isolated lung and spleen tissues of each group (E and F) Representative dot plots and replicated quantification of PD-L1 positive MDSCs identified as CD11b+Ly6chiLy6GlowPD-L1+ populations in the isolated pulmonary tumors. Data presented here are from three mice and are representative of two independent experiments. .... 72

Figure 4.4 Sequential combination of FIIN4 and immune-checkpoint-blockade enhanced survival of pulmonary tumor-bearing mice. (A) Survival analysis of BALB/c mice bearing pulmonary 4T07 tumors with indicated therapies (n=5 mice per groups). The combination group of mice received both FIIN4 (100mg/kg/day for seven days via oral gavage) and  $\alpha$ PD-L1 (four doses of 200  $\mu$ g once every three days via intraperitoneal injections) simultaneously. The 14 day FIIN4 treatment is indicated by the solid black line and each  $\alpha$ PD-L1 administration is denoted by an arrowhead (B) 4T07 cells were cocultured *in vitro* with spleenocytes from 4T07 tumor bearing mice in the presence or absence of FIIN4 and tumor cell lysis was quantified as described in the materials and methods. (C) Jurkat T-cells pretreated with either DMSO or 1 $\mu$ M FIIN4 overnight were stimulated with  $\alpha$ CD3 antibody for the indicated time points, and cell lysates were collected and assayed via immunoblot for phosphorylation of p-Lck, p-PLC $\gamma$ 1, p-SLP76, p-ZAP70(Y319), p-LAT, and  $\beta$ -tubulin ( $\beta$ -Tub) as a loading control. Data in panel C are representative of at least two independent experiments. (D) Survival analyses of BALB/c mice bearing pulmonary 4T07 tumors treated with indicated therapies (n=10 mice per group). As in panel A, FIIN4 treatment duration (100 mg/kg/day) is indicated by the solid line and  $\alpha$ PD-L1 doses (200  $\mu$ g) are indicated by the arrowheads. Survival data were analyzed by a log rank test. (E) Bioluminescent images of the different treatment groups described in panel D at Day 17 post tail vein injections. .... 74

Figure 5.1 Minimal residual disease post T-DM1 treatment. (A) HER2 driven tumors exhibit the loss of Her2 expression following prolong treatments of T-DM1 followed by the activation of FGFR signaling. The induction of EMT helps the selection of cancer cell types that exhibits a switch of growth-promoting pathways. (B) Schematic presentation of various stages of HER2+ xenografts. Initially, HER2+ cells are sensitive to T-DM1 treatments that result in the development of minimal residual diseases (MRD) when the diseases are below the threshold for detection. While in the state of MRD, these cancer cells acquire new growth-promoting pathways FGFR while downregulating Her2 driven signaling. These tumors, when they relapse out of MRD, show little sensitivity towards T-DM1 but can be targeted with FGFR inhibitors. .... 78

Figure 5.2 Model of 4T07 immune-mediated dormancy. (A) Immune dormancy is defined as a state of equilibrium between tumor cell's growth rate and cell-death due to clearance by immune cell activity. Any events that may compromise the immune system can shift the balance favoring the recurrence of metastatic tumors. (B) Systemically disseminated 4T07 cells are immunogenic and susceptible to the adaptive immune system. Following the depletion of CD8+ T cells, these disseminated micrometastasis of 4T07 tumors break their dormancy and give rise to overt macrometastatic growth. .... 81

Figure 5.3 Compositions of tumor immune microenvironment of 4T07 pulmonary metastatic niche with FGFR inhibition. 4T07 tumors can develop macrometastasis in the pulmonary region when delivered via tail vein injections. 4T07 metastatic niche is characterized as immune-exclusive phenotype with few cytolytic T lymphocytes presence. Systemic inhibition of FGFR can bring significant changes in the composition of different immune cell populations favoring tumor clearance. An increase in the number of CD8+ T lymphocytes and a decrease in the MDSCs number are two major changes with FGFR inhibition. There is an elevated expression of PD-L1 on MDSCs within these proinflammatory environments as well. Such changes in immune cell populations and their phenotypes opened up an excellent opportunity for combination therapies with FGFR kinase inhibitor and immune checkpoint blockade therapies. .... 84

Figure 5.4 FIIN4 affects T lymphocytes signaling and its effector functions. FGFR inhibition with covalent FIIN4 molecule downregulates the TCR signaling cascade and subsequently affects the T-lymphocyte mediated cancer cell killings. More experiments are needed to establish if FIIN4 can modulate the secretion of effector molecules by activated T-lymphocytes..... 86

## LIST OF ABBREVIATIONS

BC:	Breast Cancer
ADC:	antibody-drug conjugate
PFS:	progression-free survival
EMT:	epithelial-mesenchymal transition
TIME:	tumor immune-microenvironment
MDSCs:	myeloid-derived suppressor cells
TAM:	tumor associated macrophages
FGFR:	fibroblast growth factor receptor
ICB:	immune-checkpoint blockade
FIIN4:	FGFR irreversible inhibitor 4
HER2:	human epidermal growth factor receptor-2
HME2:	HER2 transformed mammary epithelial cells
LAPR:	lapatinib resistant cells
MRD:	minimal residual disease
PDX:	patient-derived xenograft
TCR:	T cell receptor
T-DM1:	Trastuzumab-emtansine
DTC:	disseminated tumor cells
TDM1R:	T-DM1 resistant cells
TGF- $\beta$ :	transforming growth factor beta

## ABSTRACT

Breast cancer (BC) is one of the deadliest forms of cancers with high incidence and mortality rates, especially in women. Encouragingly, targeted therapies have improved the overall survival and quality of life in patients with various subtypes of BC. Unfortunately, these first-line therapies often fail due to inherent as well as acquired resistance of cancer cells. Treatment-evading cancer cells can exhibit systemic dormancy in patients over a long period of time without manifesting any symptoms. In a suitable environment, these undetected disseminated tumor cells can relapse in the form of metastasis. Therefore, it is essential to understand the mechanisms of BC recurrence and to develop durable therapeutic interventions to improve patient's survival. In this dissertation work, we studied fibroblast growth factor receptors (FGFR), as therapeutic targets to treat the recurrence of drug-resistant and immune-dormant BC metastasis.

The HER2 subtype of BC is characterized by the overexpression of human epidermal growth factor receptor 2 (HER2), which drives elevated downstream signaling promoting tumorigenesis. Trastuzumab emtansine (T-DM1) is an antibody-drug conjugate in which an anti-HER2 antibody targets HER2 overexpressing tumor cells and delivers a highly potent microtubule inhibitor. Using novel models of minimal residual disease (MRD) following T-DM1 treatments, we found that epithelial to mesenchymal transition is a critical process for cells to persist the T-DM1 treatments. The upregulation of FGFR1 may facilitate insensitivity to T-DM1. Our data also showed that FGFR1 overexpression in HER2+ tumors leads to a higher incidence of recurrence, and these recurrent tumors show sensitivity towards covalent inhibition of FGFR.

In addition to drug-induced MRD in the primary tumor sites, disseminated tumor cells (DTCs) can demonstrate dormant phenotype via maintaining an equilibrium with immune-mediated tumor clearance. Factors affecting such equilibrium may contribute to the recurrence of breast cancers metastasis. We show that such immune-mediated dormancy can be modeled with the 4T07 tumors. These tumors display immune-exclusion phenotypes in metastatic pulmonary organs. The inhibition of FGFR modulates the immune cell compositions of pulmonary organs favoring anti-tumor immunity. However, inhibition of FGFR may also affect T cell receptor downstream signaling, resulting in the inhibition of cytolytic T cell's function. Finally, we report

that combination therapy using the FGFR kinase inhibitor and an immune checkpoint blockade showed effective targeting of metastatic 4T07 tumors.

FGFR signaling as a therapeutic target in various tumors has been an active focus of cancer research. In this dissertation work, we have expanded our understanding of the role of FGFR in the recurrence of drug-resistant breast cancers as well as in the maintenance of an immune evasive microenvironment promoting pulmonary growth of tumors. Moreover, we presented evidence that it is possible to repurpose FGFR targeted therapy alone or in combination with checkpoint blockades to target recurrent metastatic BCs. In the future, our novel models of minimal residual diseases and systemic immune dormancy may act as valuable biological tools to expand our understanding of the minimal residual disease and dormant tumor cells.

## **CHAPTER 1. INTRODUCTION**

Cancer, rightfully considered to be the emperors of all maladies, is the disease of our times to beat. To current days, cancer causes significant health and financial burden to people all over the world. The development of durable therapeutic interventions is hindered by the complexity of cancerous diseases (Dagogo-Jack and Shaw, 2018; Fisher et al., 2013). Inherently different mechanisms are at play in the initiation, development, and maintenance of various forms of cancers. Additionally, the limitations in experimental models pose significant scientific challenges to understand the critical steps of cancer progression.

### **1.1 Cancer dormancy**

Evolution is the fundamental characteristic of neoplastic cells (Yates and Campbell, 2012; Yates et al., 2017). Transformed cells have to undergo continuous phenotypic changes and selection events that enable them to survive and fit at different stages of metastatic progressions. Early dissemination of cells, even before the clinical detection of the disease, is a well-established phenomenon of cancers (Aslakson and Miller, 1992; Rhim et al., 2012; Röcken, 2010). These disseminated tumors often evolve to a slowly growing dormant state known as cancer dormancy (Figure 1.1). Additionally, these dormant cells are resistant to various therapies and can remain in such a state for an extended period of time (Ebinger et al., 2016; Quesnel, 2013).

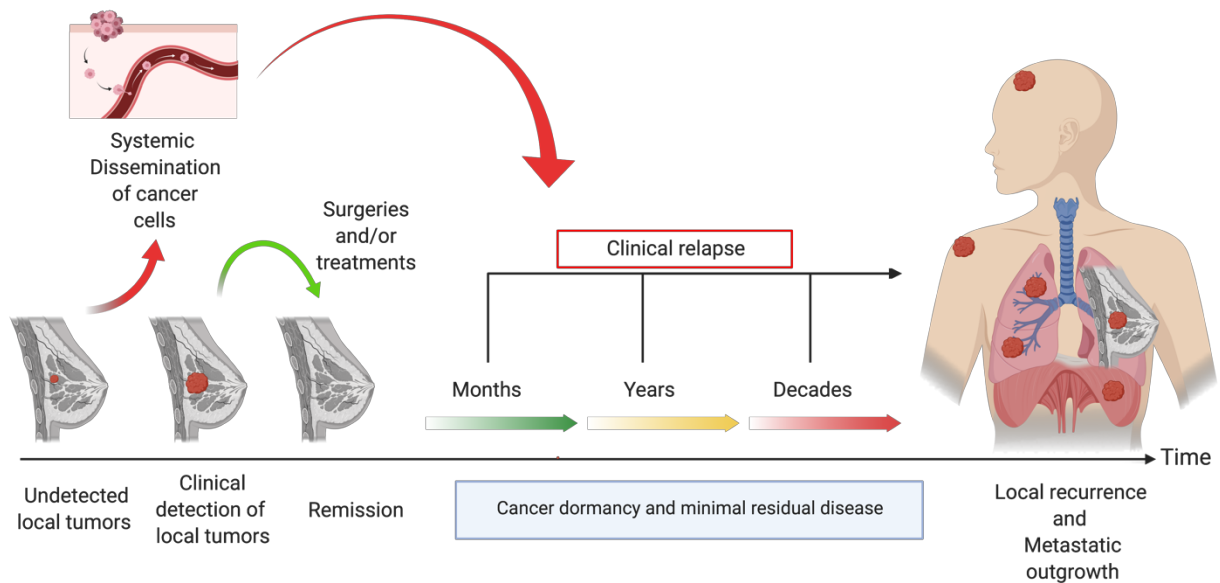


Figure 1.1 Cancer Dormancy and minimal residual disease. Cancer cells exit primary tumor sites even before the clinical detection of the local tumors. These disseminated tumors can maintain a dormant state and survive for months, years, or even decades. With the detection of the disease, patients undergo surgeries and therapeutic treatments leading to clinical remission. However, disseminated cells remain undetected and survive therapeutic treatments. Usually, there are three types of dormancy such as a) cellular dormancy b) vasculature mediated dormancy and c) immune-surveillance mediated dormancy. Various external stimuli and internal physiological factors can liberate these cells from dormancy and make them proliferative, ultimately results in the disease recurrence. Eventually, patients suffer from both local recurrences as well as systemic metastatic diseases.

The phase of minimal residual disease is defined when cancer cells exist in a clinically undetected and dormant state after treatments or surgeries. Inter and intracellular signaling pathways and external factors that influence the maintenance of such dormancy have been active fields of research. Usually, the maintenance of dormancy is categorized into three different means such as a) cellular dormancy b) angiogenic dormancy, and b) immune surveillance-mediated dormancy (Aguirre-Ghiso, 2007).

From a therapeutic standpoint, understanding the biology of dormancy inducer, maintenance and recurrence could be very exciting. Such knowledge would enable us to develop novel therapeutics to drive actively growing tumors towards dormancy, prevent or delay their recurrence, and even induce cell death in the state of dormancy. In this dissertation work, we studied the recurrence of minimal residual disease and immune-dormant breast cancer cells.

## **1.2 Breast cancer**

Breast cancer (BC) shows the highest incidence in women worldwide and causes significant mortalities (DeSantis et al., 2014). Traditional classifications of BC have been used for patient's prognosis and choice of therapeutics. These classifications of BC relied on various pathohistological features such as tumor grade, size, and node status, and immunohistochemistry for estrogen receptor alpha (ER- $\alpha$ ), progesterone receptor (PR) and human epidermal growth factor receptor 2 (Her2) receptor (Ali et al., 2017). More recently, cDNA microarray-based gene expression analyses enabled molecular subtyping of breast cancers (Hu et al., 2006; Perou et al., 2000; Sørlie et al., 2001; Sotiriou et al., 2003). Molecular subtyping such as PAM50 with several others MammaPrint and OncotypeDX are currently being used clinically for stratifications of patients and the treatment decisions (Parker et al., 2009)(Brandão et al., 2019)(McVeigh and Kerin, 2017).

The HER2 subtype of breast cancer (BC) accounts for about 20% of all BC patients (Ali et al., 2017). This subtype is defined by the overexpression of human epidermal growth factor receptor 2 (HER2), which drives elevated downstream signaling inducing tumorigenesis. Overexpression of HER2 leads to self-dimerization of the surface receptors that can initiate downstream signaling in a ligand-independent manner (Moasser, 2007). Aberrant activation of

HER2 downstream signaling cascades promotes cancer proliferation, migration, invasion, and metastasis (Johnson et al., 2010; Prior et al.). As a result, there have been significant research efforts in inhibiting HER2 driven tumorigenic signaling that lead to the emergence of successful kinase inhibitors and monoclonal antibody therapies.

Oncogenic addiction of tumors to HER2 signaling for their growth makes them susceptible to those small molecule inhibitors. Several kinase inhibitors, such as Lapatinib and Neratinib, can inhibit HER2 and other members of ErbB family receptors (Di Leo et al., 2008; Geyer et al., 2006). These drugs have shown significant efficacies in combination with chemotherapies to treat Her2-amplified advanced BC. In addition to kinase inhibitors, several monoclonal antibodies have also been developed targeting the extracellular domain of the kinase receptor. Monoclonal antibodies such as Trastuzumab and Pertuzumab can selectively bind to Her2 overexpressing cells and induce cytotoxicity by inhibiting Her2 signaling (Miller et al., 2014; Nahta, 2012). These drugs have shown significant clinical benefits and have been granted FDA approval for the treatment of metastatic Her2-amplified BC patients (Perez et al., 2014).

### **1.3 Trastuzumab-emtansine (T-DM1)**

T-DM1 is an antibody-drug conjugate (ADC) where HER2 targeting antibody trastuzumab is conjugated with a potent cytotoxic moiety, DM1, via nonreducible thioether linkage. Mechanistically, humanized monoclonal antibody Trastuzumab selectively binds with HER2-expressing cancer cells triggering receptor-mediated endocytosis of the drug. Following internalization, the linker undergoes proteolytic degradation in the lysosome releasing the DM1 drug. Upon the release of the DM1 in the cytoplasm, it can negatively affect they microtubule assembly/disassembly dynamics ultimately results in a mitotic arrest, apoptosis, and mitotic catastrophe (Barok et al., 2014a)(Barok et al., 2011)(Lewis Phillips et al., 2008).

Clinical trials with patient cohorts such as EMILIA, TH3RESA have established T-DM1 as a standard treatment for patients stratified as Her2+ BC subtype (2013)(Welslau et al., 2014)(Amiri-Kordestani et al., 2014). T-DM1 are being used both as first-line treatments for patients that progressed early to the adjuvant therapy and as second or further line treatments for patients with metastasis. EMILIA study reported 9.6 months of median progression-free survival

(PFS), whereas TH3RESA reported 6.2 months. The reported overall survivals for EMILIA and TH3RESA were 30.9 and 22.7 months, respectively. A more recent clinical study, KAMILLIA, observed similar PFS of 6.9 months for patients with advanced breast cancer (Montemurro et al., 2019). KAMILLIA trials also reported a comparable overall survival of 27.2 months. All of these studies supported the continued use of T-DM1 in patients with advanced Her2-positive breast cancer (Hardy-Werbin et al., 2019).

Despite such encouraging responses of T-DM1 in HER2-positive breast cancer, clinical data also indicate that patients eventually progress (Barok et al., 2014a). Additionally, a subset of HER2-positive patients can be non-responsive to the drug. Thus, understanding the molecular mechanisms of such inherent and acquired resistance towards T-DM1 may lead to the development of novel therapies.

#### **1.4 Fibroblast growth factor receptors (FGFR)**

Fibroblast growth factor receptors are the group of four receptor tyrosine kinases (FGFR1-4) involved in crucial physiological processes in developmental and adult cells (Dai et al., 2019). Genomic amplifications and aberrant transcriptional activation of FGFR and their downstream signaling have been implicated in various diseases. Different external stimuli and subsequent activation of various transcription factors such as E2F-1, SP1, Sp3 can drive the expression of distinct members of FGFR (Kanai et al., 2009; Tashiro et al., 2003)(McEwen and Ornitz, 1998). Additionally, the transcription factor Twist can induce FGFR upregulations during the process of EMT (Brown et al., 2016a). Such over activations are critical to sustaining tumorigenesis in various cancers (Helsten et al., 2014). Additional to such transcriptional deregulations, analyses of large set of patient's tumors revealed that FGFR signaling can also be activated via genomic amplifications, chromosomal translocation, and activating mutations (Ciriello et al., 2015)(Helsten et al., 2014)(Patani et al., 2016).

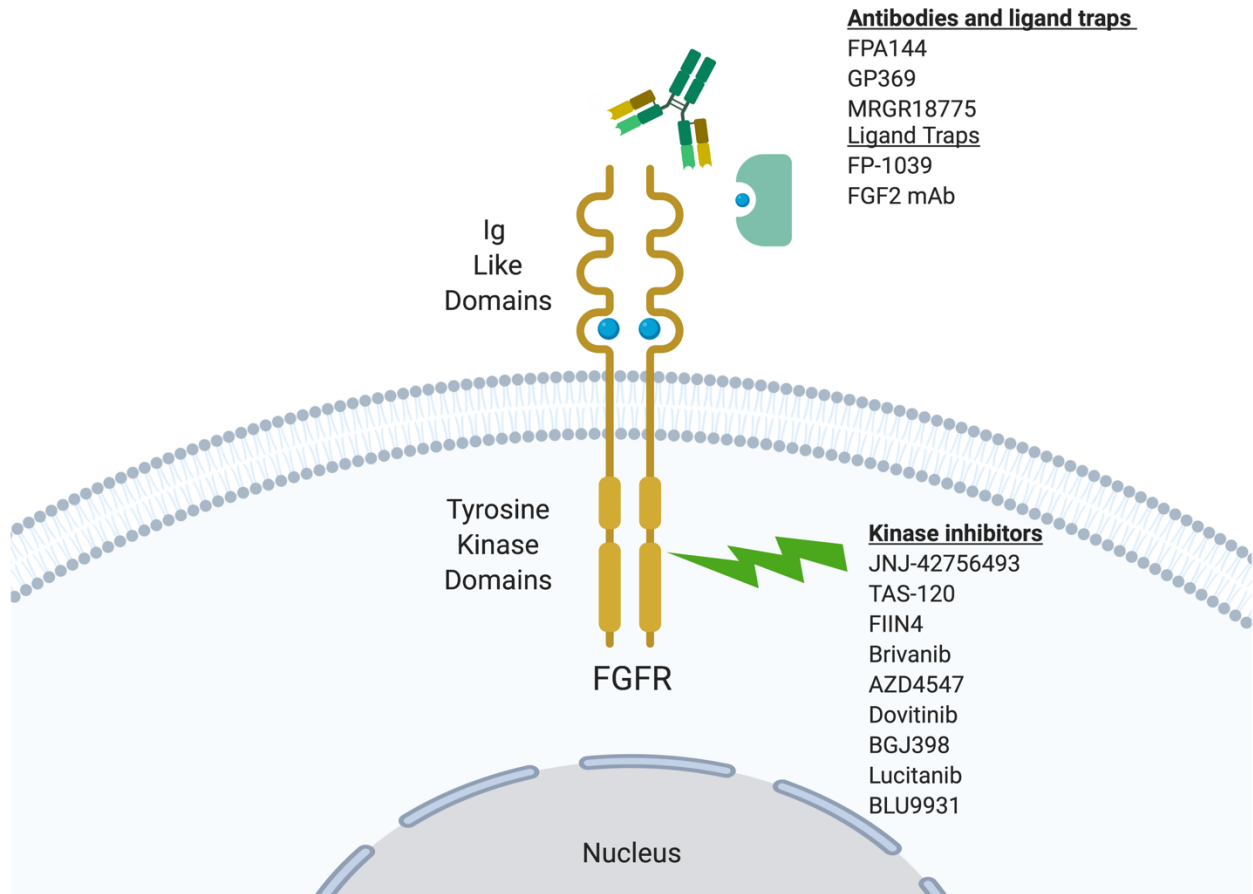


Figure 1.2 Different therapeutic options for targeting FGFR signaling. Various options are available to target FGFR in different types of cancer. Current approaches to targets FGFR include selective and non-selective tyrosine kinase inhibitors and the monoclonal antibodies to block receptor function and sequester ligands. Different competitive and covalent inhibitors are also being developed that bind to the ATP-binding sites of the intracellular kinase domains of the receptors and prevent initiation of phosphorylation cascade of the FGFR signaling. Antibody therapies like FPA144, GP369, and MRGR18775 target the external domains of the kinase receptors. Additionally, Various engineered IgG are also being pursued to traps ligands that sequester the available ligands of the receptors and subsequent downregulation of the signaling.

FGFR signaling pathway heavily dependent on its interactions with membrane co-receptors. Hepran sulfate proteoglycans(HSPGs), N-cadherin,  $\beta$ 3-integrin, neural cell adhesion molecule(NCAM), and neuropilin-1 are some of the co-receptors FGFR are found to be interacting with leading to various downstream regulations of FGFR (Fernig et al., 2000; Rahmoune et al., 1998)(Hazan et al., 2000; Williams et al., 2001)(Brown et al., 2016a; Mori et al., 2015)(Francavilla et al., 2009). Close associations of such receptors dictate the specificity and affinity of these receptors for various growth factor ligands. Interestingly, alternative splicing events of the 20 exons of the FGFR also give rise to different splice variants of these receptors with differential binding preferences for growth factor ligands (Ali et al., 2017). Additionally, cellular localization of FGFR can also influence different physiological events of the cells in the context of disease (Fang et al., 2005; Lee et al., 2013; Stachowiak and Stachowiak, 2016).

In breast cancer, FGFR1 is the most frequently amplified member of the FGFR family. FGFR1 is found to be involved in the acquisition of resistance to HER2 targeted and endocrine therapies in HER2-positive and luminal B subtype of BC, respectively (Turner et al., 2010)(Azuma et al., 2011)(Brown et al., 2016b). FGFR1 is also reported to influence multidrug efflux pumps and confer resistance to chemotherapies (Patel et al., 2013). All of these studies underscored the importance of FGFR signaling as a therapeutic target, and that led to the ongoing development of various therapies that are summarized in figure 1.2. Understanding the roles of FGFR in breast cancer progression and the acquisition of drug resistance have been the major focus of the scientific research so far. However, the influence of FGFR as a secondary driver pathway in the context of disease recurrence remains to be poorly understood. Additionally, studying off-tumor effects of FGFR inhibition is also necessary to achieve combination therapies to increase the overall survival of the patients.

## **1.5 Epithelial to mesenchymal transition (EMT)**

Tumor cells are inherently heterogeneous with distinct metastatic potential (Marusyk and Polyak, 2010). A conserved physiological process known as epithelial to mesenchymal transition (EMT) contributes to such heterogeneity by bringing transcriptional and epigenetic changes to the cancers (Meacham and Morrison, 2013). This process is essential for cellular differentiation during development as well as in wound healing in adult life (Nakaya and Sheng, 2013). Unfortunately,

cancer cells can exploit these processes to evolve as tumors with more stemness, migratory, invasive, and drug-resistant potential. When the EMT program is activated, the cancer cells can undergo dedifferentiation, lose their polarity and cell-cell junctions coupled with upregulation of various mesenchymal markers (figure 1.3) (Rhim et al., 2012; Singh and Settleman, 2010a). Unsurprisingly, EMT plays critical roles in various cancers such as pancreatic cancer, hepatocellular carcinoma, squamous cell carcinoma, urothelial carcinoma, renal cancer, colorectal cancer, cervical cancer, melanoma, prostate cancer, ovarian cancer and breast cancer (Heerboth et al., 2015).

In Breast cancer, EMT has been found to influence various aspects of the disease. Cells that have undergone EMT are found to be resistant to chemotherapy and targeted therapies (Singh and Settleman, 2010a). EMT-related transcription factors have also been found to regulate gene signatures that promote distant metastasis (Heerboth et al., 2015). However, how EMT plays a role in the recurrence of minimal residual diseases is yet to be fully elucidated. Additionally, it is of great importance to continue research on the importance of determining the underlying mechanisms by which EMT drives metastasis in cancers. Continuous improvements in our understanding of how EMT facilitates metastasis, resistance to drugs, and recurrence of the dormant disease would be of great importance.

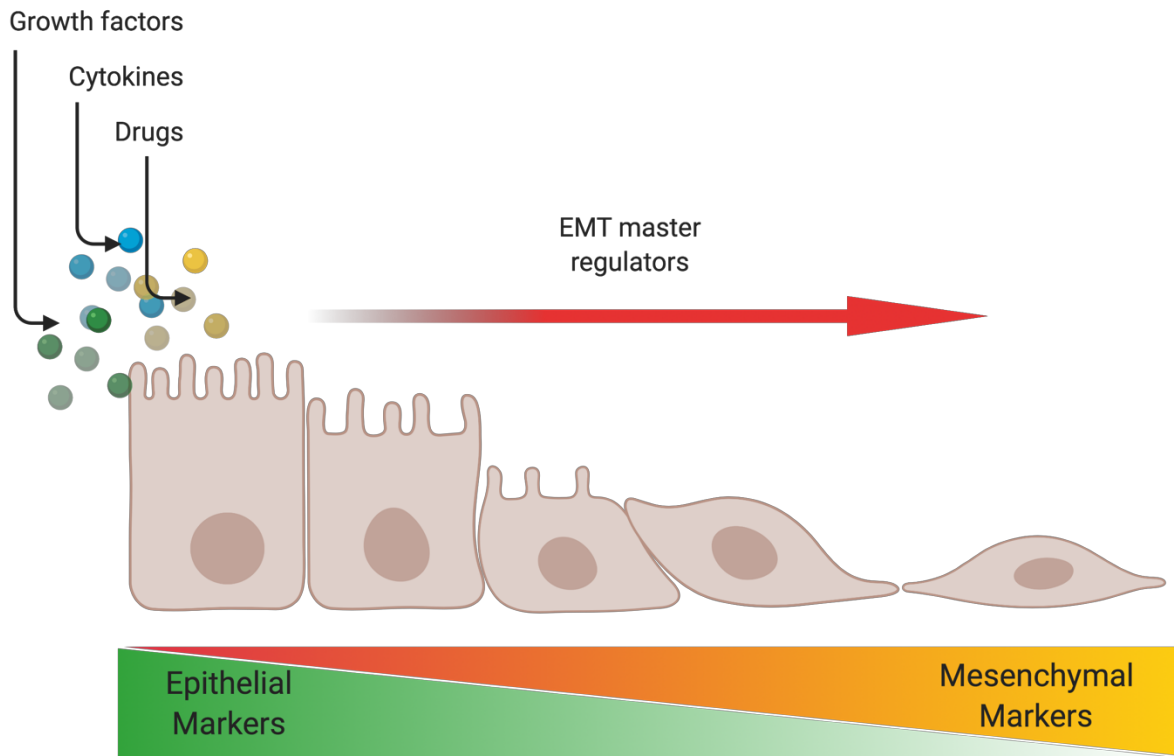


Figure 1.3 Epithelial to mesenchymal transition. Growth factors, cytokines, and even different therapies can trigger EMT processes. The EMT program is orchestrated via upregulation of master regulators and subsequent modulation of transcription factors that result in several critical gene expression changes. Along the process, epithelial cells lose the expression of epithelial markers such as E-cadherin, EPCAM, claudins, cytokeratin, and upregulate the expression of mesenchymal markers such as vimentin, N-cadherin, fibronectin, and various MMPs. As a result of such drastic changes in gene expression, polarized epithelial cells lose their cell polarity, and adhesion rendered them with more migratory and invasive potentials.

## 1.6 Tumor immune microenvironment

Neoplastic cells are rapidly dividing and congregate as cell masses of heterogeneous phenotypes. These heterogeneous tumor masses have unique metabolic needs and require special structural supports in three-dimensional space. As a result, these tumors are surrounded and infiltrated by different types of host cells, creating a specialized environment (Wang et al., 2017). Various secreted growth and chemokine factors, as well as matrix proteins, are integral parts of this environment. Such a specialized complex structure, also known as the tumor microenvironment, is the place for a vibrant relationship orchestrated by different cellular and extracellular components (Balkwill et al., 2012). Tumor-infiltrating immune cells are the integral components of the tumor microenvironment; and composition of which is known as tumor immune microenvironments (TIME) (Binnewies et al., 2018) (figure 1.4).

TIMES are composed of cytolytic lymphocytes, myeloid-derived suppressors cells (MDSCs), tumor-associated macrophages (TAM), various neutrophils, NKT cells, and B cells. Spatial distribution, overall compositions, and functional states of various immune cell populations contribute to the functional outcome of immunity against tumors (Keren et al., 2018)(Research, 2018). T cells, B cells, NKT cells, NK cells, and  $\gamma\delta$  T cells are the major components of immune surveillance program specifically recognizes and eliminates cancer cells (Swann and Smyth, 2007). On the other hand, MDSCs, TAMs, a regulatory subset of T cells (Tregs) repress such cancer eliminating immune surveillance programs (Blomberg et al., 2018). Additionally, TAMs, CD11b<sup>+</sup> myeloid cells and neutrophils are found to promote early disseminations of cancer cells and the formation of premetastatic niches in metastatic organs (Lee and Naora, 2019)(Liu and Cao, 2016)(Lin et al., 2019)(Wang et al., 2019b).

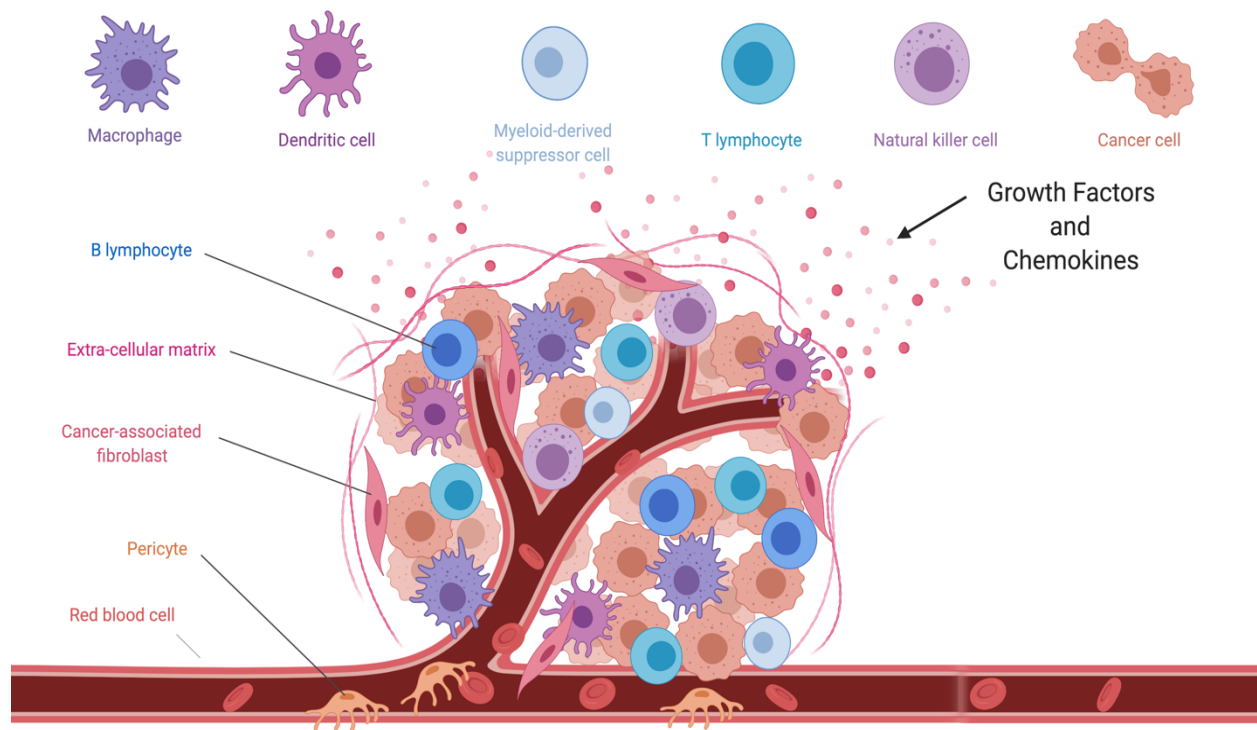


Figure 1.4 The tumor microenvironment is a complex structure with vibrant cellular interactions. Cancer cells in the tumor lesions are surrounded by stromal fibroblasts, endothelial cells of blood vasculatures, and different types of immune cells. These multicellular structures are constantly interacting in paracrine and autocrine manners via various secreted growth factors, chemokines, and matrix proteins. Different types of immune cells play distinct roles leading to both metastasis promotion and cancer clearance.

The success and failures of immune checkpoint therapies such as  $\alpha$ PD1,  $\alpha$ PD-L1, and  $\alpha$ -CTLA-4, etc. that are designed to maintain and potentiate immune surveillance, depends on the composition and phenotypes TIME (Binnewies et al., 2018). Solid tumors are classified as ‘cold tumors’ or ‘non-inflamed’ tumors when the TIMEs are less infiltrated with T lymphocytes (Trujillo et al., 2018). There is a major gap in our understanding of the cellular intrinsic signaling events that are necessary to maintain such T lymphocyte’s exclusion within tumor microenvironments. Additionally, the development of therapeutic interventions to change the composition of TIME by converting them more inflamed with T lymphocytes is also very desirable.

## **CHAPTER 2. FIBROBLAST GROWTH FACTOR RECEPTOR FACILITATES RECURRENCE OF MINIMAL RESIDUAL DISEASE FOLLOWING TRASTUZUMAB EMTANSINE THERAPY**

### **2.1 Disclaimer**

The material in this chapter has been submitted for publications as a manuscript.

### **2.2 Introduction**

Human epidermal growth factor receptor 2 (HER2) is a member of the ErbB family of receptor tyrosine kinases. HER2-amplified breast cancers respond to treatment with the HER2-targeted monoclonal antibodies pertuzumab and trastuzumab at a high rate but acquired resistance to these therapies remains a major clinical problem for patients with this breast cancer subtype. Trastuzumab-emtansine (T-DM1) is an antibody-drug conjugate (ADC) that provides a mechanism to deliver a potent microtubule-targeting cytotoxin to HER2 overexpressing cells. Initial enthusiasm for T-DM1 based on dramatic preclinical results has been diminished by the inability of T-DM1 to improve patient outcomes as compared to the current standard of care therapy, unconjugated trastuzumab in combination with a taxane. These clinical data suggest that uncharacterized drivers of resistance are at play (Barok et al., 2014b). An underlying mechanism of resistance to all ErbB-targeting compounds is the downregulation of ErbB receptors during the processes of invasion and metastasis. Indeed, clinical findings demonstrate discordance in HER2 expression when metastases are compared to the corresponding primary tumor from the same patient (Choong et al., 2007; Niikura et al., 2011).

Epithelial-mesenchymal transition (EMT) is a normal physiological process whereby polarized epithelial cells transition into motile, apolar fibroblastoid-like cells to facilitate several developmental events and to promote wound repair in response to damaged tissues (Wendt et al., 2012). In contrast, initiation of pathological EMT engenders the acquisition of invasive, metastatic and drug resistant phenotypes to developing and progressing carcinomas (Wendt et al., 2010)(Wendt et al., 2011a, 2013a). Physiologic and pathologic EMT can be induced by cytokines such as TGF- $\beta$  and HGF (Kalluri and Weinberg, 2009). More recent findings demonstrate that

EMT can be initiated by treatment with kinase inhibitors and that this transition to a mesenchymal state facilitates tumor cell persistence in the sustained presence of these molecular-targeted compounds (Sharma et al., 2010). In contrast to kinase inhibition, very little is known about the mechanisms by which EMT may facilitate resistance to antibody and ADC therapies.

Induction of EMT increases the expression of fibroblast growth factor receptor 1 (FGFR1) (Warzecha et al., 2010; Wendt et al., 2014a). FGFR1 can also undergo gene amplification and translocation, and elevated expression of FGFR1 is associated with decreased clinical outcomes of breast cancer patients (Madden et al., 2013)(Elbauomy Elsheikh et al., 2007; Turner et al., 2010). Work from our lab and others suggest that upregulation of FGFR and FGF ligands can serve as resistance mechanisms for tumor cells that were originally sensitive to ErbB and endocrine-targeted therapies (Brown et al., 2016b; Hanker et al., 2017; Mao et al., 2019; Raoof et al., 2019; Turner et al., 2010). In addition to enhanced expression of the receptor, our recent studies demonstrate that the processes involved in EMT work en masse to support FGFR signaling through diminution of E-cadherin and enhanced interaction with integrins (Brown et al., 2016c). Several different Type I, ATP-competitive kinase inhibitors against FGFR have been developed, and we and others have demonstrated their *in vivo* efficacy in delaying the growth of metastatic breast cancers (Wendt et al., 2014a)(Dey et al., 2010; Sharpe et al., 2011). Based on the potential of FGFR as a clinical target for cancer therapy we recently developed FIIN4, a highly specific and extremely potent covalent kinase inhibitor of FGFR, capable of *in vivo* tumor inhibition upon oral administration in rodent models (Brown et al., 2016c, 2016b).

In the current study, we address the hypothesis that FGFR can act as a driver of resistance to T-DM1. The use of *in vivo* and *in vitro* models demonstrate that unlike ErbB-targeted kinase inhibitors, EMT cannot overtly elicit resistance to T-DM1. Instead, induction of EMT and upregulation of FGFR1 induce a cell population with reduced trastuzumab binding. This minimal residual disease (MRD) is able to persist in the presence of T-DM1 and eventually reemerge as recurrent tumors that lack HER2 expression. In this recurrent setting, FGFR acts as a major driver of tumor growth, which can be effectively targeted with FIIN4. Overall, our studies strongly suggested that combined therapeutics targeting HER2 and FGFR will delay tumor recurrence and prolong response times of patients with HER2<sup>+</sup> breast cancer.

## **2.3 Methods and materials**

### **2.3.1 Cell cultures and reagents**

Bioluminescent, HER2-transformed HMLE cells (HME2) were constructed as previously described [20]. These cells are cultured in DMEM containing 10% FBS. HME2 and BT474 cells stably overexpressing FGFR1 were also previously described [20]. Trastuzumab and trastuzumab emtansine (T-DM1) were obtained from Genentech Biotechnology Company through the material transfer agreement program. Where indicated HME2 cells were treated with TGF- $\alpha$ 1 (5 ng/ml) every three days for a period of 4 weeks to induce EMT. These EMT-induced HME2 cells were further treated with T-DM1 (250 ng/ml) every three days until resistant colonies emerged, these cells were pooled and cultured as the TDM1R population. Cells were validated for lack of mycoplasma contamination using the IDEXX Impact III testing on July 24th, 2018.

### **2.3.2 Xenograft studies and drug treatments**

HME2 cells ( $2 \times 10^6$ ) expressing firefly luciferase were injected into the duct of the 4th mammary fat pad of female NRG mice. When tumors reached a size of 200 mm<sup>3</sup>, mice were treated with the indicated concentrations of T-DM1 via tail vein injection. Presence of tumor tissue was visualized by bioluminescence imaging following I.P. administration of luciferin (Gold Bio). Where indicated viable pieces of HME2 tumor tissue were directly transplanted into the exposed fat pad of recipient NRG mice. Similarly, pieces of human derived HCI-012 PDX (Huntsman Preclinical Research Resource) were engrafted onto the exposed mammary fat pad of female NRG mice. Tumor bearing mice were treated with T-DM1 as indicated followed by FIIN4 (25 mg/kg/q.o.d) resuspended in DMSO and then further diluted in a solution 0.5% carboxymethyl cellulose and 0.25% Tween-80 to a final concentration of 10% DMSO, for administration to animals via oral gavage. Mammary tumor sizes were measured using digital calipers and the following equation was used to approximate tumor volume ( $V = (\text{length}^2) * (\text{width}) * (0.5)$ ). All animal experiments were conducted under IACUC approval from Purdue University.

### **2.3.3 Cell Biological assays**

For ex-vivo 3D culture, viable human PDX tissues were dissected as above but instead of transfer onto recipient animals, pieces were further mechanically dissected and treated with trypsin-EDTA. These cells were shaken several times and incubated at 37°C. Cells were then filtered through a 50 µm filter and plated onto a 50 µl bed of growth factor reduced cultrex (Trevigen) in a white walled 96 well plate. These cultures were allowed to grow for 20 days in the presence or absence of the indicated kinase inhibitors (1 µM). Two-dimensional cell growth dose response assays were conducted in white walled 96 well plates. Cells (5000 cell/well) were plated in the presence of the indicated concentrations of T-DM1 or kinase inhibitors and cultured for 96 hours. In both cases cell viability was determined by Cell Titer Glo assay (Promega).

### **2.3.4 Immuno-assays**

For immunoblot assays, lysates were generated using a modified RIPA buffer containing 50mM Tris pH 7.4, 150 mM NaCl, 0.25% Sodium deoxycholate, 0.1% SDS, 1.0% NP-40, containing protease inhibitor cocktail (Sigma), 10 mM Sodium Orthovanadate, 40 mM β-glycerolphosphate, and 20 mM Sodium Fluoride. Following SDS PAGE and transfer, PVDF membranes were probed with antibodies specific for FGFR1 (9740), HER2 (4290; Cell signaling technologies), E-cadherin (610182), N-cadherin (610920), Vimentin (550513; BD biosciences), or β-Tubulin (E7-s; Developmental Studies Hybridoma Bank). For immunocytochemistry, formalin fixed paraffin embedded tissue sections were deparaffinized and stained with antibodies specific for HER2 (4290), FGFR1 (HPA056402; Sigma), Ki67 (550609; BD biosciences) or were processed using the TUNEL Assay Kit (ab206386). Additionally, cells were trypsinized and incubated with antibodies specific for FITC conjugated CD44 (338804) and PerCP conjugated CD24 (311113; Biolegend) or trastuzumab conjugated with Alexafluor 647 according to the manufacturer's instructions (A20181; Thermo Scientific). Following antibody staining these cells were washed and analyzed by flow cytometry.

### **2.3.5 Kinomic analyses**

Lysates from HME2 cell conditions indicated above, were analyzed on tyrosine chip (PTK) and serine-threonine chip (STK) arrays using 15ug (PTK) or 2ug (STK) of input material as per

standard protocol in the UAB Kinome Core as previously described [24,25]. Three replicates of chip-paired samples were used and phosphorylation data was collected over multiple computer controlled kinetic pumping cycles, and exposure times (0,10,20,50,100,200ms) for each of the phosphorylatable substrates. Slopes of exposure values were calculated, log<sub>2</sub> transformed and used for comparison. Raw image analysis was conducted using Evolve2, with comparative analysis done in BioNavigator v6.2 (PamGene, The Netherlands).

### **2.3.6 Statistical analyses**

Data from the Long-HER study were obtained from GSE44272. Expression values of FGFR1-4 were obtained from Affymetrix probes, 11747417\_x\_at, 11740159\_x\_at, 11717969\_a\_at, 11762799\_a\_at, respectively. Expression values were normalized to the average probe value for the entire group and differences between the long term responders (Long-HER) and control (Poor response) groups were compared via an 2-sided, unpaired T-test. 2-way ANOVA or 2-sided T-tests were used where the data met the assumptions of these tests and the variance was similar between the two groups being compared. No exclusion criteria were utilized in these studies. A Log-rank test was performed to calculate statistically significant differences in disease-free survival of HME2-GFP and HME2-FGFR1 tumor-bearing mice. P values for all experiments are indicated, values of less than 0.05 were considered significant.

## **2.4 Results**

### **2.4.1 HER2 is diminished following recurrence of T-DM1 resistant minimal residual disease**

Human mammary epithelial (HMLE) cells can be transformed by overexpression of wild type HER2 (Brown et al., 2016b; Mani et al., 2008). Additionally, HER2 overexpression allows for these cells to be cultured outside of the defined growth factor rich mammary gland media required for HMLE culture. In addition to antibiotic selection, this change from a defined media to FBS-containing media prevents the growth of non-HER2 expressing cells, driving a uniform HER2<sup>+</sup> culture that is highly sensitive to inhibition of HER2 (Brown et al., 2016b). Engraftment of these HER2-transformed HMLE cells (HME2) onto the mammary fat pad results in robust formation of highly differentiated, nonmetastatic, secretory tumors that demonstrate robust HER2<sup>+</sup>

expression consistent with that of HER2<sup>+</sup> patient tumors (Shinde et al., 2019). Here, we engrafted the HME2 cells onto the mammary fat pad and upon formation of orthotopic tumors mice received four intravenous injections of T-DM1 administered once a week for four weeks (Figure 2.1A,2.1B). This treatment protocol led to robust regression of these tumors to a point which they were no longer palpable and therefore immeasurable by digital calipers (Figure 2.1A). However, these HME2 cells were constructed to stably express firefly luciferase and MRD was still detectable via bioluminescent imaging (Fig. 2.1B). Cessation of T-DM1 treatment led to recurrence of mammary fat pad tumors in 3 of 5 mice over approximately a 150-day period (Figure 2.1A). Importantly, these recurrent tumors were nonresponsive to additional rounds of T-DM1 (Figure 2.1A). Histological assessment of the recurrent tumors clearly demonstrated reduced levels of HER2 as compared to the untreated HME2 tumors (Figure 2.1C). Overall these data demonstrate that even cells specifically transformed by HER2 overexpression are capable of establishing drug persistent MRD in response to T-DM1 and recurring in a HER2-independent manner.

#### **2.4.2 In vitro establishment of T-DM1 resistant cells requires prior induction of epithelial-mesenchymal transition**

Attempts to subculture the T-DM1 recurrent HME2 tumors were unsuccessful, suggesting that these cells had evolved mechanisms of tumor growth that were not present under *in vitro* culture conditions. Therefore, we sought to establish a T-DM1 resistant cell line via prolonged *in vitro* ADC treatment. However, progressive treatment of HME2 cells with T-DM1 over extended periods of time failed to yield a spontaneously resistant population (Figure 2.2A). We recently demonstrated that induction of EMT in the HME2 model is sufficient to facilitate immediate resistance to the ErbB kinase inhibitors, lapatinib and afatinib (Brown et al., 2016b). In contrast, induction of EMT via pretreatment with TGF- $\beta$ 1 did not induce immediate resistance to T-DM1 (Figure 2.2A; 2 weeks). Consistent with the inhibition of microtubules being the mechanism of emtansine, treatment of parental and TGF- $\beta$ 1 pretreated HME2 cells with T-DM1 prevented cell division leading to the formation of non-dividing groups of cells and large senescent cells (Figure 2.2A, 2.2B). Importantly, only those cells that had undergone EMT via pretreatment with TGF- $\beta$  were capable of giving rise to extremely mesenchymal daughter cells that were capable of replicating in the continued presence of T-DM1 (Figure 2.2A, 2.2B). This *in vitro*-derived T-DM1 resistant (TDM1R) cell population continued to thrive in culture and maintained their

mesenchymal phenotype and resistance to T-DM1 even after several passages in the absence of the drug (Figure 2.2C). To gain insight into the mechanisms by which induction of EMT facilitates acquisition of resistance to T-DM1 we fluorescently labeled trastuzumab and utilized flow cytometry to quantify changes in drug binding. Consistent with their complete eradication upon T-DM1 treatment, the HME2 parental cells presented as a single population of trastuzumab<sup>+</sup> cells (Figure 2.2A, 2.2D). In contrast, induction of EMT with TGF- $\beta$  clearly produced a distinct population of cells that were resistant to trastuzumab binding, giving rise to a more uniform reduction in trastuzumab binding in the TDM1R cell population (Figure 2.2D). These findings suggest that prior induction of cytokine-mediated EMT contributes to diminished trastuzumab binding and is required for acquisition of resistance to T-DM1.

### **2.4.3 FGFR1 is sufficient to reduce T-DM1 binding and efficacy**

Our previous studies establish that following TGF- $\beta$ 1 treatment, the purely mesenchymal HME2 culture will asynchronously recover producing a heterogenous population of both epithelial and mesenchymal cells (Brown et al., 2016b). These morphologically distinct populations can also be readily visualized via flow cytometric analyses for CD44 and CD24 (Figure 2.3A and 2.3B). Consistent with the stable mesenchymal morphology of the TDM1R cells they presented as a single population with high levels of CD44, but lacked the diminished expression of CD24 characteristic of TGF- $\beta$ -induced EMT (Figure 2.3A and 2.3B)(Mani et al., 2008). Other markers of EMT were enhanced upon acquisition of T-DM1 resistance, including loss of E-cadherin and potentiated gains in N-cadherin and vimentin (Figure 2.3C). Consistent with the diminished trastuzumab binding observed in figure 2, we also observed HER2 expression to be decreased in whole cell lysates from TDM1R cells (Fig. 2.3C). To elucidate a mechanistic characterization of potential mediators of T-DM1 resistance we compared the TDM1R cells to their T-DM1 sensitive, post-TGF $\beta$  HME2, counterparts using kinomic profiling on the PamStation-12 platform. Lysates from TDM1R cells had an increased ability to phosphorylate peptides from FKBP12-rapamycin associated protein (FRAP), a result consistent with enhanced PI3 kinase-mTOR signaling. This finding is supported by the Long-HER study, which compared global gene expression of HER2<sup>+</sup> patients that experienced a long-term response to trastuzumab with those whose disease progressed within the first year of initiating trastuzumab (Gámez-Pozo et al., 2014).

Looking upstream to receptors potentially responsible for these events, we observed the autophosphorylation sites of several other ErbB receptors, VEGFRs and FGFR to be increased in the TDM1R lysates. Upon further investigation into the potential of these receptors in facilitating resistance to T-DM1 we found that the expression level of FGFR1 induced by TGF- $\beta$  was further enhanced upon acquisition of T-DM1 resistance (Figure 2.3C). Directed analysis of the Long-HER dataset indicated that enhanced expression of FGFR1 and FGFR2 are significantly associated with a poor clinical response to trastuzumab (Figure 2.3D). To elucidate if FGFR1 is sufficient to provide resistance to T-DM1 we constructed HME2 cells to specifically overexpress FGFR1 in the absence of other EMT-associated factors (Figure 2.3C; (Brown et al., 2016b)). Using this approach we found that overexpression of FGFR1, when in the presence of exogenous ligand, was sufficient to significantly reduce the dose response to T-DM1 (Figure 2.3E). Unlike the TDM1R cell line, we did not detect an appreciable decrease in HER2 expression upon directed overexpression of FGFR1 (Figure 2.3C). However, FGFR1 overexpression, in the absence of other EMT-associated events, was sufficient to cause a significant reduction in trastuzumab binding as determined by flow cytometry (Figure 2.3F).

#### **2.4.4 FGFR1 increases tumor recurrence following T-DM1-induced minimal residual disease**

We next sought to evaluate the impact of FGFR1 expression on HME2 tumor growth and response to T-DM1. Overexpression of FGFR1 promoted a significant increase in growth rate of HME2 tumors upon mammary fat pad engraftment, leading to differential TDM1 treatment initiation times for matched tumor sizes (Figure 2.4A). Irrespective of FGFR1 expression, the liquid filled masses characteristic of large HME2 tumors quickly became necrotic after a single dose of TDM1 (Figure 2.4B). However, following this initial rapid reduction in tumor size, only the FGFR1 overexpressing tumors maintained a more solid mass which required two additional rounds of T-DM1 treatment to achieve complete tumor regression (Figure 2.4B). As we observed in Figure 2.1 the MRD associated with these nonpalpable lesions could still be detected by bioluminescence (Figure 2.4B). Following achievement of T-DM1-induced MRD, none of the control tumors progressed within the 40 day post-treatment observation period (Figure 2.4C). In contrast, over 50% of the FGFR1 overexpressing tumors underwent disease progression during this same post-treatment time frame (Figure 2.4C). In contrast to the marked loss of HER2

expression in the spontaneously resistant HME2 lesions noted in figure 2.1, the FGFR1 overexpressing recurrent tumors were capable of maintaining heterogeneous HER2 expression (Figure 2.4C). Taken together, these data strongly suggest that enhanced expression of FGFR1 inhibits T-DM1 binding, facilitating therapeutic persistence of HER2<sup>+</sup> cells and post-treatment tumor recurrence.

#### **2.4.5 T-DM1 resistant cells are sensitive to covalent inhibition of FGFR**

Given the changes in ErbB kinase signaling observed in the TDM1R cells and the ability of FGFR overexpression to facilitate recurrence following ADC therapy we next sought to evaluate the ability of specific kinase inhibitors to target TDM1R cells as compared to their T-DM1 sensitive counterparts. Lapatinib is a clinically used kinase inhibitor that targets both EGFR and HER2, and we recently developed FIIN4, a covalent kinase inhibitor that targets FGFR1-4 (Brown et al., 2016c). Treatment of the HME2 parental cells with lapatinib led a robust inhibition of HER2 phosphorylation and downstream blockade of ERK1/2 phosphorylation (Figure 2.5A). Consistent with the reduced expression of total HER2, phosphorylated levels of HER2 were undetectable in the TDM1R cells and ERK1/2 phosphorylation was minimally inhibited by lapatinib (Figure 2.5A). In contrast, treatment of the HME2 parental cells with FIIN4 had no effect on HER2 or ERK1/2 phosphorylation, but FIIN4 markedly diminished ERK1/2 phosphorylation in the TDM1R cells (Figure 2.5A). Importantly, TDM1R cells also demonstrated robust resistance to lapatinib, even though they had never been exposed to this compound previously (Figure 2.5B). Similarly, TDM1R cells were also resistant to afatinib, a more potent second-generation covalent kinase inhibitor capable of targeting EGFR, HER2, and ErbB4 (Figure 2.5C;(Hirsh, 2015)). In contrast, HME2 cells that had previously been selected for resistance to lapatinib (LAPR) maintained expression of HER2 and were similarly sensitive to T-DM1 as compared to the HME2 parental cells (Figure 2.5D;(Brown et al., 2016b)). Finally, TDM1R cells were significantly more sensitive to FIIN4 as compared to the HME2 parental cells (Figure 2.5E). Taken together these data indicate that resistance to HER2-targeted ADC therapy predicates acquisition of resistance to ErbB-targeted kinase inhibitors but the reverse is not true. Importantly, these drug resistant populations become increasingly sensitive to covalent inhibition of FGFR.

#### 2.4.6 T-DM1 resistant tumors respond to systemic inhibition of FGFR

We next sought to validate our *in vitro* findings by evaluating the efficacy of FGFR inhibition in the treatment of tumors that had acquired *in vivo* resistance to T-DM1. To do this we treated HME2 tumor bearing mice with T-DM1 and prior to complete MRD, sections of the tumors were directly passaged onto additional mice. This process was repeated twice until we obtained a cohort of mice with growing tumors that did not respond to T-DM1 (Figure 2.6A). Similar to what was observed in tumors that were recovered following induction of MRD and in our *in vitro* TDM1R cells, these serially passaged *in vivo*-derived T-DM1 resistant tumors also demonstrated a diminution in HER2 expression and modulated markers of EMT, including enhanced FGFR1, as compared to untreated HME2 tumors (Figure 2.6A). Importantly, treatment with FIIN4 was capable of significantly inhibiting the growth of these T-DM1-resistant tumors (Figure 2.6B-2.6D). This inhibition of tumor growth was consistent with induction of apoptosis and decreased proliferation as visualized by TUNEL and Ki67 staining in tumors from FIIN4 treated mice as compared to untreated controls (Figure 2.6E).

Next, we utilized a patient-derived xenograft (PDX) that was isolated from a pleural effusion of a patient originally diagnosed with a HER2<sup>+</sup> primary tumor (Figure 2.7A). This patient's disease progressed while on trastuzumab therapy (Figure 2.7A). Consistent with this clinical failure of trastuzumab, these PDX tumors displayed non-plasma membrane staining for HER2 and mice bearing these PDX tumors failed to respond to T-DM1 treatment (Figure 2.7B, 2.7C). These PDX tumors also demonstrated readily detectable staining for FGFR1 (Figure 2.7C). Clinically, lapatinib is indicated as a second line therapy in HER2<sup>+</sup> patients that do not respond to trastuzumab. Treatment with lapatinib did blunt the 3D invasive phenotype of the HCI-012 PDX when cultured under 3D *ex-vivo* conditions. However, consistent with our data from figure 5, the overall growth of these T-DM1-resistant PDX *ex-vivo* cultures was not inhibited by lapatinib treatment (Figure 2.7D). In contrast, treatment of these *ex-vivo* cultures or tumor bearing mice with FIIN4, the covalent FGFR inhibitor, led to significant inhibition of tumor growth (Figure 2.7B, 2.7D). Consistent with our previous studies, FIIN4 also demonstrated enhanced potency as compared to an identical concentration of its ATP competitive structural analogue, BGJ-398 (Figure 2.7D). Taken together these data indicate that T-DM1 resistant tumors can be effectively targeted via covalent inhibition of FGFR kinase activity.

## 2.5 Figures

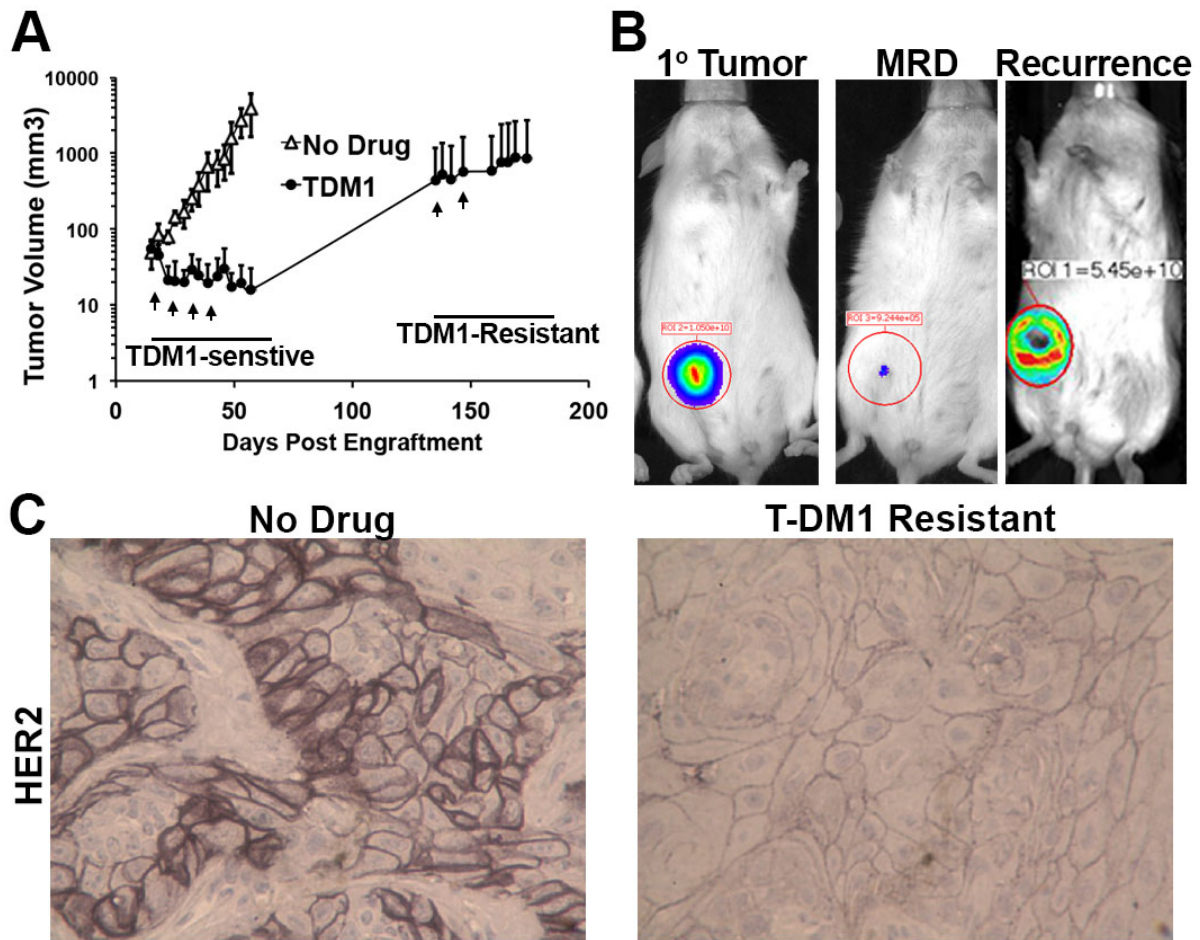


Figure 2.1 HER2 is diminished following recurrence of T-DM1 resistant minimal residual disease. A Mice were inoculated with HME2 cells ( $2 \times 10^6$  cells/mouse) via the mammary fat pad and tumors were allowed to form for a period of 14 days. At this point mice were split into two cohorts (5 mice/group) and left untreated (no drug) or were treated with T-DM1 (9 mg/kg) at the indicated time points (arrows). Following complete regression of palpable tumors T-DM1 treatment was stopped. Recurrent tumors (3 mice) were again treated with T-DM1 (arrows). B Representative bioluminescent images of tumor bearing mice before T-DM1 treatment (1° tumor), following T-DM1 treatment (MRD), and upon tumor recurrence. C Immunohistochemistry for HER2 expression in control and recurrent, T-DM1 resistant HME2 tumors.

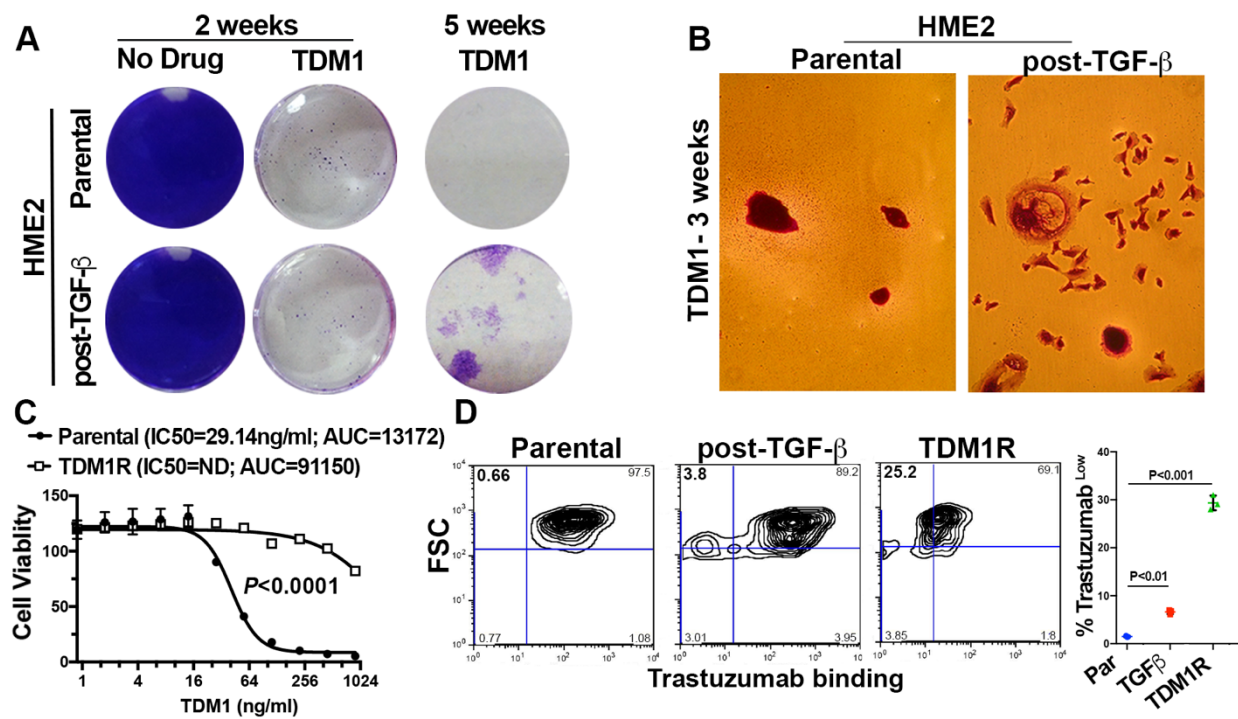


Figure 2.2 *In vitro* establishment of T-DM1 resistant cells requires prior induction of epithelial-mesenchymal transition. A HME2 cells were left untreated (parental) or were stimulated with TGF- $\beta$ 1 and allowed to recover (Post-TGF- $\beta$ ) as described in the materials and methods. These two cell populations were subsequently treated with T-DM1 (250 ng/ml) every three days for a period of 5 weeks. Representative wells were stained with crystal violet at the indicated time points to visualize viable cells. B Brightfield microscopy of crystal violet stained HME2 parental and post-TGF- $\beta$  cells following 3 weeks of continuous T-DM1 treatment. C The T-DM1 resistant (TDM1R) cells that survived 5 weeks of treatment were further expanded and cultured for a period of 4 weeks in the absence of T-DM1. These cells along with passage-matched parental HME2 cells were subjected 96 hour treatments with the indicated concentrations of T-DM1 and assayed for cell viability. Data are the mean  $\pm$ SE of three independent experiments resulting in the indicated P value. D Parental, post-TGF- $\beta$ , and TDM1R HME2 cells were stained with Alexafluor 647-labeled trastuzumab and antibody binding was quantified by flow cytometry. The percentage of cells in each quadrant with reference to forward scatter (FSC) is indicated. Also shown is the mean,  $\pm$ SD, percentages of low trastuzumab binding (Trastuzumab<sup>Low</sup>) cells of three independent experiments resulting in the indicated P values.

Figure 2.3 FGFR1 is sufficient to reduce T-DM1 efficacy. A Brightfield microscopy of HME2 parental, post-TGF- $\beta$ , and T-DM1 resistant (TDM1R) cells. B The cells described in panel A were analyzed by flow cytometry for cell surface expression of CD24 and CD44. The percentage of cells in each quadrant is indicated. C Whole cell lysates from HME2 parental, Post-TGF- $\beta$ , T-DM1 resistant (TDM1R), and HME2 cells constructed to stably express FGFR1 or GFP as a control were analyzed by immunoblot for expression of FGFR1, HER2, E-cadherin (Ecad), N-cadherin (Ncad), vimentin, and  $\beta$ -tubulin ( $\beta$ -Tub) served as a loading control. Data in panels B and C are representative of at least three separate analyses. D Expression values for FGFR1-4 were analyzed in the Long-HER data set. Data are the relative expression of individual patients that demonstrated long-term (Long-HER) or short-term (Poor-response) response to trastuzumab treatment, resulting in the indicated *P* values. E HME2 cells expressing FGFR1 or GFP as a control were treated with the indicated concentrations of T-DM1 for 96 hours at which point cell viability was quantified. Data are normalized to the untreated control cells and are the mean  $\pm$ SE of three independent experiments resulting in the indicated *P* value. F HME2 cells expressing FGFR1 or GFP as a control were incubated with Alexafluor 647-labeled trastuzumab and antibody binding was quantified by flow cytometry. Data are the mean fluorescence intensities, normalized to total HER2 levels as determined by immunoblot,  $\pm$ SD for three independent experiments resulting in the indicated *P* value.

Figure 2.3 continued

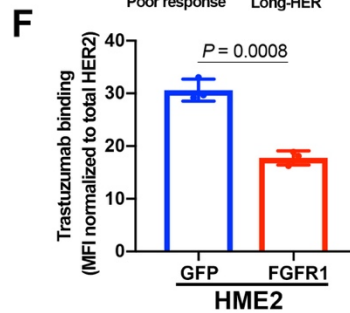
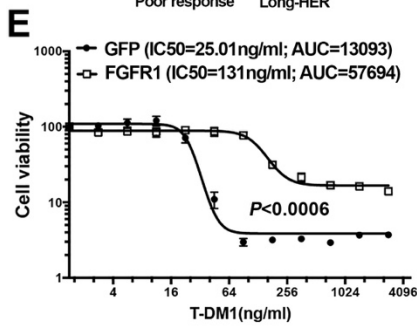
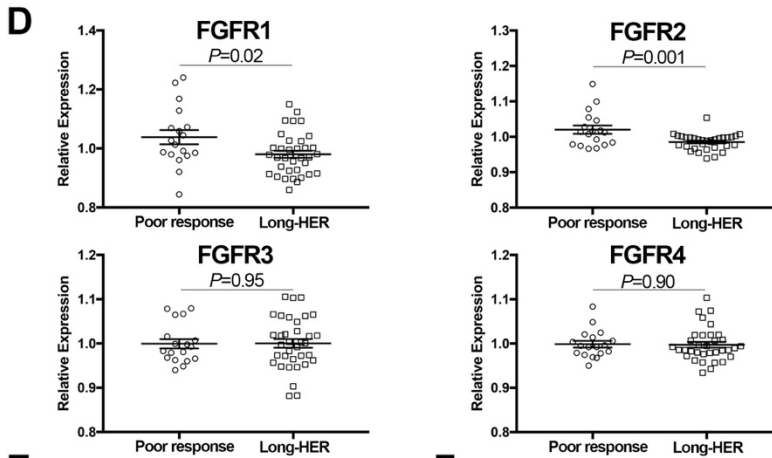
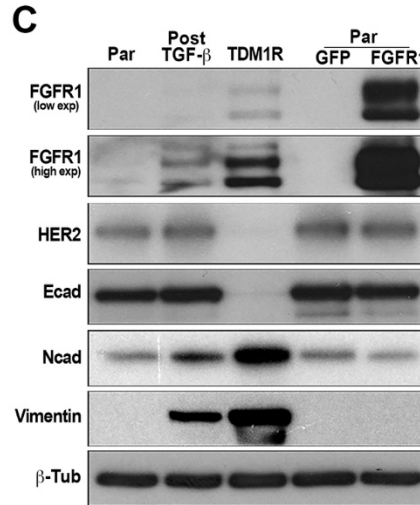
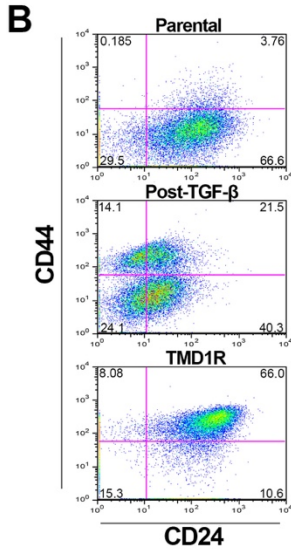
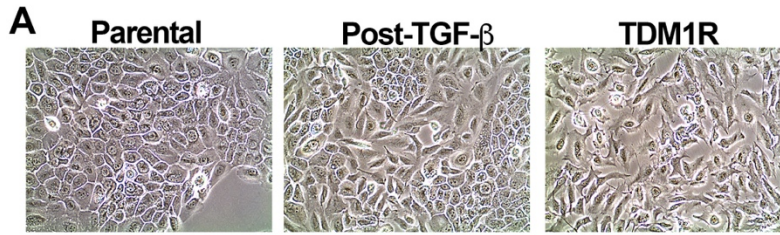


Figure 2.4 FGFR1 increases tumor recurrence following T-DM1-induced minimal residual disease. A Time line demarking the primary tumor growth period for HME2 cells constructed to express FGFR1 or GFP as a control. Cells were engrafted onto the mammary fat pad of female NRG mice ( $2 \times 10^6$  cells/mouse;  $n=5$  mice per group). Tumor growth was monitored via digital caliper measurements at the indicated time points. T-DM1 treatment was initiated in each group when tumors reached an average of  $1000 \text{ mm}^3$ , horizontal line. Representative bioluminescent images for each group are shown at the indicated time points. Days are in reference to tumor engraftment (Day 0). B Time line demarking the T-DM1 treatment periods for each group. T-DM1 was administered via I.V. injections ( $9 \text{ mg/kg}$ ) at day 0 for HME2-GFP tumors and days 0, 7 and 14 for HME2-FGFR1 tumors (arrows). Tumor regression was monitored via digital caliper measurements at the indicated time points. Representative bioluminescent images for each group are shown at the indicated time points. Days are in reference to initiation of T-DM1 treatment (Day 0) for each group. C Time line demarking the post-treatment observation period for each group. Once tumors regressed to a non-palpable state of minimal residual disease (MRD) mice were left untreated and monitored for tumor recurrence via digital caliper measurements. Representative bioluminescent images for each group are shown at the indicated time points. Days are in reference to achievement of MRD (Day 0) for each group. A representative HER2 IHC is shown for the recurrent tumors. Survival data in panel C were analyzed via a log rank test where tumor recurrence of  $>50 \text{ mm}^3$  was set as a criteria for disease progression. Data in panel A are the mean  $\pm$ SD of five mice per group resulting in the indicated P value. In panel B tumor size for each mouse is plotted individually. Data in panels A and B were analyzed via a two-way ANOVA.

Figure 2.4 continued

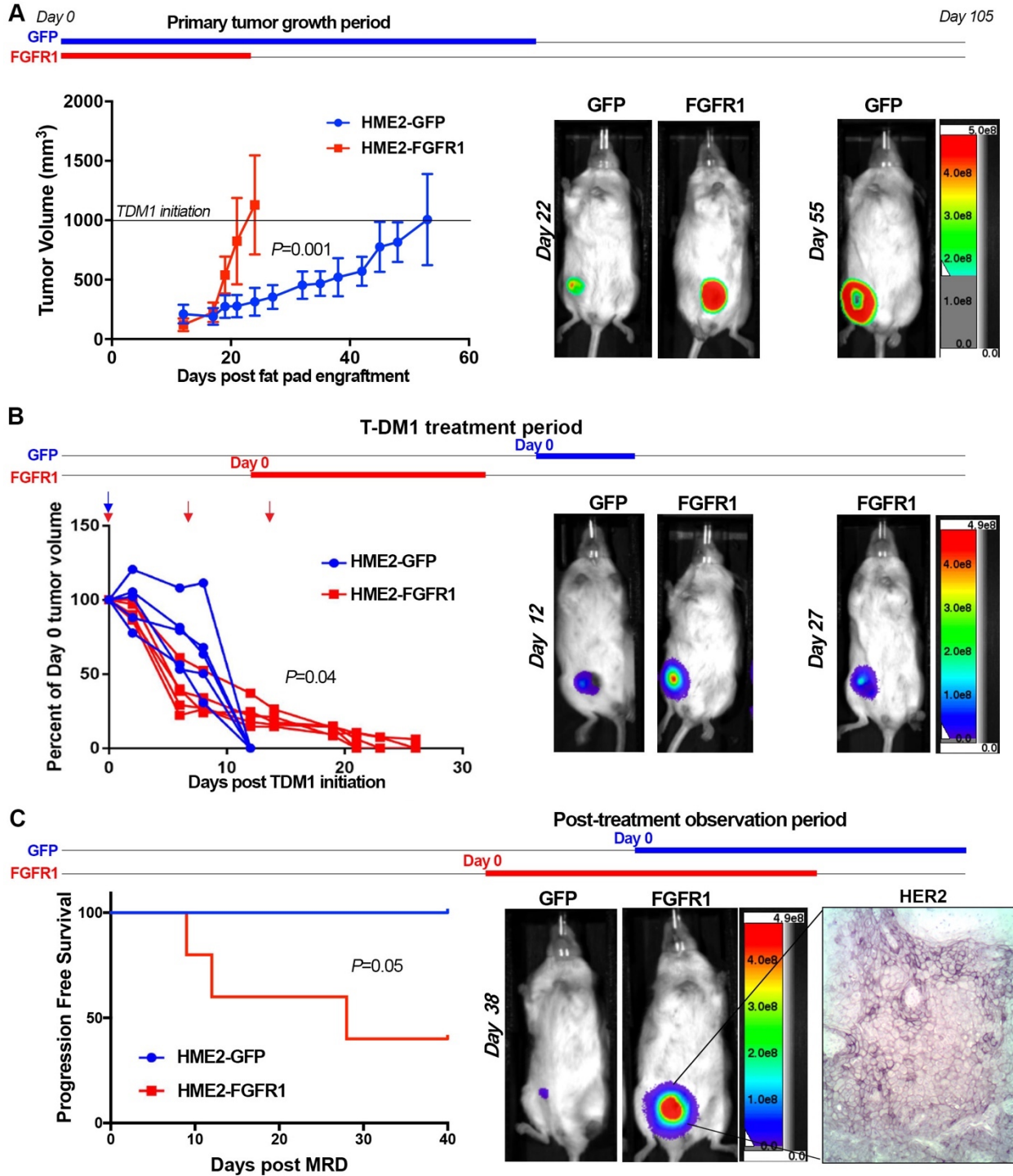
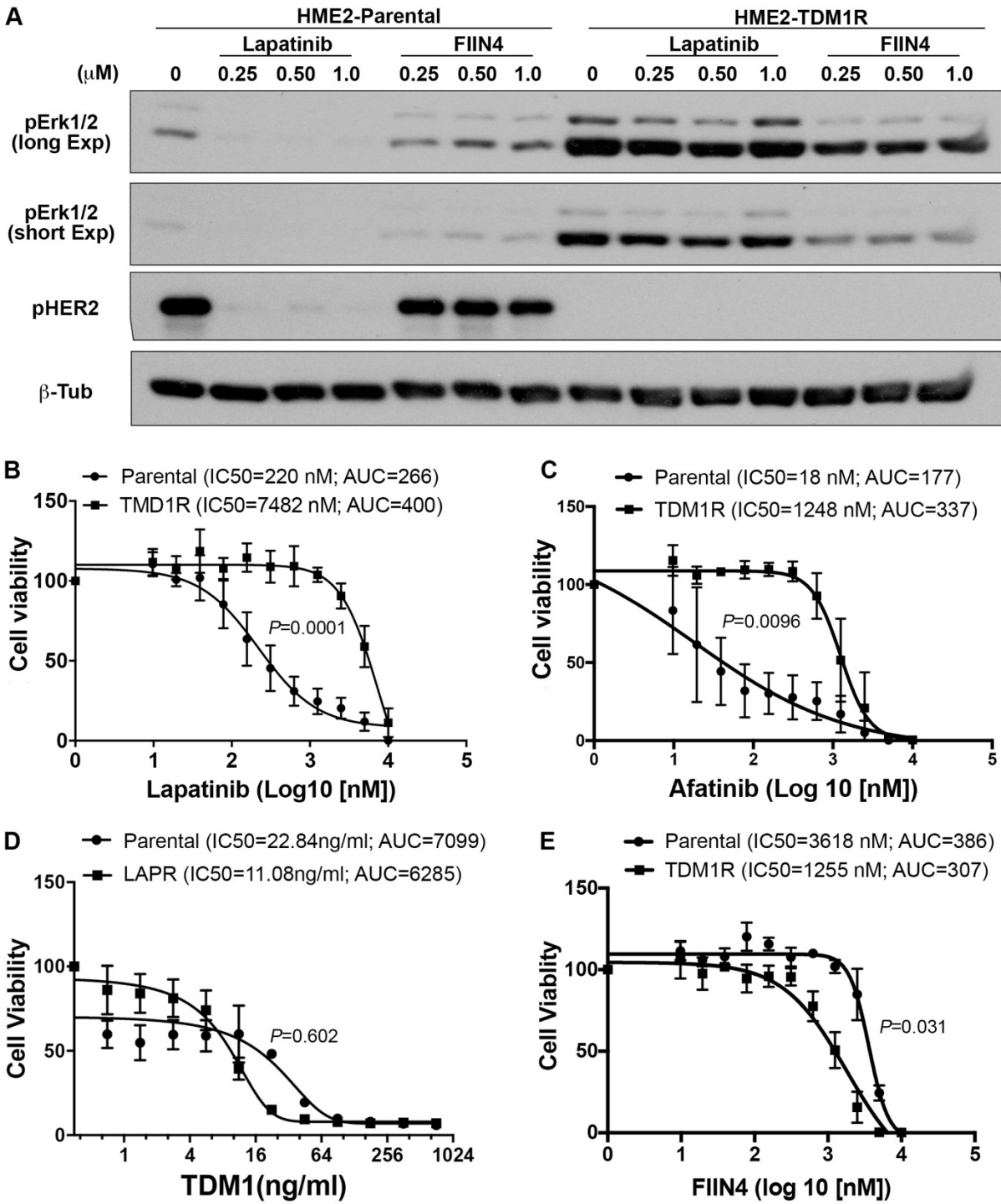


Figure 2.5 T-DM1 resistant cells are sensitive to covalent inhibition of FGFR. A HME2 parental and T-DM1 resistant (TDM1R) cells were treated with the indicated concentrations of lapatinib or FIIN4 for 2 hours. Cell lysates were subsequently assayed by immunoblot for phosphorylation of ERK1/2 and HER2,  $\beta$ -tubulin ( $\beta$ -Tub) served as a loading control. Data in panel A are representative of at least two independent experiments. B HME2 parental cells (parental) and TDM1R cells were plated in the presence of the indicated concentrations of lapatinib for 96 hours at which point cell viability was determined. C HME2 parental and TDM1R cells were plated in the presence of the indicated concentrations of afatinib for 96 hours at which point cell viability was determined. D HME2 parental and lapatinib resistant (LAPR) cells were plated in the presence of the indicated concentrations of T-DM1 for 96 hours at which point cell viability was determined. E HME2 parental and TDM1R cells were plated in the presence of the indicated concentrations of FIIN4 for 96 hours at which point cell viability was determined. Data in panels B-E are the mean  $\pm$ SE of at least three independent experiments resulting in the indicated P values.

Figure 2.5 continued



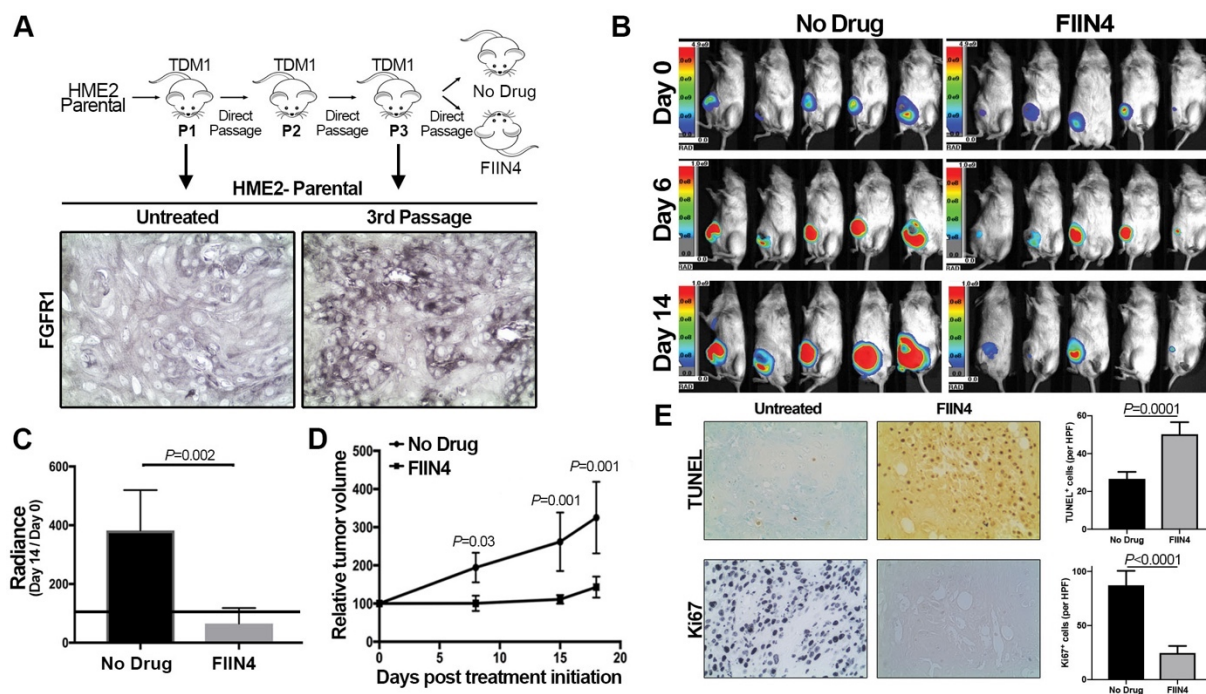


Figure 2.6 T-DM1 resistant tumors respond to systemic inhibition of FGFR. A Schematic representation of the *in vivo* derivation of T-DM1 resistant HME2 tumors. HME2 parental cells ( $2 \times 10^6$ ) were engrafted onto the mammary fat pad of an NSG mouse. This mouse was treated with T-DM1 until tumor regression was observed. Sections of the remaining tumor were directly transferred onto recipient mice. This was repeated twice until transferred tumors that no longer responded to T-DM1 therapy were identified. At this point sections of a T-DM1 resistant tumor were assessed by IHC for FGFR1 expression as compared to the originally engrafted HME2 tumors. Representative FGFR1 IHC staining is shown. B Bioluminescent imaging of mice bearing the T-DM1 resistant tumors described in panel A. These mice were left untreated (No Drug) or were treated with FIIN4 (100 mg/kg/q.o.d.). C Bioluminescent quantification of control and FIIN4-treated animals bearing T-DM1 resistant tumors. Data are normalized to the tumor luminescence values at the initiation of FIIN4 treatment (day 0). D Tumor size as determined by digital caliper measurements at the indicated time points during FIIN4 treatment. For panels C and D data are the mean  $\pm$ SE of five mice per group resulting in the indicated P-values. E Representative Ki67 and TUNEL staining of P3, T-DM1 resistant tumors from untreated and FIIN4 treated groups. Also shown are the mean  $\pm$ SD of TUNEL and Ki67 positive cells per high powered field (HPF), n=5, resulting in the indicated P values.

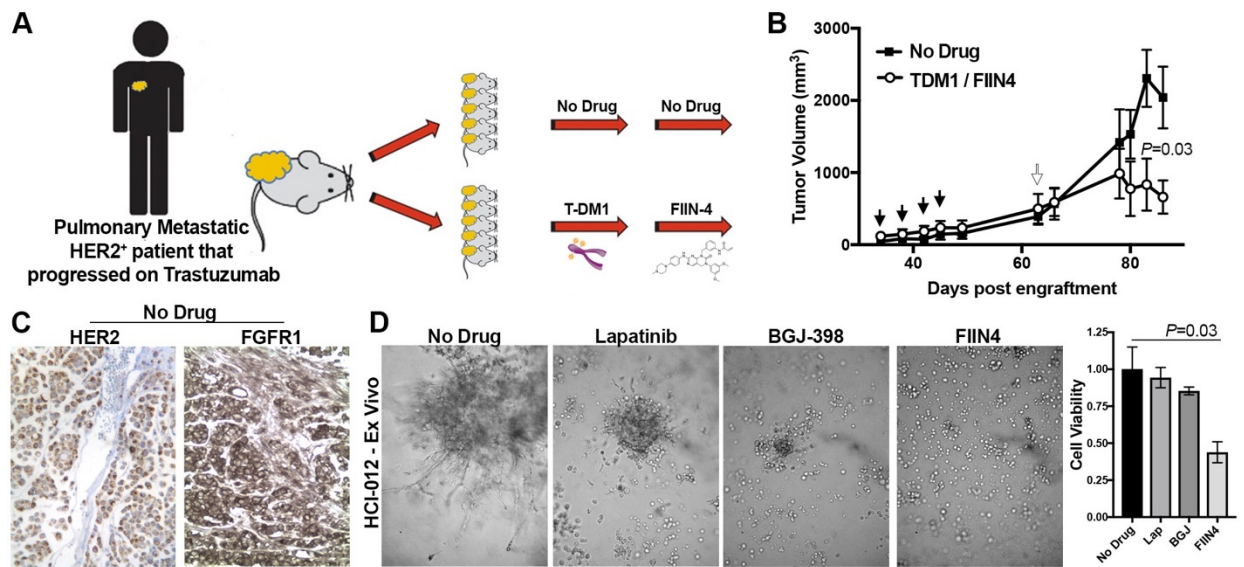


Figure 2.7 Trastuzumab-resistant patient derived xenografts are sensitive to covalent inhibition of FGFR. A Schematic representation of the expansion protocol of HCl-012. Tumor bearing mice were split into two cohorts consisting of an untreated group and a group that was initially treated with T-DM1 (5 mg/kg) and then switched to FIIN4 (25 mg/kg/p.o.d). B PDX tumor bearing mice were treated as described in panel A and tumor size was measured by digital caliper measurements at the indicated time points. Closed arrows indicate T-DM1 treatments, open arrow indicates initiation of FIIN4 treatment. Data are the mean  $\pm$ SE of 5 mice per group resulting in the indicated p-value. C Representative histological sections of untreated HCl-012 tumors stained with antibodies for HER2 and FGFR1. D *Ex-vivo* HCl-012 tumor cells were grown for 20 days under 3D culture conditions in the presence or absence of the indicated compounds. Representative images are shown and cell viability was quantified by cell titer glow. Data are mean  $\pm$ SD of triplicate wells treated with the indicated compounds.

## 2.6 Conclusion

The Her2 subtype of breast cancer (BC) accounts for about 20% of all BC patients (Kümler et al., 2014). This subtype is defined by the overexpression of human epidermal growth factor receptor 2 (Her2) which drives elevated downstream signaling promoting tumorigenesis. Overexpression of Her2 leads to self-dimerization of the surface receptors that can initiate downstream signaling in a ligand independent manner. Trastuzumab-DM1 (T-DM1) is an antibody drug conjugate in which an anti-Her2 antibody targets Her2 overexpressing tumor cells and delivers emtansine, a high potent inhibitor of microtubule formation (Boyraz et al., 2013; Junttila et al., 2011b). Metastatic BC patients who have progressed on Trastuzumab show improved overall survival with T-DM1 treatment. However, there is an unmet medical need in a group of patients where their initial response is followed by disease recurrence due to the development of acquired resistance. Here, we presented data showing FGFR as a potential therapeutic target for such recurrent tumors.

In this study, we established minimal residual disease following T-DM1 treatment of HMLE-Her2 xenografts. Upon removal of the drug, tumors relapsed in a few weeks that were no longer responsive to T-DM1. In addition, immunohistochemistry staining revealed that these T-DM1 drug persistent tumors lost their *Her2* expression. Interestingly, continuous treatment of HMLE-ErbB2 cell line with T-DM1 failed to show any acquired resistance *in vitro*. However, induction of epithelial-mesenchymal transition (EMT) via pretreatment with TGF- $\beta$  facilitated acquisition of drug resistance to T-DM1. Similar to our *in vivo* resistant model, these *in vitro* resistant cells showed diminution in Her2 expression. Flow cytometry analysis suggested that TGF- $\beta$  treatment may promote a heterogeneous expression of Her2 in HMLE-E2 cell line, which helps the selection of a low Her2 expressing TDM1 resistant population. To uncover a targetable tyrosine kinase pathway in the resistant cell line, we performed cell viability assay in the presence various inhibitors. While the resistant cells were not sensitive to the broad spectrum ErbB inhibitors Lapatinib and Afatinib; they showed a dramatic response to a covalent FGFR inhibitor, FIIN-4. Previously, we have reported that FGFR signaling is important in EMT-driven drug persistent cells (Brown et al., 2016d). To complement these inhibitor studies, we have found that ectopic overexpression of FGFR1 in HMLE-ErbB2 and the Her2 amplified BT474 cell line was sufficient to increase survival in the presence of T-DM1. Mechanistically, overexpressed FGFR1

receptors perturbed the trastuzumab binding to ErbB2 receptors (Figure 2). Overexpression of FGFR1 is sufficient to increase tumor growth and drive T-DM1 resistance in *in vivo* mouse xenograft as well. Moreover, we observed rapid recurrence of tumors after clearance of primary tumors with T-DM1 in FGFR1 overexpressing HMLE-ErbB2 cells. In line with these observations, we found that a patient derived xenograft (PDX) from a Her2+ BC patient who had been progressed on trastuzumab, were responsive to FIIN-4 while showing limited response to T-DM1 (Figure 3).

Overall, Our studies present covalent inhibition of FGFR as a potential approach for targeting T-DM1 resistance tumors. We developed FIIN4 as the first-in-class covalent inhibitor of FGFR, and an additional covalent FGFR inhibitor, TAS-120, is currently in phase 2 clinical trials in patients with advanced solid tumors (NCT02052778)(Brown et al., 2016c). These studies and the studies herein demonstrate the enhanced efficacy of covalent kinase inhibition of FGFR as compared to first generation ATP competitive inhibitors. This may be a result of the structural stabilization of the inactivate conformation that results upon covalent engagement of FGFR (Tan et al., 2014). However, erdafitinib, an extremely potent competitive inhibitor of FGFR has recently been FDA approved. Therefore, clinical investigation of sequential and/or direct combinations of FGFR inhibitors with T-DM1 in the HER2<sup>+</sup> setting is possible and clearly warranted.

## **CHAPTER 3. THE SYSTEMICALLY DORMANT PHENOTYPE OF 4T07 BREAST CANCER CELLS IS MEDIATED BY THE IMMUNE SYSTEM**

### **3.1 Disclaimer**

The material in this chapter has been prepared for submission to a journal for publication as a manuscript.

### **3.2 Introduction**

During the stage of minimal residual diseases cancer cells remain dormant within the tumor microenvironment for an extended period of time. The tumor microenvironment consists of tumor cells and tumor-associated stromal and immune cells(Wang et al., 2017). The intricate relationships among different cell types in both primary and metastatic microenvironment greatly influence the outcome of the disease (Binnewies et al., 2018). Predictably, cancer cells maintain unique relationships with surrounding immune cells during the state of dormancy. Indeed, various experimental and clinical studies reported that immune systems play important roles in the maintenance of cancer cells dormancy(Dahlke et al., 2014)(Valente et al., 2012). Previous studies proposed that humoral immune response drives cancer dormancy in a spontaneous model of BCL1 mouse lymphoma. CD8+ T lymphocytes are found to be critical for the maintenance of dormancy in this model (Rabinovsky et al., 2007). Both CD8+ and CD4+ T lymphocytes are found to be important in conserving the dormancy phenotype of a metastatic fibrosarcoma mouse model(Romero et al., 2014a). Additionally, experimental and clinical data showed that memory T lymphocytes play a role in cancer cells dormancy in the bone marrow (Feurerer et al., 2001; Mahnke et al., 2005; Müller et al., 1998). These studies establish that cancer dormancy is the result of an active immune surveillance program. On the other hand, disseminated dormant cells evolved to display immune evasion via overexpression of checkpoint ligands such as B7H1 or B7.1, to inactivate anti-tumor responses that result in the breakage of immune dormancy in a model of dormant acute myeloid leukemia (Saudemont and Quesnel, 2004).

In addition to adaptive immune cells, members of innate immunity also can display direct and indirect influence on cancer dormancy. Natural killer(NK) cells are found to be highly associated with the dormant sarcomas in mice(Wu et al., 2013). Moreover, NK cells are also implicated in metastatic latency (Nair and Malladi, 2019). Myeloid-derived suppressor cells (MDSCs) can also influence the latency period of dormant cancers via affecting the tumor suppressor gene(Pten) and tumor angiogenesis (Di Mitri et al., 2014; Murdoch et al., 2008; Safarzadeh et al., 2018).

In addition to targeting primary tumors and overt metastasis, targeting dormant cancer cells is an exciting therapeutic option(Romero et al., 2014b)(Wang et al., 2019a). Awakening of dormant metastasis due to immunosuppressive treatments or external factors is a potential threat for patients with suspecting immune-mediated latent tumors. As a result, it is essential to expand our understanding of the immune-mediated dormancy in the relevant cancer models. In this chapter, we presented an immune-mediated dormant breast cancer model following surgical removal of the primary tumor. Metastatic recurrence of these disseminated dormant cells with the weakening of the immune systems made this model a valuable tool to study novel therapies.

### **3.3 Methods and materials**

#### **3.3.1 Animal studies**

All the mouse xenograft studies were conducted according to the IACUC approval from Purdue University. Female BALB/c and Nude(Nu/J) mice of 5-6 weeks old were purchased from Jackson Laboratories. The procedures for tumors implantations and treatment administrations for all of the animal experiments are detailed in the respective figures.

#### **3.3.2 Cell Line and reagents**

The 4T07 cells were acquired from the Fred Miller (Wayne State University) lab. DMEM media with 10% FBS and penicillin/streptomycin(Life technologies) supplementations were used to culture and expand these breast cancer cells. The bioluminescent 4T07 cells were developed via stable expression of firefly luciferase gene as described previously(Wendt and Schiemann, 2009; Wendt et al., 2013a).

### **3.3.3 Statistics**

Statistically significant differences were calculated via conducting a log-rank test. Relevant statistical analyses and the p values are described in the respective figures.

## **3.4 Results**

### **3.4.1 4T07 cells are metastatic in immunodeficient mice.**

In our efforts to develop immune-directed approaches to be used in combination with FIIN4, we first sought to better characterize the role of the immune system in regulating the metastatic potential of the 4T07 cells. Therefore, we established orthotopic primary tumors in the mammary fat pad of immunodeficient NU/NU and immunocompetent BALB/c mice (Figure 3.1A). The 4T07 cells formed primary tumors in both groups of mice, however the growth rate was significantly slower in BALB/c mice as compared to NU/NU animals (Figure 3.1A-3.1C). Bioluminescent tracking of metastasis following primary tumor removal demonstrated that 4T07 cells can disseminate and form macroscopic metastases in NU/NU mice but not in BALB/c (Figure 3.1D-3.1E). These data suggest that the previously reported systemically dormant phenotype of the 4T07 cells is dependent on adaptive immune function .

### **3.4.2 Primary tumor exposure prevents systemic tumor growth**

To further explore the immunogenicity of the 4T07 tumor model we conducted primary tumor immunization experiments (Figure 3.2A). Here, control non-luminescent 4T07 cells were engrafted onto the mammary fat pad and these primary tumors were removed 14 days later (Figure 3.2B). Following this primary tumor exposure and a prolonged period of recovery firefly luciferase expressing 4T07 cells were delivered via the tail vein to the primary tumor exposed and age matched primary tumor naïve littermates (Figure 3.2C). Bioluminescent imaging demonstrated pulmonary tumor growth typical of the 4T07 model in the control animals (Figure 3.2C-3.2E). In contrast, animals that were exposed to primary tumors failed to form pulmonary tumors (Fig. 3.2C-3.2E). These findings suggest that orthotopic, 4T07 tumors elicit a systemic immune response capable of preventing cellular outgrowth even if they are delivered directly to an alternate organ system (Aslakson et al., 1991).

### **3.4.3 CD8<sup>+</sup> cells depletion promotes pulmonary outgrowth of systemically dormant 4T07 cells**

Our previous studies strongly indicate that immune function is required for regulation of 4T07 systemic dormancy. To more specifically characterize the role of the adaptive immune system in regulating 4T07 dormancy, orthotopic or pulmonary tumors were grown in BALB/c for 14 days. The resultant tumors were subsequently analyzed for the presence of CD8<sup>+</sup> immune cells present in the tumors versus the spleens of tumor bearing mice (Figure 3.3A-3.3C). These analyses demonstrated that while either route of tumor cell engraftment similarly resulted in a systemic immune response, CD8<sup>+</sup> cells were more restricted from 4T07 pulmonary lesions established via tail vein injection as compared to orthotopic mammary fat pad tumor (Figure 3.3A-3.3C). To establish the role of CD8<sup>+</sup> immune cells in mediating the systemically dormant 4T07 phenotype, these cells were engrafted onto the mammary fat pad of BALB/c mice and allowed to develop and disseminate for a period of four weeks (Figure 3.3D). Following surgical removal of the primary tumor mice were treated with either an  $\alpha$ CD8 depleting antibody or with an isotype control IgG (Figure 3.3D). Bioluminescent imaging clearly indicated that mice depleted for CD8<sup>+</sup> cells demonstrated significantly more frequent incidence of metastasis compared to those that received control IgG (Figure 3.3E, 3.3F). These findings clearly demonstrate that restricted infiltration of CD8<sup>+</sup> immune cells is critical for the metastatic progression of the 4T07 tumor model.

### 3.5 Figures

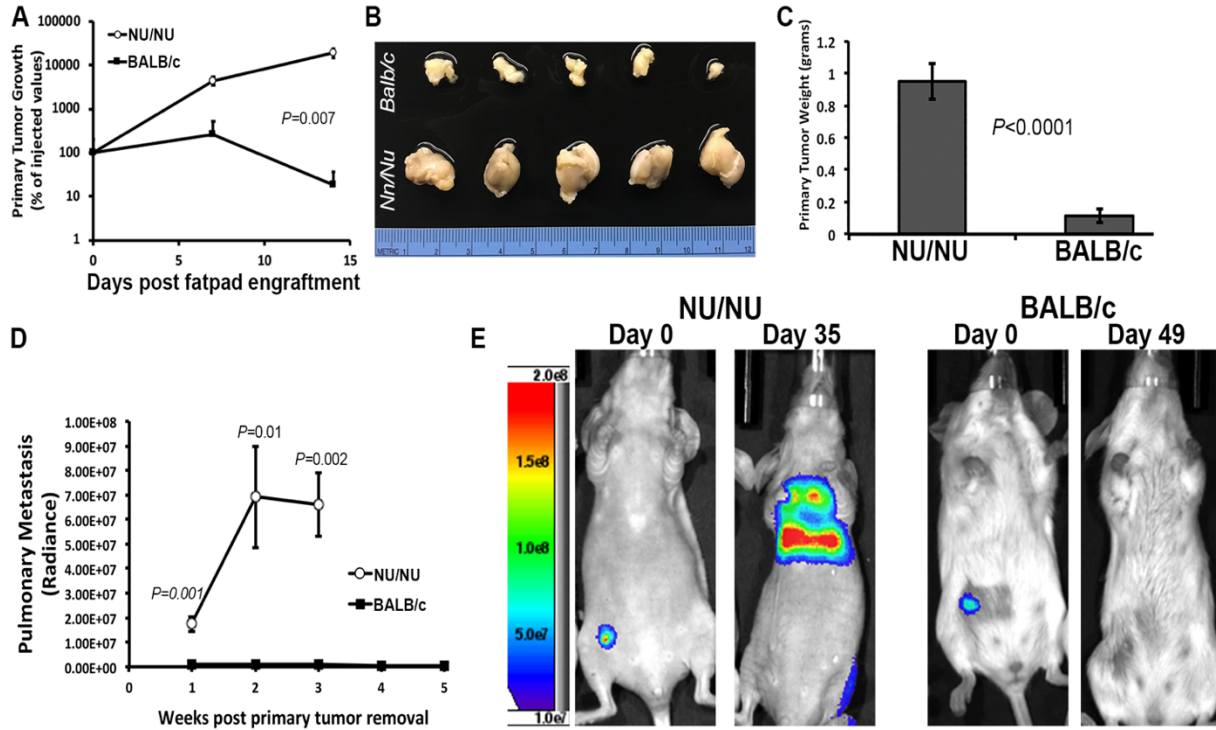


Figure 3.1 4T07 cells are metastatic in immunodeficient mice. (A) Both immunodeficient(NU/NU) and immunocompetent(BALB/c) mice (n=5 mice per group) were engrafted with 4T07 cells ( $1 \times 10^6$ ) via the mammary fat pad. Engraftment and primary tumor growth were monitored by bioluminescence at the indicated time points. (B and C) Fourteen days after engraftment the resulting primary lesions were surgically excised (B) and differences in tumor weight (n=5 mice per group) were analyzed via a paired T-test, resulting in the indicated P value. (D) These mice were subsequently monitored for pulmonary metastasis via bioluminescence imaging. The mean ( $\pm$ SE) bioluminescent values from each group taken at the indicated time points resulting in the indicated p values. (E) Bioluminescent images of representative mice from each group at the indicated timepoints.

Figure 3.2 Primary tumor exposure prevents systemic tumor growth A) Schematic timeline of primary and systemic tumor engraftments. One group of mice (n=5) were engrafted with wild type 4T07 cells on the mammary fat pad. The primary tumors were grown for 14 days, surgically excised and mice were allowed to recover. These mice and primary tumor naïve littermates were subsequently challenged with firefly luciferase expressing 4T07 cells via the lateral tail vein and pulmonary tumor growth was quantified by bioluminescence. All time points are in reference to primary tumor engraftment (D0). (B) Excised wild type 4T07 primary tumors, 14 days after fat pad engraftment. (C) Bioluminescent images of three representative mice from the primary tumor naïve group and the group exposed to primary tumor formation. Images were taken immediately after tail vein injection (D41) to demonstrate equal pulmonary tumor cell challenge and 12 days later (D53). (D) The mean ( $\pm$ SE) bioluminescent values from each group taken at the indicated time points (n=5 mice per group) resulting in the indicated P value. Data are normalized to the challenge values obtained immediately following tail vein injection. (E) Survival analysis of primary tumor naïve mice and those exposed to primary tumor formation following pulmonary tumor challenge (n=5 mice per group).

Figure 3.2 continued

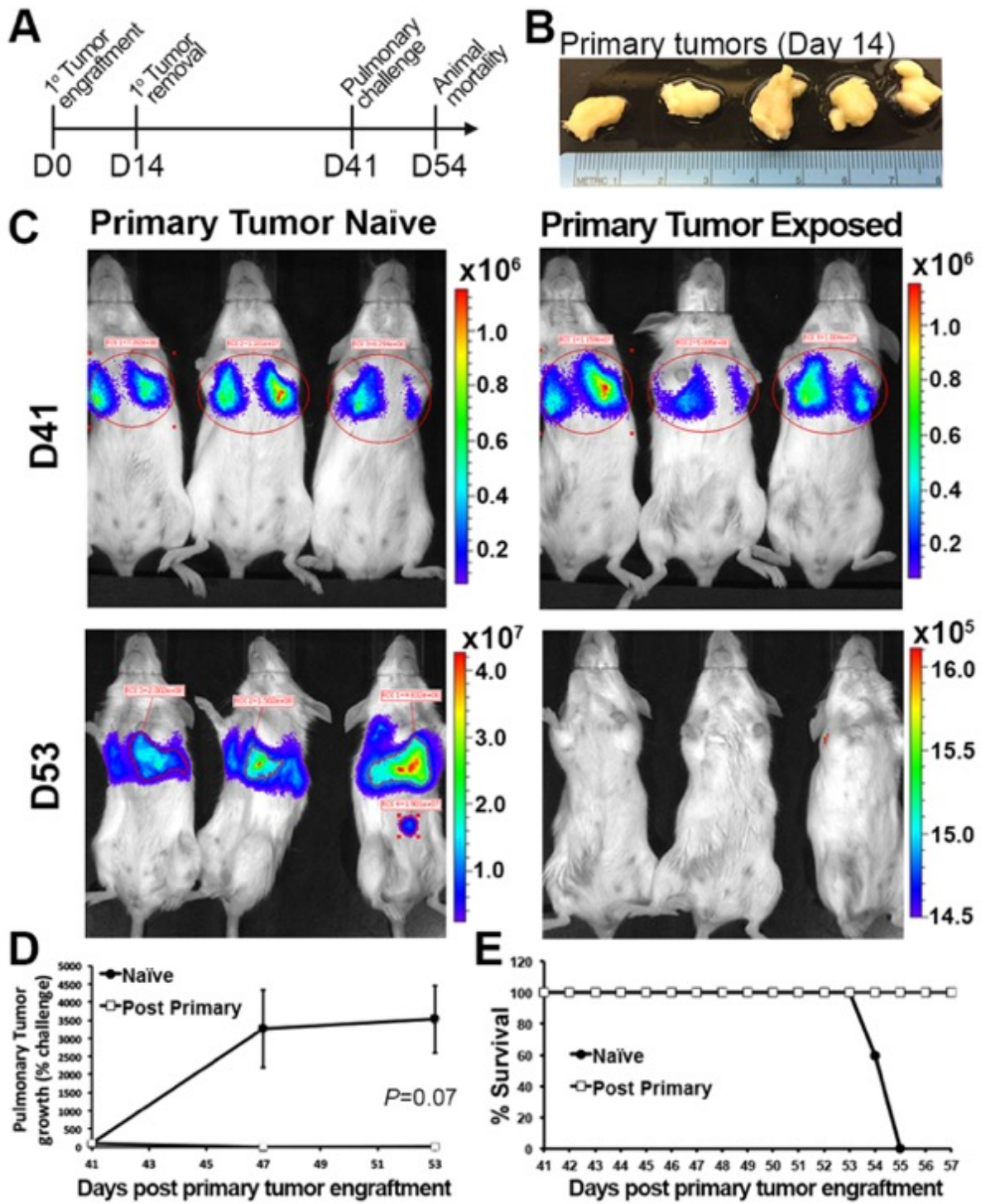
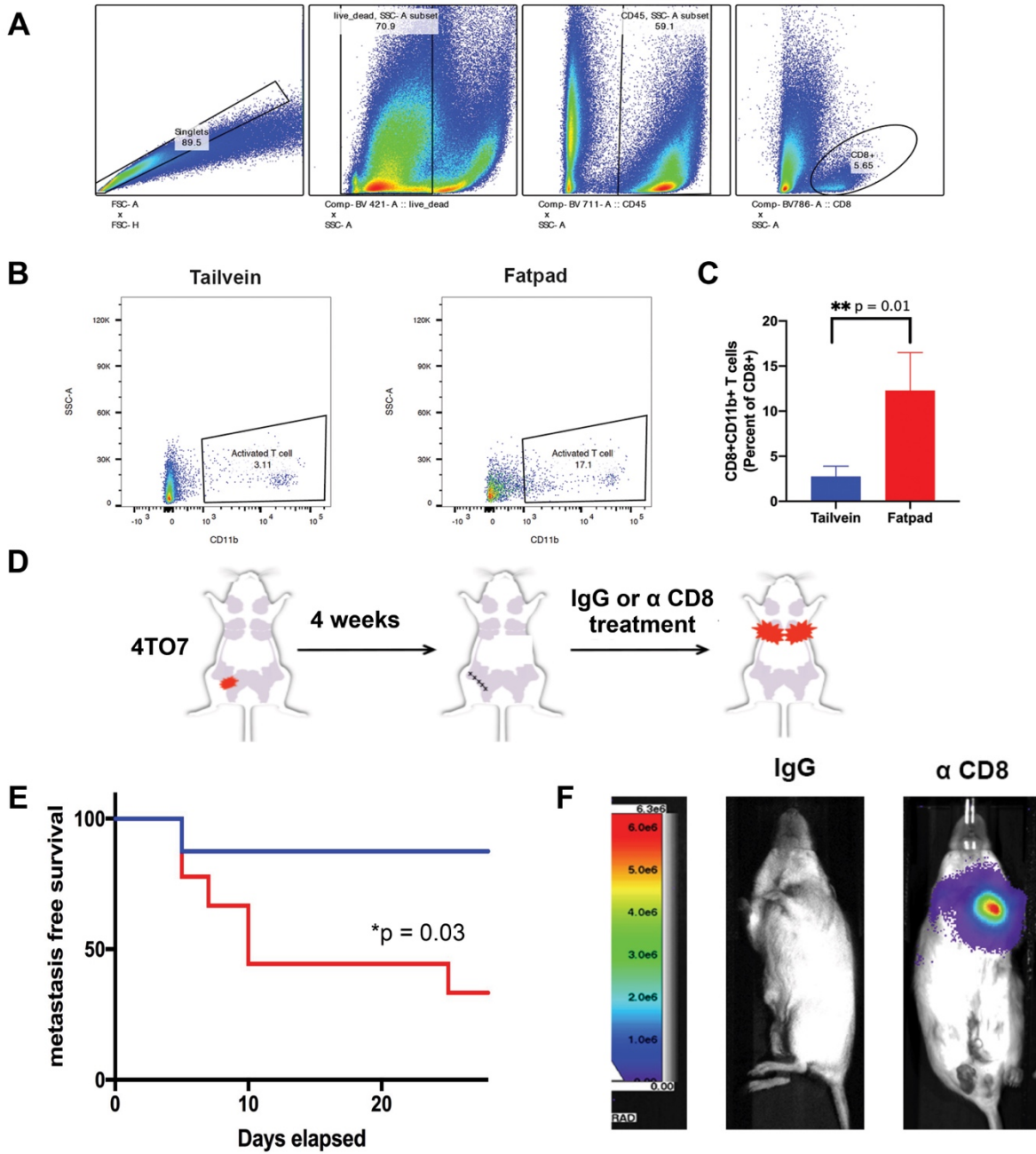


Figure 3.3 Systemically-dormant 4T07 cells can undergo metastatic outgrowth upon depletion of CD8<sup>+</sup> cells. (A-C) Two groups of BALB/c mice were engrafted with 4T07 cells (5x10<sup>5</sup>) either via the fat pad or the tail vein. Mice were sacrificed at Day 14 and tissues were collected for flow cytometric analysis. In panels A and B, dot plots showing ancestry of the gated CD11b<sup>+</sup>CD8<sup>+</sup> cells in the indicated tissues. In panel C, the presence of CD8<sup>+</sup>CD11b<sup>+</sup> cells was quantified as a percent of CD8<sup>+</sup> cells in the indicated tissues (n=4 mice per group). (D) Schematic timeline detailing timing in which BALB/c mice (n=16 mice) were engrafted with 4T07 cells (1X10<sup>5</sup>) via the mammary fat pad. The primary tumors were grown for 4 weeks, surgically excised and mice were subsequently treated with either IgG or  $\alpha$ CD8 antibodies (200  $\mu$ g) via intraperitoneal injections once every three days for the length of the experiment (n=8 mice per group). (E) Metastasis free survival analysis of IgG control mice (blue line) and CD8 depleted mice (red line) in days following the primary tumor removal (n=8 mice per group). The indicated p-value was calculated using a log rank test. (F) Bioluminescent images of representative mice at the 23 days after primary tumor removal.

Figure 3.3 continued



### **3.6 Conclusion**

Dissemination of tumor cells occurs years before the detection and treatment of primary tumors. These disseminated can be held dormant by a number of mechanisms including the establishment of a balance with the immune system (Romero et al., 2014b). Here we report that the systemically dormant phenotype of the BALB/c mouse model 4T07 is dependent on the function CD8<sup>+</sup> immune cells (Aslakson et al., 1991). Direct delivery of the 4T07 cells into the lungs is capable of overcoming this immune response via physical exclusion of CD8<sup>+</sup> lymphocytes.

Previous studies have characterized the 4T07 tumor model as a highly immunogenic tumor model capable of dissemination but not macrometastatic outgrowth (Aslakson et al., 1991). Our findings expand upon these conclusions by clearly demonstrating that CD8<sup>+</sup> cells are required for maintenance of 4T07 systemic tumor dormancy following surgical resection of the primary tumor. These data establish the 4T07 cells as a true model of immune-mediated tumor dormancy. This opens up opportunities for the use of this post-surgical system for the study of various dietary and other environmental influences on metastatic tumor relapse.

## **CHAPTER 4. PHARMACOLOGICAL INHIBITION OF FGFR MODULATES THE METASTATIC IMMUNE MICROENVIRONMENT AND PROMOTES RESPONSE TO CHECKPOINT BLOCKADE**

### **4.1 Disclaimer**

The material in this chapter has been prepared for submission to a journal for publication as a manuscript.

### **4.2 Introduction**

Immune checkpoint blockade therapy is approved for the treatment of metastatic breast cancer, but the clinical benefits of these treatments are limited in comparison to other cancer types (Li et al., 2016). A major rate-limiting aspect of antibody-based immuno-checkpoint-blockade (ICB) therapies such as  $\alpha$ PD-L1 is that breast cancer metastases are poorly infiltrated with inflammatory lymphocytes (Binnewies et al., 2018)(Garber, 2019). Indeed, recent studies indicate that as compared to matched primary mammary tumors, breast cancer metastases have decreased immune cell infiltration (Dieci et al., 2018; Zhu et al., 2019a). The drivers of these immune cold phenotypes in metastatic disease remain to be definitively determined. Therefore, there is clear clinical need to develop therapeutic interventions capable of altering the composition of the metastatic immune microenvironment to enhance the success of ICB therapies.

Fibroblast growth factor receptors (FGFR) are a family of receptor tyrosine kinases whose aberrant functions facilitate cancer cell proliferation, migration, and resistance to currently used therapeutics (Helsten et al., 2014; Porta et al., 2017). Recent studies have identified overexpression and activation of FGFR1 as a marker of epithelial-mesenchymal transition (EMT) and metastasis (Brown et al., 2016a; Wendt et al., 2014b). Additionally, *FGFR1* is genomically amplified in 13% of primary breast cancers and the FGFR1 locus can also become amplified *de novo* in metastatic tumors as compared to the primary tumor from which they were derived (Curtis et al., 2012; Yates et al., 2017). Several different selective and non-selective inhibitors of FGFR kinase activity demonstrate efficacy against *in vitro* cell lines as well as in pre-clinical mouse models (Ali et al., 2017). Recent studies have begun to demonstrate the impact of systemic inhibition of FGFR on

various aspects of the primary tumor microenvironment such as angiogenesis and infiltration by various immune cells (Holmström et al., 2018; Yu et al., 2017)(Palakurthi et al., 2019; Ye et al., 2014a). For instance, FGFR-mediated mTOR signaling drives expression of G-CSF leading to enhanced recruitment of myeloid-derived suppressor cells MDSCs (Welte et al., 2016).

However, It's not well understood how systemic inhibition of FGFR signaling during the treatment of pulmonary metastasis may change the immune landscape and potentiate a response to immunotherapy. Here we sought to address the hypothesis that modulation of the metastatic immune microenvironment via inhibition of FGFR would enhance the efficacy of immune checkpoint blockade.

### **4.3 Methods and materials**

#### **4.3.1 Animal studies and drug dosing**

All mouse experiments were performed in accordance with the IACUC approval from Purdue University. Five to 6 week old female BALB/c and athymic Nude(NU/J) mice were purchased from Jackson Laboratories. Female NRG(NOD-Rag1<sup>null</sup> IL2rg<sup>null</sup>, NOD<sup>rag gamma</sup>) were purchased from Biological Evaluation Shared Resource facility at Purdue University. Methods used for cancer cell engraftments and drug dosing are described in the respective figure legends for all animal experiments.

#### **4.3.2 Cell lines and reagents**

The 4T1, 4T07 and D2.A1 cell lines were obtained from the lab of Fred Miller (Wayne State University). These cells were cultured in DMEM media supplemented with 10% FBS and penicillin/streptomycin (Life Technologies). Stable expression of firefly luciferase was established via stable transfection under Zeocin selection as previously described (Wendt and Schiemann, 2009; Wendt et al., 2013a). Jurkat (clone e6-1) cells were obtained from Kazemian lab at Purdue University. The Jurkat cells were cultured in RPMI 1640 media supplemented with 10% FBS and penicillin/streptomycin. Depletion of FGFR1 in the D2.A1 cells was achieved via stable shRNA expression as described previously (Wendt et al., 2014a). All cell lines were subjected to tests for

mycoplasma contamination. The development and synthesis of FIIN4, the covalent FGFR inhibitor, were described previously (Brown et al., 2016c).

### **4.3.3 Flow cytometry**

Single-cell suspensions were prepared from isolated lung tumors and spleens. Briefly, collected tumor bearing lung tissues were minced and digested for 1 hour at 37°C in HBSS media containing collagenase type II. Isolated spleens were mechanically disrupted by grinding. Samples were treated with ACK buffer to lyse red blood cells before being filtered with 70µm sterile cell strainers. To characterize the immune microenvironment, the resultant single-cell suspensions were incubated with TruStain (FcR blocker) and Zombie violet (live/dead stain)(Biolegend). After that, they were stained with CD45-PerCP, CD11b-PE/Cy7, CD8-PacificBlue, ly6C-FITC, ly6G-APC/Cy7, F4/80-BV 605, and PD-L1-PE (Biolegend). A BD Fortessa LSR flow cytometry cell analyzer was used to perform the experiments and the resulting data were analyzed using Flowjo software.

### **4.3.4 Immunoassays**

Immunoblot assays were performed on cell lysates prepared by lysing the samples with modified RIPA lysis buffer containing 50 mM Tris, 150mM NaCl, 0.25% Sodium Deoxycholate, 1.0% NP40 and 0.1% SDS supplemented with protease inhibitor cocktails (Sigma), 10 mM Sodium Orthovanadate, 40 mM b-glycerolphosphate, and 20 mM Sodium Fluoride. For immunohistochemistry, formalin fixed and paraffin embedded tissue sections were deparaffinized, rehydrated and boiled on 10mM sodium citrate buffer (pH 6.0) to retrieve antigens. These processed sections were stained with antibodies specific for CD4, CD8, and CXCL16 (Cell Signaling). Staining was detected using the appropriate biotinylated secondary antibodies in combination with an ABC and DAB reagents (Vector). Sections were counter stained with hematoxylin. At least two people who were blinded in regards to the experimental groups counted the positively stained cells in the multiple fields of the stained sections.

#### **4.3.5 mRNA expression analyses**

4T1 cells treated with either 500nM FIIN4 or DMSO for 24 hours and total RNA was isolated using an RNeasyPlus Kit (Qiagen). cDNA libraries were synthesized using iScriptcDNA Synthesis System (Bio-Rad). Semiquantitative real-time PCR was performed using iQ SYBR Green (Bio-Rad) as previously reported (Wendt et al., 2011b). The unique primers used for CXCL16 were Forward: 5'-CTCTGCAGGTTTGCAGCTCT-3' and Reverse: 5'-CACTGATGGAGACGAGCCTG-3'

#### **4.3.6 T-cell signaling and immune cell killing assays**

Jurkat cells ( $1 \times 10^4$ ) were pretreated with indicated doses of FIIN4 for 2 hours in 24-well plates. Next, these cells were washed with sterile PBS twice and incubated with  $5 \mu\text{g/ml}$  anti-CD3 (Biolegend, LEAF) for the indicated amounts of time. Following incubation, cells were isolated via centrifugation and lysed as described above. Following SDS PAGE and transfer, the PVDF membranes were probed with the indicated antibodies (Cell Signaling Technologies). For tumor cell killing assays 4T07 cells ( $5 \times 10^4$ ) were incubated for 6 hours in the presence of spleenocytes ( $5 \times 10^5$ ) derived from 4T07 tumor bearing mice. Following this incubation the supernatants were collected, mixed with luciferin and assayed for luminescence as a measure of tumor cell lysis.

#### **4.3.7 Statistics**

Bonferroni-corrected threshold (significance level 0.05) was used to compare the survival of multiple groups in the combination studies. A log-rank study was performed to identify statistically significant differences between the DMSO and FIIN4 treated group in figure S1 and S2 . All the performed statistical analyses and associated P values are indicated in the respective figure legends.

## 4.4 Results

### 4.4.1 Inhibition of metastatic tumor growth by FGFR targeted agents is enhanced by the immune system.

We recently reported that pulmonary growth of the 4T1 model of metastatic breast cancer can be inhibited by pharmacological inhibition of FGFR following via tail vein injection of cells (Brown et al., 2016c). Delivery of the related 4T07 cell model similarly results in robust pulmonary tumor formation within three weeks of tumor cell inoculation (Wendt et al., 2013b). To further investigate the ability of FIIN4 to inhibit pulmonary tumor growth, we treated animals bearing pulmonary 4T07 cells tumors with FIIN4 (Figure 4.1). As shown in figure 1 both immunodeficient NRG mice and syngeneic BALB/c mice were injected with 4T07 cells and drug treatment was initiated 48 hours later (Figure 4.1a). A seven day treatment course with FIIN4 significantly delayed pulmonary tumor outgrowth in NRG mice, but this same treatment actually led to transient regression of tumor cell presence in BALB/c animals (Figure 4.1B-C). Moreover, upon cessation of FIIN4 treatment, BALB/c mice experienced a significant survival benefit whereas the NRG mice did not (Figure 4.1D).

### 4.4.2 Inhibition of FGFR increases CD8<sup>+</sup> cell in pulmonary tumors

Given the importance of the adaptive immune system on both 4T07 metastasis and response to FGFR inhibition we next sought to utilize this model system to further characterize the impact of FGFR on immune function (Palakurthi et al., 2019; Welte et al., 2016; Ye et al., 2014b). To this end, mice bearing pulmonary 4T07 tumors mice were split into four separate cohorts and treated with increasing doses of FIIN4 (Figure 4.2A). Consistent with our data in figure one, FIIN4 treatment led to a dose-dependent inhibition of pulmonary tumor growth (Figure 4.2A and 4.2B). Histological examination of these pulmonary tumors demonstrated that the 4T07 pulmonary tumors that form following tail vein engraftment are nearly devoid of CD8<sup>+</sup> cytolytic lymphocytes (Fig. 4.2A). In contrast, systemic administration of FIIN4 produced a dose-dependent increase in the number of CD8<sup>+</sup> cells present in these pulmonary lesions (Fig. 4.2C). In attempts to identify a mechanism of FIIN4-mediated recruitment of CD8<sup>+</sup> cells we examined the dataset GSE52452. These gene expression data were derived from urothelial carcinoma cells treated with an alternative FGFR inhibitor, PD173074 ([CSL STYLE ERROR: reference with no printed

form.]). Examination of this dataset for differential expression of T-cell recruitment molecules revealed a significant increases in expression of the chemokine CXCL16 upon inhibition of FGFR (Figure 4.2D; (Matsumura et al., 2008)). Consistent with these findings, CXCL16 mRNA was increased upon treatment with FIIN4, and IHC analyses of 4T07 pulmonary lesions demonstrated a marked increase in CXCL16 staining upon administration of FIIN4 (Figure 4.2E and 4.2F). Importantly, these drug-induced immune phenotypes could be recapitulated genetically as shRNA-mediated depletion of FGFR1 in tumor cells also led to increased presence of CD8<sup>+</sup> cells in pulmonary tumors (Fig. 4.2G; (Wendt et al., 2014a)).

#### **4.4.3 FIIN4 treatment modulates immune suppressive populations in pulmonary tumors**

In addition to exclusion of CD8<sup>+</sup> lymphocytes, FGFR also contributes to an immune suppressive microenvironment via recruitment of myeloid-derived suppressor cells (MDSCs) and tumor associated macrophages (Welte et al., 2016). As a result, we sought to define how FIIN4 treatment affects these immune regulatory cells in pulmonary 4T07 tumors. Flow cytometry analyses of isolated spleen and lung tissues from pulmonary tumor bearing BALB/c mice revealed that systemic administration of FIIN4 reduced the number of MDSCs in pulmonary tumors (Figure 4.3A and 4.3B). In contrast, FIIN4 did not change the number of macrophages in the tumor bearing lung tissue (Figure 4.3C and 4.3D). Further characterization of the MDSCs that remained after FIIN4 treatment revealed enhanced expression of the immunosuppressive molecule programmed death ligand 1 (PD-L1) (Figure 4.3E and 4.3F). Taken together, these data suggest that FGFR signaling actively contributes to an immunosuppressive microenvironment in pulmonary metastases via simultaneous exclusion of CD8<sup>+</sup> lymphocytes and recruitment of MDSCs.

#### **4.4.4 Combination of FIIN4 and immune-checkpoint-blockade therapy**

To translate the observations above we initiated combination therapy approaches using both FIIN4 and checkpoint blockade antibodies. Initially, addition of PD-1 or PD-L1 blocking antibodies failed to show any improvement in FIIN4-mediated survival of mice bearing either 4T07 pulmonary tumors (Figure 4.4A). Previous studies have found that FGFR can participate T cell receptor (TCR) signaling and in the activation of a T cell response (Byrd et al., 2003a). Therefore, we hypothesized that pharmacological inhibition of FGFR signaling may actually be

inhibiting the antitumor activity of cytolytic lymphocytes. To test this hypothesis we cocultured spleenocytes from 4T07 primary tumor bearing mice with 4T07 cells and assayed for tumor cell lysis (Figure 4.4B). As predicted, the spleenocytes from *in vivo* primed, tumor bearing animals efficiently killed the 4T07 cells (Figure 4.4B). However, this immune-mediated killing was nullified in the presence of FIIN4 (Figure 4.4B). To further investigate the inhibition of T-cell function by FIIN4 we stimulated Jurkat cells *in vitro* with  $\alpha$ CD3 antibodies in the presence or absence of FIIN4 and assayed for differential phosphorylation of downstream signaling molecules. This approach clearly indicated that FIIN4 potently inhibits TCR proximal signaling events (Figure 4.4C). Given these inhibitory effects of FIIN4 on T-cell function we reasoned that sequential combination of FIIN4 and  $\alpha$ PD-L1 would first abrogate the immunosuppressive microenvironment followed by enhanced T-cell activity via checkpoint blockade. Indeed, sequential dosing of FIIN4 followed by  $\alpha$ PD-L1 significantly limited pulmonary tumor growth and increased overall survival as compared to either monotherapy (Figure 4.4D,4.4E).

## 4.5 Figures

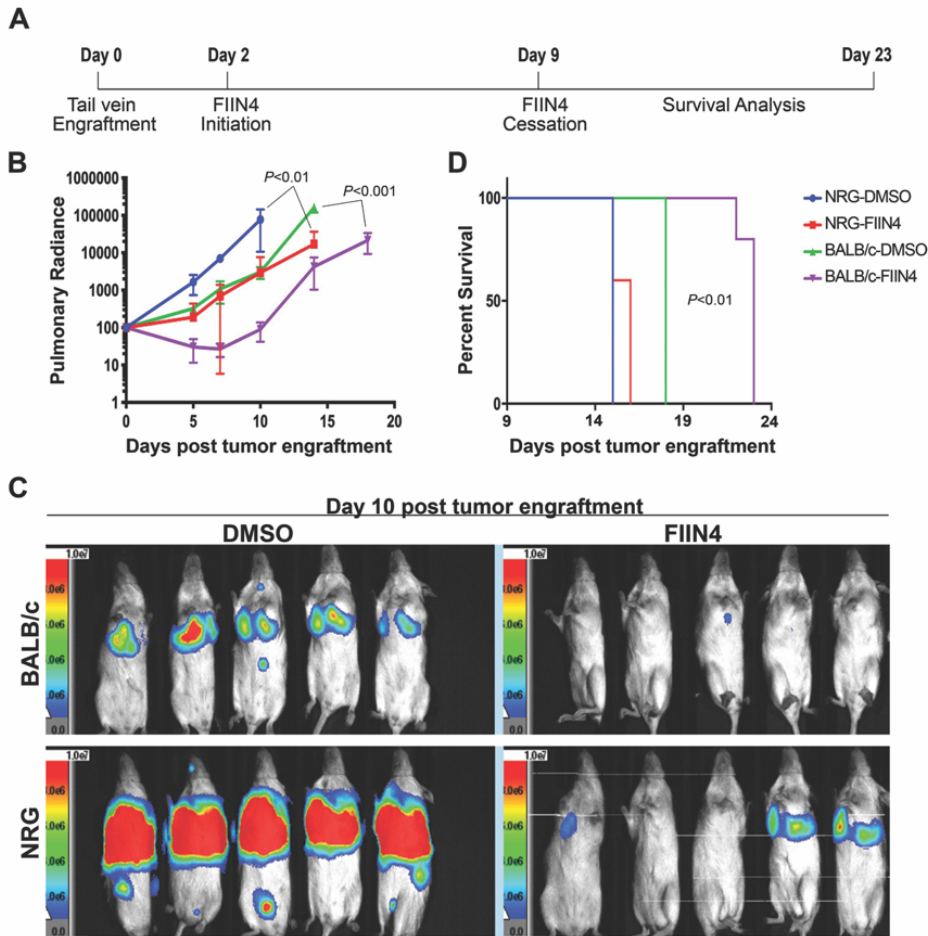


Figure 4.1 Immune competent mice demonstrate prolonged antitumor effects following systemic inhibition of FGFR. (A) Timeline of the engraftment and treatment approaches. Firefly luciferase-expressing 4T07 cells ( $5 \times 10^5$ ) were injected into the lateral tail vein of both BALB/c and NRG mice ( $n=10$  mice each group) and cells were allowed to seed for two days. These mice were then treated with either DMSO or FIIN4 (100 mg/kg/po/qd) for 7 days. (B) The mean ( $\pm$ SE) pulmonary radiance values from each group was taken at the indicated time points ( $n=5$  mice per group). Data are normalized to the load values obtained immediately following tail vein injection and were analyzed using a 2-way ANOVA. (C) Representative bioluminescent images of both BALB/c and NRG mice at Day 10 post tumor engraftment. (D) Survival analysis of indicated groups mice after stopping the treatment ( $n=5$  mice per group). These data were analyzed using a log rank test.

Figure 4.2 FIIN4 treatment leads to an elevated level of CD8+ cells in pulmonary tumors. (A, B and C) 4T07 cells ( $5 \times 10^5$ ) were delivered to the lungs of BALB/c mice ( $n=20$ ) via tail vein injection, and the mice were allowed to recover for two days. Mice were administered either DMSO or FIIN4 (25, 50 and 100 mg/kg/day) via oral gavage for 7 days. ( $n=5$  mice per group). Following this treatment, mice were sacrificed and lungs were collected and fixed in paraformaldehyde for downstream histological analysis. (A) Representative images of pulmonary histological sections of each treatment group stained with H&E, or antibodies specific for CD8 or CD4. (B) Bioluminescent images of each group treatment group 10 days after pulmonary engraftment. (C) The mean ( $\pm$ SD) of CD8 and CD4 positive cells per high powered field (HPF),  $n=5$ . (D) Differential CXCL16 expression levels were obtained from the dataset GSE52452 in which MGHU3 were treated with the FGFR inhibitor PD173074. (E) RT-PCR analysis for CXCL16 obtained from 4T1 cells treated with 500 nM FIIN4 for 24 hours. (F) IHC analysis for CXCL16 in the control and FIIN4 treated (100 mg/kg/day) pulmonary tumors as described in panel A. (G) IHC analysis for CD8+ cells in control D2.A1 pulmonary tumors expressing a scrambled shRNA (shscram) and those depleted for FGFR1 expression (shFGFR1).

Figure 4.2 continued

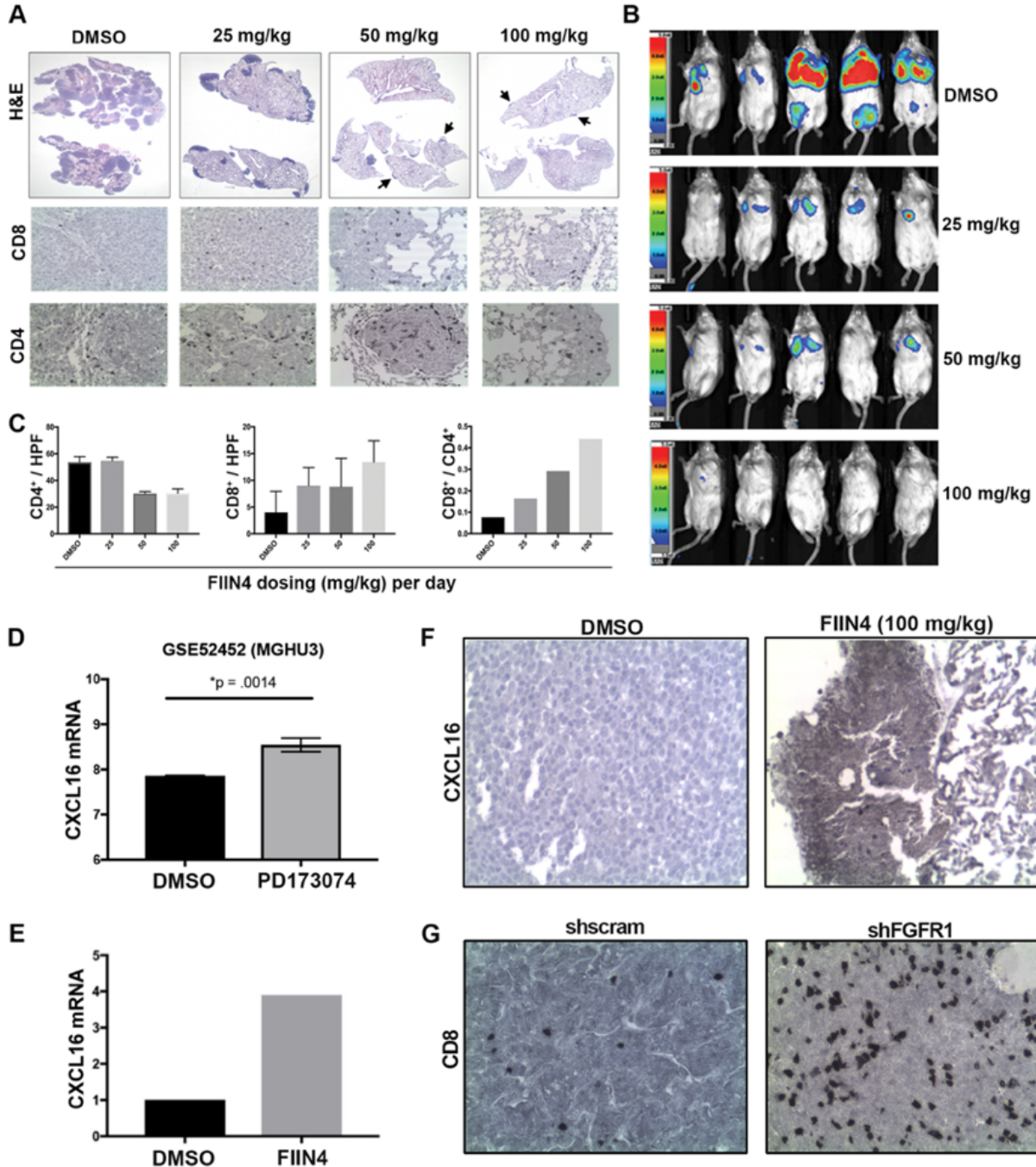
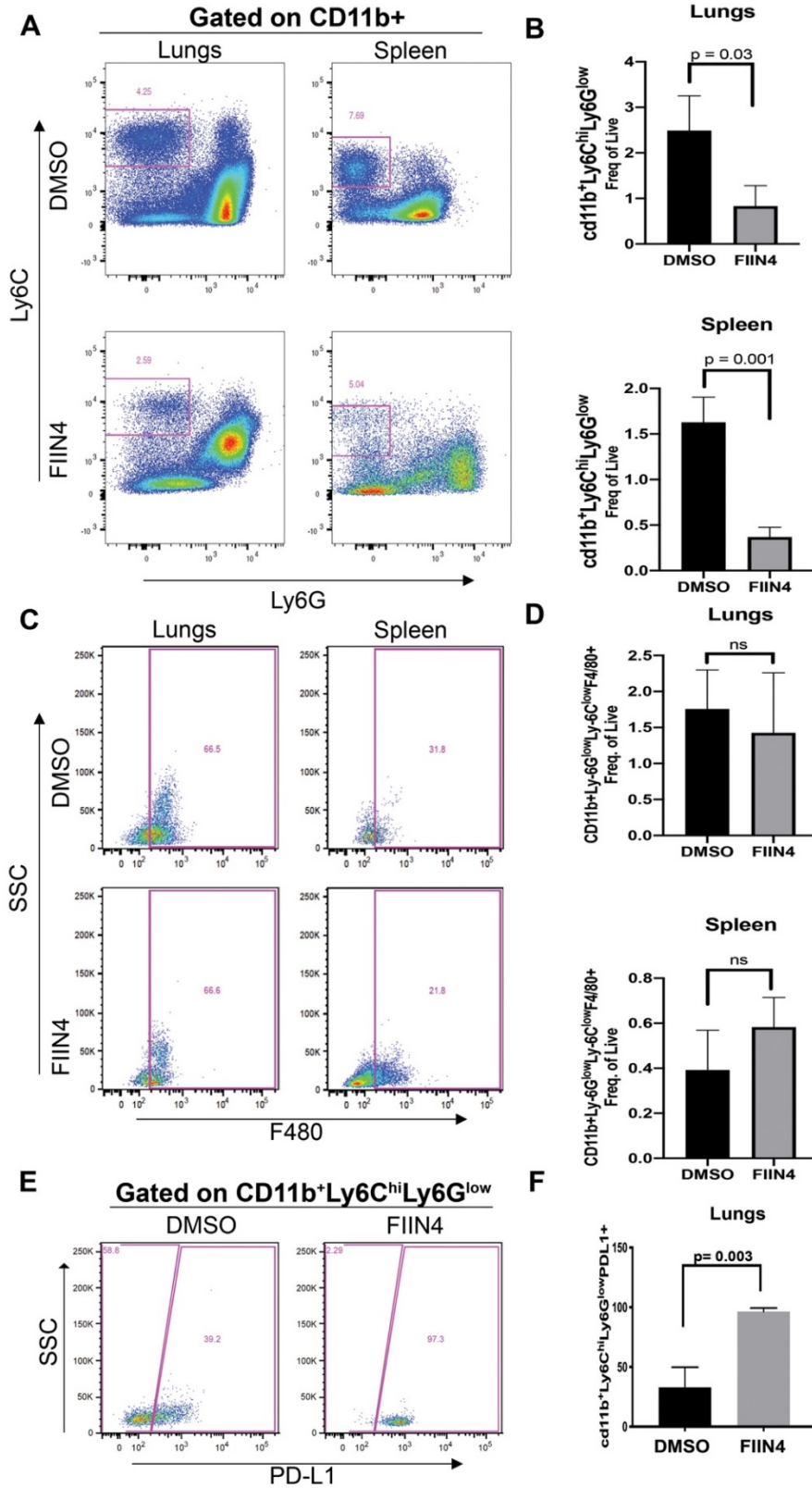


Figure 4.3 FIIN4 treatment modulates pulmonary immune populations in 4T07 tumor-bearing mice. Multicolor flow cytometry analyses were performed to measure the changes in various immune cell populations in the spleen and lungs of BALB/c mice bearing 4T07 pulmonary tumors following 7 days of systemic administration of FIIN4 (100 mg/kg,po,qd). (A and B) Representative dot plots and replicated quantification of myeloid-derived suppressor cells (MDSCs) identified as CD11b+Ly6chiLy6Glow populations and quantified as a frequency of live events in isolated lung and spleen tissues of each group. (C and D) Representative dot plots and replicated quantification of macrophages identified as CD11b+Ly6clowF4/80+ populations and quantified as a frequency of live events in the isolated lung and spleen tissues of each group. (E and F) Representative dot plots and replicated quantification of PD-L1 positive MDSCs identified as CD11b+Ly6chiLy6GlowPD-L1+ populations in the isolated pulmonary tumors. Data presented here are from three mice and are representative of two independent experiments.

Figure 4.3 continued



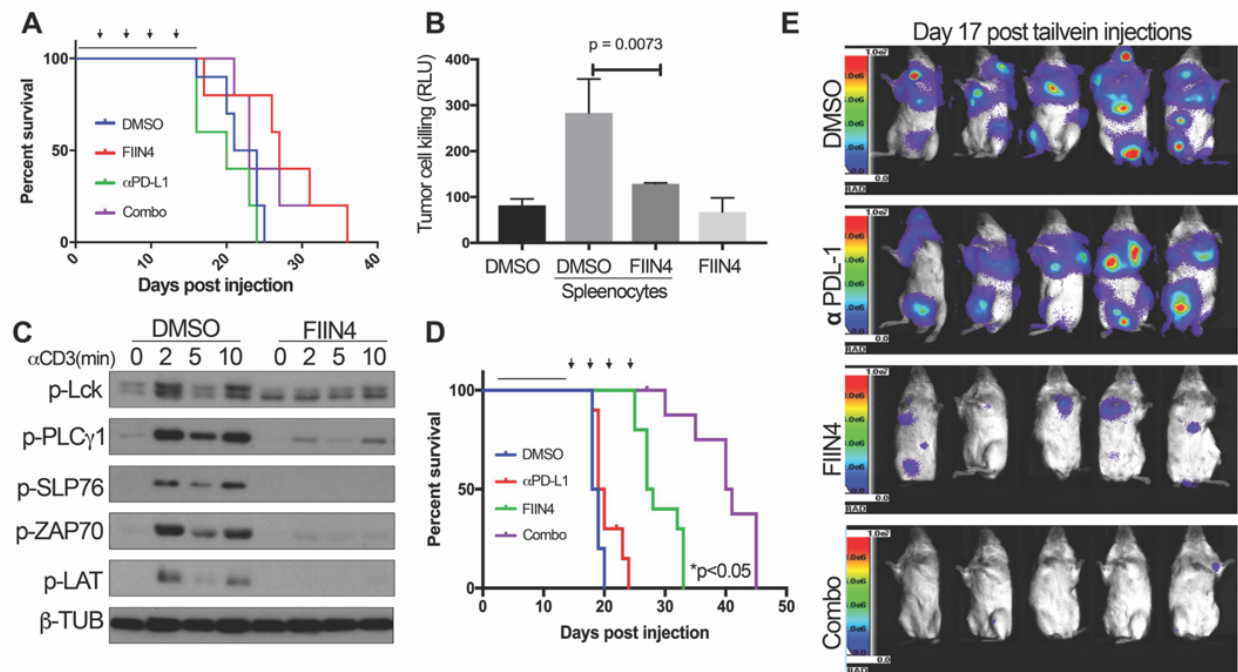


Figure 4.4 Sequential combination of FIIN4 and immune-checkpoint-blockade enhanced survival of pulmonary tumor-bearing mice. (A) Survival analysis of BALB/c mice bearing pulmonary 4T07 tumors with indicated therapies (n=5 mice per groups). The combination group of mice received both FIIN4 (100mg/kg/day for seven days via oral gavage) and  $\alpha$ PD-L1 (four doses of 200  $\mu$ g once every three days via intraperitoneal injections) simultaneously. The 14 day FIIN4 treatment is indicated by the solid black line and each  $\alpha$ PD-L1 administration is denoted by an arrowhead (B) 4T07 cells were cocultured *in vitro* with spleenocytes from 4T07 tumor bearing mice in the presence or absence of FIIN4 and tumor cell lysis was quantified as described in the materials and methods. (C) Jurkat T-cells pretreated with either DMSO or 1 $\mu$ M FIIN4 overnight were stimulated with  $\alpha$ CD3 antibody for the indicated time points, and cell lysates were collected and assayed via immunoblot for phosphorylation of p-Lck, p-PLC $\gamma$ 1, p-SLP76, p-ZAP70(Y319), p-LAT, and  $\beta$ -tubulin ( $\beta$ -Tub) as a loading control. Data in panel C are representative of at least two independent experiments. (D) Survival analyses of BALB/c mice bearing pulmonary 4T07 tumors treated with indicated therapies (n=10 mice per group). As in panel A, FIIN4 treatment duration (100 mg/kg/day) is indicated by the solid line and  $\alpha$ PD-L1 doses (200  $\mu$ g) are indicated by the arrowheads. Survival data were analyzed by a log rank test. (E) Bioluminescent images of the different treatment groups described in panel D at Day 17 post tail vein injections.

## 4.6 Conclusion

Immunotherapies are promising therapeutic avenues in various types of cancers(Li et al., 2016). Despite recent clinical trials showing durable response of different immunotherapies in many patients, a significant number remain unresponsive. The immunosuppressive nature of the tumor immune microenvironment (TIME) in different cancers presents grounds for such contrasting efficacies(Binnewies et al., 2018). Solid tumors, for instance in Breast cancer, are infiltrated with a low number of inflammatory lymphocytes, thus, contributing to a limited sensitivity to antibody-based immuno-checkpoint-blockade (ICB) therapies such as anti-PDL1 ( $\alpha$ PDL1)(Binnewies et al., 2018)(Garber, 2019). Here, we presented systemic inhibition of FGFR as a potential therapeutic strategy to alter the composition of TIME that favors the activity of  $\alpha$ PDL1 to prolong the survival of mice with pulmonary tumors.

Using this 4T07 cancer model, we found that FIIN4, the covalent inhibitor of FGFR, has greater efficacy in mice with competent immune systems, implicating its immunomodulatory functions. Importantly, pharmacological inhibition of FGFR markedly increases number of CD8<sup>+</sup> T lymphocytes within pulmonary tumors via induction of the T cell chemoattractant CXCL16. Besides, FIIN4 treatments decrease the number of immune-suppressive myeloid-derived suppressor cells (MDSCs) but elevate the level of PD-L1 expression while macrophages remain unchanged. These data suggest the combination of FGFR inhibition and PD-L1 targeting as an effective anti-metastatic therapy. However, we demonstrate that pharmacological inhibition of FGFR can interfere with T cell receptor signaling, inhibit T cell-mediated killing of tumor cells, and prevent a therapeutic benefit upon direct combination of FIIN4 with anti-PD-L1 checkpoint blockade. To overcome this, we were able to optimize a sequential dosing strategy consisting of FGFR inhibition followed by anti-PD-L1. This sequential combination approach significantly improves the overall survival of mice with pulmonary tumors as compared single treatment therapies. Collectively, our results indicate that in addition to direct inhibition of tumor cell growth, systemic targeting of FGFR signaling can sensitize metastatic tumors to  $\alpha$ PD-L1 immune checkpoint therapy by changing the immune microenvironment.

Additionally, we demonstrate that upon tail vein injection of 4T07 cells, the resulting pulmonary tumors demonstrate an immune exclusion phenotype. These findings nicely recapitulate patient data in which metastases are less infiltrated with immune cells as compared to matched primary tumors (Zhu et al., 2019b). These data point to the importance of the tumor microenvironment in dictating response to kinase inhibitors as well as immunotherapy. In contrast to the 4T07 cells the highly metastatic 4T1 model contains a high number of T-cells in both the primary tumor and the resulting metastases. This raises the interesting question of whether metastases that manifest quickly following primary tumor interventions evolve more active modes of immune suppression, where metastases that only emerge following prolonged periods of remission rely on immune exclusion to maintain tumor cell survival and outgrowth.

Overall, in this chapter, we presented evidence that systemic FGFR inhibition transform the composition of immune microenvironment within metastatic niche which allow a combination therapy with  $\alpha$ PD-L1 to prolong patient's survival. We also reported novel mechanistic links between FGFR signaling and T lymphocyte's migration and function in cancer. Further analysis of the mechanism of FGFR mediated chemokine expression and subsequent lymphocyte recruitment will be critical to develop novel small molecule immune modulators .

## CHAPTER 5. DISCUSSION AND FUTURE DIRECTIONS

At the onset of this dissertation work, we set out to develop novel biological models with the goal of understanding the mechanism of disease recurrence in breast cancers. Disease recurrence in cancer can occur as local, regional, and distant metastasis (Holleczek et al., 2019). Different factors affect the risk of disease recurrence such as the age of the patients, tumor size, time of tumor detection, lymph node involvement, type of cancers (Mannell, 2017). Various cellular signaling events are also implicated in the disease recurrence (Ahmad, 2013). To date, toxic hormonal chemo and radiation therapies are common approaches to target these relapsed diseases. As a result, continuous research is vital to identify targetable pathways to inhibit recurrent tumors. Here, with our novel *in vivo* and *in vitro* models, we established fibroblast growth factor receptors (FGFR) as molecular targets to treat recurrent tumors. In the future, continual efforts in improving the experimental models for better recapitulation of various aspects of disease recurrence will be key to unlock novel therapeutics against breast cancer recurrence.

### 5.1 Recurrence of minimal residual disease

Treatment of HMLE-HER2 xenografts with antibody-drug conjugates T-DM1 established drug-induced minimal residual diseases (MRDs). Upon removal of drugs, these MRDs exhibited disease recurrence with the acquisition of new cellular phenotypes. Analyses of relapsed tumors from MRDs revealed that the T-DM1 drug persistent tumors significantly lost *Her2* expression. These observations have important implications on the choice of drug treatment sequences in the HER2+ subtype of breast cancer. We reported that upon the acquisition of lapatinib resistance, HER2 can still be expressed in the cancer cells and be targeted with T-DM1. However, the development of T-DM1 resistance comes with Her2 downregulations, which eventually makes them inherently resistant to other Her2 kinase inhibitors. As a result, our results recommend that a better sequence of Her2 targeted therapies for this subset of patients would consist of kinase inhibitors as first-line treatments followed by Her2 targeted antibodies and T-DM1. Similar to our findings of Her2 discordance, recent studies with doxycycline inducible

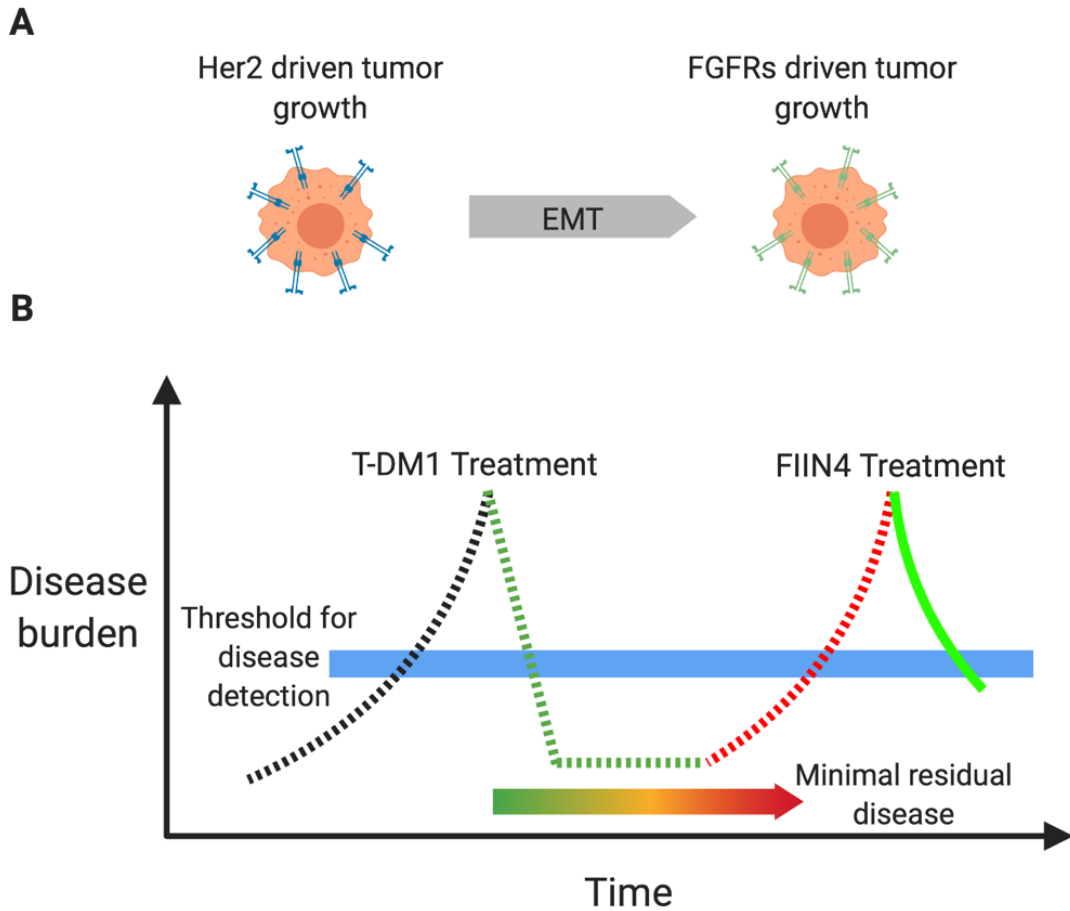


Figure 5.1 Minimal residual disease post T-DM1 treatment. (A) HER2 driven tumors exhibit the loss of Her2 expression following prolonged treatments of T-DM1 followed by the activation of FGFR signaling. The induction of EMT helps the selection of cancer cell types that exhibit a switch of growth-promoting pathways. (B) Schematic presentation of various stages of HER2+ xenografts. Initially, HER2+ cells are sensitive to T-DM1 treatments that result in the development of minimal residual diseases (MRD) when the diseases are below the threshold for detection. While in the state of MRD, these cancer cells acquire new growth-promoting pathways FGFR while downregulating Her2 driven signaling. These tumors, when they relapse out of MRD, show little sensitivity towards T-DM1 but can be targeted with FGFR inhibitors.

HER2 expression tumor models, showed that recurrent tumors can evolved via loss of HER2 expression and grow using alternative signaling pathways (Abravanel et al., 2015; Mabe et al., 2018). Additional studies also reported similar downregulation of target receptors following antibody treatments (Duman et al., 2012). More complete analysis of the molecular and signaling mechanism of such active HER2 downregulation or loss of expression post T-DM1 treatments are necessary. Understanding such mechanisms may lead to the development of combination therapies to significantly delay the recurrence of the disease.

Our *in vitro* models suggest that cytokine-induced EMT programs facilitate the selection of a small subset of the population that exhibits diminished Her2 expression along with high level expression of FGFR1. These data are consistent with previous observations of Inducible activation of the FGFR following the initiation of EMT programs (Brown et al., 2016b; Raoof et al., 2019). With the downregulation of the Her2 growth pathway, the drug persisted cells need alternative signaling pathways for growing as relapsed tumors. Indeed, we found that elevated expression of FGFR1 inhibits T-DM1 mediated cell growth arrest, at least partially, via interfering with the antibody binding of Her2 and may drive tumor regrowth in these Her2 discordant tumors. As a result, our data suggest that FGFR1 can act as a major driver of tumor recurrence following the onset of HER2 discordance and acquisition of resistance to T-DM1 and other ErbB-targeted therapies. EMT has been linked with the development of resistance to various targeted therapies (Singh and Settleman, 2010b). EMT driven FGFR1 upregulations and development of T-DM1 persistent MRDs presents a functional and targetable link between EMT and the acquisition of drug resistance. However, the mechanisms of FGFR1 upregulation during EMT need to be fully elucidated in the future. Also, the role of EMT-driven FGFR1 upregulations in the acquisition of T-DM1 resistance need to be established in other HER2+ BC cells and xenograft models. FGFR signaling is capable of acting as a bypass pathway during the acquisition of resistance to ErbB kinase inhibitors. However, our current data suggest that enhanced FGFR1 expression also plays a more active role in manifesting T-DM1 resistance by disrupting trastuzumab's ability to bind to HER2. In the future, the exact mechanisms by which FGFR prevents trastuzumab binding need to be explored.

Our xenografts studies suggest that, in the recurrent setting, FGFR acts as a major driver of tumor growth, which can be effectively targeted with FIIN4. Overall, our studies strongly suggested that combined therapeutics targeting HER2 and FGFR will delay tumor recurrence and prolong response times of patients with HER2+ breast cancer. In the future, these combination approaches need to be validated in the relevant preclinical models. Due to the origin of the T-DM1, all of our preclinical studies were performed using human cancer cell lines and PDXs in mice with compromised immune systems. Similar studies using mouse tumors lines in preclinical mice model with competent immune systems will define the role of immune systems in the recurrence of minimal residual diseases.

## **5.2 Recurrence of immune mediated dormant tumors**

In addition to drug-induced dormant MRDs, as described in the previous chapter, cancer cells also demonstrate immune-mediated dormancy. As cancer initiates and progresses to develop metastatic growth in distant sites, it has to overcome body's various defense mechanisms continually. With high mutational rates, cancer cells can present numerous neoantigens that can be identified by the adaptive immune system (Castle et al., 2019). Systemically disseminated tumor cells (DTCs) are similarly susceptible to immune-mediated clearance as they leave immune-suppressive tumor microenvironments (Mohme et al., 2017). Among other mechanisms, these DTCs can survive in a dormant state for an extended period of time by maintaining an equilibrium of its proliferation and the immune-cells mediated growth inhibition (figure 5.2.A) (Romero et al., 2014b).

Here, we established 4T07 tumors as a model of immune-mediated dormancy. Previously, it has been reported that highly immunogenic 4T07 tumors can disseminate systemically from primary tumors but unable to form macrometastatic lesions (Aslakson et al., 1991). While comparing the metastatic progression of 4T07 tumors in mice with differential immune capabilities, we found that 4T07 tumors maintain their ability to form macrometastasis in mice with impaired immune systems. These observations suggested an active inhibition of 4T07 DTCs growth in the lungs via adaptive immune systems.

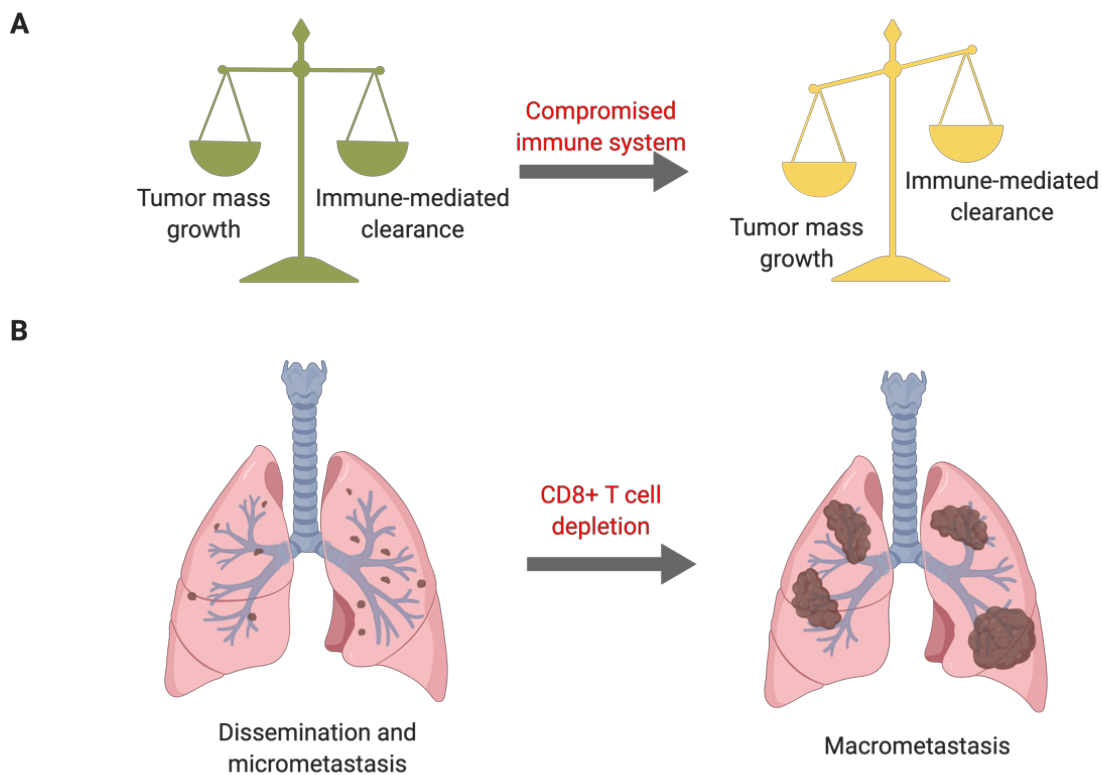


Figure 5.2 Model of 4T07 immune-mediated dormancy. (A) Immune dormancy is defined as a state of equilibrium between tumor cell's growth rate and cell-death due to clearance by immune cell activity. Any events that may compromise the immune system can shift the balance favoring the recurrence of metastatic tumors. (B) Systemically disseminated 4T07 cells are immunogenic and susceptible to the adaptive immune system. Following the depletion of CD8<sup>+</sup> T cells, these disseminated micrometastasis of 4T07 tumors break their dormancy and give rise to overt macrometastatic growth.

Moreover, we find that the systemic immune response developed with the implantation of 4T07 cells in mouse fat pad provides protection of pulmonary tumors growth delivered via tail-vein injection. These observations further indicated that the growth of 4T07s in the pulmonary regions are susceptible to systemically educated immune-mediated defense. Supporting this hypothesis, we found that 4T07 tumors, when delivered to the lungs, demonstrate immune exclusion phenotypes allowing them to manifest macrometastasis. Additionally, we found that dormant 4T07s are capable of forming macrometastasis in the lung with the depletion of cytolytic T lymphocytes (figure 5.2.B). These observations strongly underscored the importance of CD8+ cells for the maintenance of the equilibrium that results in 4T07's systemic dormant phenotype.

Overall, in this chapter, we presented 4T07 as a model to study the recurrence of immune susceptible dormant tumors. We envision this model to be used as a powerful tool to study external interventions on disease relapse by modulating anti-tumor immunity. In the future, an in-depth analysis of immunity against 4T07 tumors will enrich the model. Identification of the specific subset of CD8+ T lymphocytes and subsequent characterization of tumor antigen-specific T cell's receptors will refine our understanding of 4T07 tumors immunogenicity. Additionally, the role of other leukocytes such as NK cells, macrophages, and neutrophils, etc. in the maintenance of 4T07's dormancy also needs to be explored. All of this knowledge will be important to bolster the model of immune-mediated dormancy.

### **5.3 A combination therapy to target metastatic tumors**

FGFR has recently been established as a key modulator of the immune microenvironment in several primary cancers (Palakurthi et al., 2019; Welte et al., 2016; Ye et al., 2014b). Recent studies have begun to identify important mechanisms by which kinase inhibitors, originally designed to have on tumor effects, can influence immune cell recruitment and or function (Goel et al., 2017). There is still a major gap in our understanding of how FGFR signaling may influence the metastatic microenvironment, particularly the pulmonary region, a common site of breast cancer metastasis (Jin et al., 2018). Our presented systemically dormant immune-excluded 4T07 tumors equipped us with an excellent opportunity to explore the immune modulation of the pulmonary metastatic niche following the inhibition of FGFR signaling.

Using the aforementioned 4T07 pulmonary tumor models, we found that mice with a functional immune system exhibit better survival with the systemic inhibition of FGFR. These data clearly implied the influence of FGFR signaling on the composition of tumor surrounding immune microenvironments in the pulmonary region (figure 5.3). Subsequently, our data showed that FGFR inhibition leads to an increase of CD8+ T lymphocytes numbers within the metastasis niche in a dose-dependent manner. Further analysis of the changes in CD8+ T lymphocytes phenotypes and their expression profiles with the systemic FGFR inhibition are necessary to better characterize the extent of FGFR influence on tumor-infiltrating cytolytic T lymphocytes. Since FIIN4 has shown potential off-target inhibitions of various kinases, the specificity of FGFR inhibition mediated CD8+ T lymphocytes recruitment remains to be determined (Brown et al., 2016c). While genetic knockdown of FGFR1 in metastatic D2A1 models showed a direct relationship of FGFR1 and CD8+ T lymphocytes recruitments, further experiments on other tumor models with different genetic backgrounds are needed to strengthen these observations.

While the exact mechanism of FGFR mediated CD8+ T lymphocytes recruitments are yet to be delineated in detail, our data suggest that the upregulation of CXCL16 chemokines following FGFR inhibition may be partially responsible. The sources of CXCL16 ligands in the metastatic niche are also needed to be determined. High levels of expression for CXCL16 are found in the pulmonary region of the body (Day et al., 2009; Zuo et al., 2019)(Allaoui et al., 2016). As a result, the effects of FGFR inhibition on the differential expression of CXCL16 in the cancer-associated lung fibroblasts need to be explored. Additionally, genetic knockdown of CXCL16 in cancer cells with FIIN4 treatments are required for establishing of FGFR–CXCL16 axis as one of the active pathways that can influence CTL recruitments in metastatic nodules. The expression of CXCL16 in cancers has been found to inhibit tumor growths via helping recruitments of tumor-targeting immune cells (Hojo et al., 2007)(Kee et al., 2014). As a result, targeted delivery of recombinant CXCL16 within the metastatic region can be explored as a therapeutic option to treat pulmonary metastasis. Along with the CXCL16 expression, other chemokines may also be altered with the FGFR inhibition. Analysis of changes in the panel of mouse chemokines may provide a more detailed listing of potential effects of FIIN4.

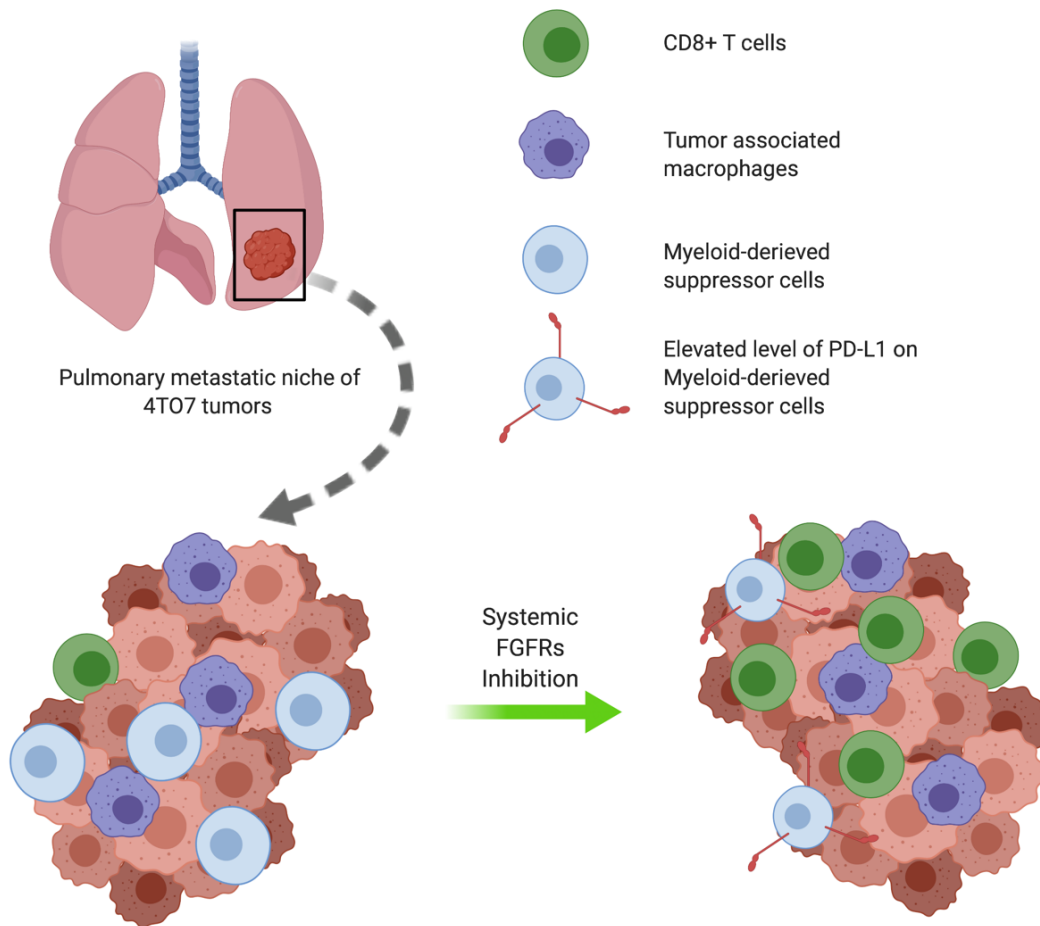


Figure 5.3 Compositions of tumor immune microenvironment of 4T07 pulmonary metastatic niche with FGFR inhibition. 4T07 tumors can develop macrometastasis in the pulmonary region when delivered via tail vein injections. 4T07 metastatic niche is characterized as immune-exclusive phenotype with few cytolytic T lymphocytes presence. Systemic inhibition of FGFR can bring significant changes in the composition of different immune cell populations favoring tumor clearance. An increase in the number of CD8+ T lymphocytes and a decrease in the MDSCs number are two major changes with FGFR inhibition. There is an elevated expression of PD-L1 on MDSCs within these proinflammatory environments as well. Such changes in immune cell populations and their phenotypes opened up an excellent opportunity for combination therapies with FGFR kinase inhibitor and immune checkpoint blockade therapies.

KinomeScan profiling for FIIN4 does suggest potential off-target inhibition of LCK, a critical mediator of TCR signaling (Brown et al., 2016c). However, other studies suggest that FGFR can interact with the TCR and participates in TCR-mediated signaling events (Byrd et al., 2003b). Indeed, our data shows that FGFR inhibition can actively inhibit cancer cell killings in vitro. Additionally, we find that FIIN4 treatment may inhibit TCR proximal signaling (figure 5.4). Further experiments are required to determine how FIIN4 treatments ultimately affect the effector functions of activated primary T lymphocytes and its production of IL2, INF- $\gamma$ , perforins, and granzymes. Screening of other small molecules inhibitors of FGFR will be necessary to determine if such effects are specific to FIIN4 only. Additionally, the activation of FGFR signaling on primary T lymphocytes via FGFR specific ligand may also strengthen the functional relationship of T cell receptors and FGFR signaling.

Eradifitinib is a competitive inhibitor and the only FGFR-targeted small molecule currently approved by the FDA. However, there are numerous other competitive and covalent FGFR-targeted molecules in various stages of clinical trials being tested (NCT03473756, NCT04024436). Our studies herein indicate that in addition to toxicity and on-target potency and specificity, the selection of these molecules should include analysis of interference with T-cell function.

Finally, we devised sequential dosing approaches with FIIN4 and  $\alpha$ PD-L1 ICB to facilitate the efficacy of checkpoint blockade in the immune-excluded 4T07 pulmonary tumors. The concept of combining kinase inhibitors with immune checkpoint blockade is clearly not without precedent. Recent studies have begun to identify important mechanisms by which kinase inhibitors, originally designed to have on tumor effects, can influence immune cell recruitment and or function (Goel et al., 2017). While some of these mechanisms can be readily targeted in direct combination with checkpoint blockade, our study is likely reflective of a common occurrence in that either on or off-target kinase inhibition can block T-cell function, thus negating the antitumor activity of checkpoint blockade. These results point to the importance of a complete understanding of the systemic effects of small molecules before they can effectively be combined with checkpoint blockade or other immune therapies.

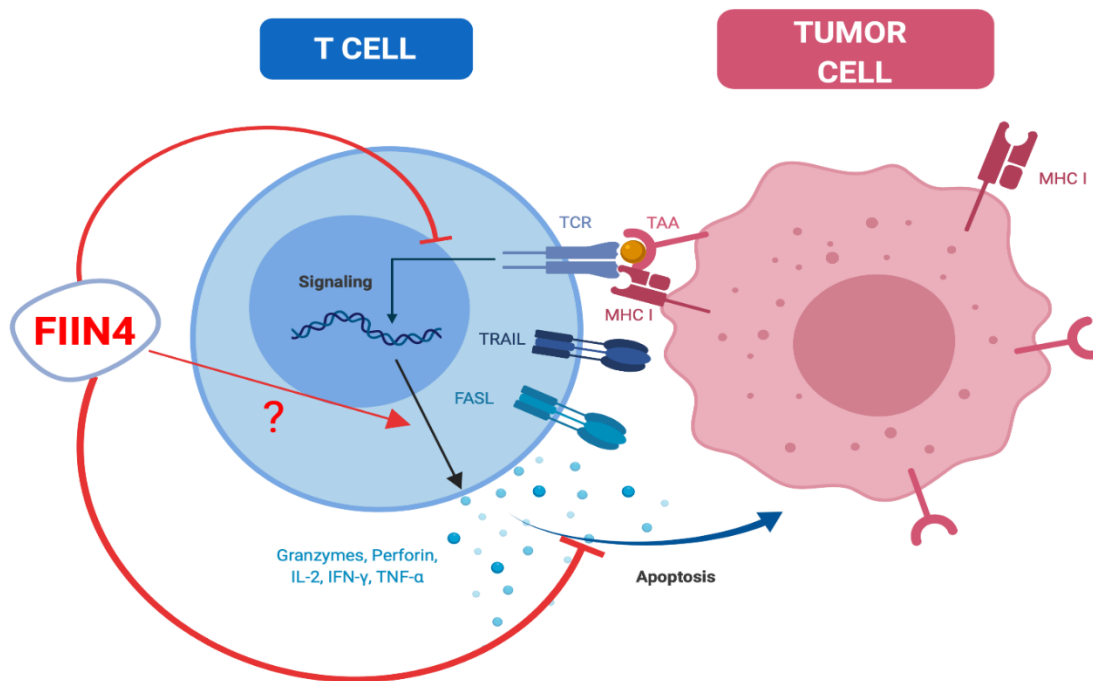


Figure 5.4 FIIN4 affects T lymphocytes signaling and its effector functions. FGFR inhibition with covalent FIIN4 molecule downregulates the TCR signaling cascade and subsequently affects the T-lymphocyte mediated cancer cell killings. More experiments are needed to establish if FIIN4 can modulate the secretion of effector molecules by activated T-lymphocytes.

## 5.4 Summary

In this dissertation work, we established FGFR signaling as an essential pathway that expedites the recurrence of the T-DM1 resistant tumors in Her2+ subtype of breast cancer. We also found that systemic FGFR inhibition changes the immune landscape of the metastatic tumors that can be exploited by combination therapy with  $\alpha$ PD-L1 to increase patient's survival with highly aggressive immune-dormant breast cancer tumors. Additionally, we suggested novel mechanistic insights into the relationship between FGFR signaling and T cell functions in cancer.

## REFERENCES

- Abravanel, D.L., Belka, G.K., Pan, T., Pant, D.K., Collins, M.A., Sterner, C.J., and Chodosh, L.A. (2015). Notch promotes recurrence of dormant tumor cells following HER2/neu-targeted therapy. *J Clin Invest* 125, 2484–2496.
- Aguirre-Ghiso, J.A. (2007). Models, mechanisms and clinical evidence for cancer dormancy. *Nat. Rev. Cancer* 7, 834–846.
- Ahmad, A. (2013). Pathways to Breast Cancer Recurrence. *ISRN Oncology* 2013, 1–16.
- Ali, R., Akhand, S.S., and Wendt, M.K. (2017). Targeting FGFR for the Treatment of Breast Cancer. In *Resistance to Targeted Therapies in Breast Cancer*, J.R. Prosperi, ed. (Cham: Springer International Publishing), pp. 117–137.
- Allaoui, R., Bergenfelz, C., Mohlin, S., Hagerling, C., Salari, K., Werb, Z., Anderson, R.L., Ethier, S.P., Jirström, K., Pählman, S., et al. (2016). Cancer-associated fibroblast-secreted CXCL16 attracts monocytes to promote stroma activation in triple-negative breast cancers. *Nat Commun* 7, 13050.
- Amiri-Kordestani, L., Blumenthal, G.M., Xu, Q.C., Zhang, L., Tang, S.W., Ha, L., Weinberg, W.C., Chi, B., Candau-Chacon, R., Hughes, P., et al. (2014). FDA Approval: Ado-Trastuzumab Emtansine for the Treatment of Patients with HER2-Positive Metastatic Breast Cancer. *Clin Cancer Res* 20, 4436–4441.
- Aslakson, C.J., and Miller, F.R. (1992). Selective events in the metastatic process defined by analysis of the sequential dissemination of subpopulations of a mouse mammary tumor. *Cancer Res.* 52, 1399–1405.
- Aslakson, C.J., McEachern, D., Conaway, D.H., and Miller, F.R. (1991). Inhibition of lung colonization at two different steps in the metastatic sequence. *Clin. Exp. Metastasis* 9, 139–150.
- Azuma, K., Tsurutani, J., Sakai, K., Kaneda, H., Fujisaka, Y., Takeda, M., Watatani, M., Arao, T., Satoh, T., Okamoto, I., et al. (2011). Switching addictions between HER2 and FGFR2 in HER2-positive breast tumor cells: FGFR2 as a potential target for salvage after lapatinib failure. *Biochem. Biophys. Res. Commun.* 407, 219–224.
- Balkwill, F.R., Capasso, M., and Hagemann, T. (2012). The tumor microenvironment at a glance. *Journal of Cell Science* 125, 5591–5596.
- Barok, M., Tanner, M., Köninki, K., and Isola, J. (2011). Trastuzumab-DM1 causes tumour growth inhibition by mitotic catastrophe in trastuzumab-resistant breast cancer cells in vivo. *Breast Cancer Res.* 13, R46.

- Barok, M., Joensuu, H., and Isola, J. (2014a). Trastuzumab emtansine: mechanisms of action and drug resistance. *Breast Cancer Res.* *16*, 209.
- Barok, M., Joensuu, H., and Isola, J. (2014b). Trastuzumab emtansine: mechanisms of action and drug resistance. *Breast Cancer Res.* *16*, 209.
- Binnewies, M., Roberts, E.W., Kersten, K., Chan, V., Fearon, D.F., Merad, M., Coussens, L.M., Gabrilovich, D.I., Ostrand-Rosenberg, S., Hedrick, C.C., et al. (2018). Understanding the tumor immune microenvironment (TIME) for effective therapy. *Nature Medicine* *24*, 541–550.
- Blomberg, O.S., Spagnuolo, L., and de Visser, K.E. (2018). Immune regulation of metastasis: mechanistic insights and therapeutic opportunities. *Dis Model Mech* *11*.
- Boyras, B., Sendur, M. a. N.N., Aksoy, S., Babacan, T., Roach, E.C., Kizilarlanoglu, M.C., Petekkaya, I., and Altundag, K. (2013). Trastuzumab emtansine (T-DM1) for HER2-positive breast cancer. *Current Medical Research and Opinion* *29*, 405–414.
- Brandão, M., Pondé, N., and Piccart-Gebhart, M. (2019). Mammaprint™: a comprehensive review. *Future Oncol* *15*, 207–224.
- Brown, W.S., Tan, L., Smith, A., Gray, N.S., and Wendt, M.K. (2016a). Covalent Targeting of Fibroblast Growth Factor Receptor Inhibits Metastatic Breast Cancer. *Molecular Cancer Therapeutics* *15*, 2096–2106.
- Brown, W.S., Akhand, S.S., Wendt, M.K., Brown, W.S., Salehin Akhand, S., and Wendt, M.K. (2016b). FGFR signaling maintains a drug persistent cell population following epithelial-mesenchymal transition. *Oncotarget* *7*, 83424–83436.
- Brown, W.S., Tan, L., Smith, A., Gray, N.S., and Wendt, M.K. (2016c). Covalent Targeting of Fibroblast Growth Factor Receptor Inhibits Metastatic Breast Cancer. *Mol. Cancer Ther.* *15*, 2096–2106.
- Brown, W.S., Salehin Akhand, S., and Wendt, M.K. (2016d). FGFR signaling maintains a drug persistent cell population following epithelial-mesenchymal transition. *Oncotarget* *7*, 83424–83436.
- Byrd, V.M., Kilkenny, D.M., Dikov, M.M., Reich, M.B., Rocheleau, J.V., Armistead, W.J., Thomas, J.W., and Miller, G.G. (2003a). Fibroblast growth factor receptor-1 interacts with the T-cell receptor signalling pathway. *Immunol. Cell Biol.* *81*, 440–450.
- Byrd, V.M., Kilkenny, D.M., Dikov, M.M., Reich, M.B., Rocheleau, J.V., Armistead, W.J., Thomas, J.W., and Miller, G.G. (2003b). Fibroblast growth factor receptor-1 interacts with the T-cell receptor signalling pathway. *Immunol Cell Biol* *81*, 440–450.
- Castle, J.C., Uduman, M., Pabla, S., Stein, R.B., and Buell, J.S. (2019). Mutation-Derived Neoantigens for Cancer Immunotherapy. *Front. Immunol.* *10*, 1856.

- Choong, L.-Y., Lim, S., Loh, M.C.-S., Man, X., Chen, Y., Toy, W., Pan, M., Chen, C.-S., Poonepalli, A., Hande, M.P., et al. (2007). Progressive loss of epidermal growth factor receptor in a subpopulation of breast cancers: implications in target-directed therapeutics. *Mol. Cancer Ther.* *6*, 2828–2842.
- Ciriello, G., Gatza, M.L., Beck, A.H., Wilkerson, M.D., Rhie, S.K., Pastore, A., Zhang, H., McLellan, M., Yau, C., Kandoth, C., et al. (2015). Comprehensive Molecular Portraits of Invasive Lobular Breast Cancer. *Cell* *163*, 506–519.
- Curtis, C., Shah, S.P., Chin, S.-F., Turashvili, G., Rueda, O.M., Dunning, M.J., Speed, D., Lynch, A.G., Samarajiwa, S., Yuan, Y., et al. (2012). The genomic and transcriptomic architecture of 2,000 breast tumours reveals novel subgroups. *Nature* *486*, 346–352.
- Dagogo-Jack, I., and Shaw, A.T. (2018). Tumour heterogeneity and resistance to cancer therapies. *Nat Rev Clin Oncol* *15*, 81–94.
- Dahlke, E., Murray, C.A., Kitchen, J., and Chan, A.-W. (2014). Systematic review of melanoma incidence and prognosis in solid organ transplant recipients. *Transplant Res* *3*, 10.
- Dai, S., Zhou, Z., Chen, Z., Xu, G., and Chen, Y. (2019). Fibroblast Growth Factor Receptors (FGFR): Structures and Small Molecule Inhibitors. *Cells* *8*.
- Day, C., Patel, R., Guillen, C., and Wardlaw, A.J. (2009). The chemokine CXCL16 is highly and constitutively expressed by human bronchial epithelial cells. *Exp. Lung Res.* *35*, 272–283.
- DeSantis, C., Ma, J., Bryan, L., and Jemal, A. (2014). Breast cancer statistics, 2013: Breast Cancer Statistics, 2013. *CA: A Cancer Journal for Clinicians* *64*, 52–62.
- Dey, J.H., Bianchi, F., Voshol, J., Bonenfant, D., Oakeley, E.J., and Hynes, N.E. (2010). Targeting fibroblast growth factor receptors blocks PI3K/AKT signaling, induces apoptosis, and impairs mammary tumor outgrowth and metastasis. *Cancer Res.* *70*, 4151–4162.
- Di Leo, A., Gomez, H.L., Aziz, Z., Zvirbule, Z., Bines, J., Arbushites, M.C., Guerrero, S.F., Koehler, M., Oliva, C., Stein, S.H., et al. (2008). Phase III, Double-Blind, Randomized Study Comparing Lapatinib Plus Paclitaxel With Placebo Plus Paclitaxel As First-Line Treatment for Metastatic Breast Cancer. *J Clin Oncol* *26*, 5544–5552.
- Di Mitri, D., Toso, A., Chen, J.J., Sarti, M., Pinton, S., Jost, T.R., D’Antuono, R., Montani, E., Garcia-Escudero, R., Guccini, I., et al. (2014). Tumour-infiltrating Gr-1+ myeloid cells antagonize senescence in cancer. *Nature* *515*, 134–137.
- Dieci, M.V., Tsvetkova, V., Orvieto, E., Piacentini, F., Ficarra, G., Griguolo, G., Miglietta, F., Giarratano, T., Omarini, C., Bonaguro, S., et al. (2018). Immune characterization of breast cancer metastases: prognostic implications. *Breast Cancer Research* *20*, 62.

- Duman, B.B., Sahin, B., Ergin, M., and Guvenc, B. (2012). Loss of CD20 antigen expression after rituximab therapy of CD20 positive B cell lymphoma (diffuse large B cell extranodal marginal zone lymphoma combination): a case report and review of the literature. *Med. Oncol.* *29*, 1223–1226.
- Ebinger, S., Özdemir, E.Z., Ziegenhain, C., Tiedt, S., Castro Alves, C., Grunert, M., Dworzak, M., Lutz, C., Turati, V.A., Enver, T., et al. (2016). Characterization of Rare, Dormant, and Therapy-Resistant Cells in Acute Lymphoblastic Leukemia. *Cancer Cell* *30*, 849–862.
- Elbauomy Elsheikh, S., Green, A.R., Lambros, M.B.K., Turner, N.C., Grainge, M.J., Powe, D., Ellis, I.O., and Reis-Filho, J.S. (2007). FGFR1 amplification in breast carcinomas: a chromogenic in situ hybridisation analysis. *Breast Cancer Res.* *9*, R23.
- Fang, X., Stachowiak, E.K., Dunham-Ems, S.M., Klejbor, I., and Stachowiak, M.K. (2005). Control of CREB-binding protein signaling by nuclear fibroblast growth factor receptor-1: a novel mechanism of gene regulation. *J. Biol. Chem.* *280*, 28451–28462.
- Fernig, D.G., Chen, H.L., Rahmoune, H., Descamps, S., Boilly, B., and Hondermarck, H. (2000). Differential regulation of FGF-1 and -2 mitogenic activity is related to their kinetics of binding to heparan sulfate in MDA-MB-231 human breast cancer cells. *Biochem. Biophys. Res. Commun.* *267*, 770–776.
- Feuerer, M., Rocha, M., Bai, L., Umansky, V., Solomayer, E.F., Bastert, G., Diel, I.J., and Schirmacher, V. (2001). Enrichment of memory T cells and other profound immunological changes in the bone marrow from untreated breast cancer patients. *Int. J. Cancer* *92*, 96–105.
- Fisher, R., Pusztai, L., and Swanton, C. (2013). Cancer heterogeneity: implications for targeted therapeutics. *Br J Cancer* *108*, 479–485.
- Francavilla, C., Cattaneo, P., Berezin, V., Bock, E., Ami, D., de Marco, A., Christofori, G., and Cavallaro, U. (2009). The binding of NCAM to FGFR1 induces a specific cellular response mediated by receptor trafficking. *J Cell Biol* *187*, 1101–1116.
- Gámez-Pozo, A., Pérez Carrión, R.M., Manso, L., Crespo, C., Mendiola, C., López-Vacas, R., Berges-Soria, J., López, I.Á., Margeli, M., Calero, J.L.B., et al. (2014). The Long-HER study: clinical and molecular analysis of patients with HER2+ advanced breast cancer who become long-term survivors with trastuzumab-based therapy. *PLoS ONE* *9*, e109611.
- Garber, K. (2019). Pursuit of tumor-infiltrating lymphocyte immunotherapy speeds up. *Nat Biotechnol* d41587-019-00023–00026.
- Geyer, C.E., Forster, J., Lindquist, D., Chan, S., Romieu, C.G., Pienkowski, T., Jagiello-Gruszfeld, A., Crown, J., Chan, A., Kaufman, B., et al. (2006). Lapatinib plus Capecitabine for HER2-Positive Advanced Breast Cancer. *New England Journal of Medicine* *355*, 2733–2743.

- Goel, S., DeCristo, M.J., Watt, A.C., BrinJones, H., Sceneay, J., Li, B.B., Khan, N., Ubellacker, J.M., Xie, S., Metzger-Filho, O., et al. (2017). CDK4/6 inhibition triggers anti-tumour immunity. *Nature* *548*, 471–475.
- Hanker, A.B., Garrett, J.T., Estrada, M.V., Moore, P.D., Ericsson, P.G., Koch, J.P., Langley, E., Singh, S., Kim, P.S., Frampton, G.M., et al. (2017). HER2-Overexpressing Breast Cancers Amplify FGFR Signaling upon Acquisition of Resistance to Dual Therapeutic Blockade of HER2. *Clin. Cancer Res.* *23*, 4323–4334.
- Hardy-Werbin, M., Quiroga, V., Cirauqui, B., Romeo, M., Felip, E., Teruel, I., Garcia, J.J., Erasun, C., España, S., Cucurull, M., et al. (2019). Real-world data on T-DM1 efficacy – results of a single-center retrospective study of HER2-positive breast cancer patients. *Sci Rep* *9*, 1–7.
- Hazan, R.B., Phillips, G.R., Qiao, R.F., Norton, L., and Aaronson, S.A. (2000). Exogenous Expression of N-Cadherin in Breast Cancer Cells Induces Cell Migration, Invasion, and Metastasis. *The Journal of Cell Biology* *148*, 779–790.
- Heerboth, S., Housman, G., Leary, M., Longacre, M., Byler, S., Lapinska, K., Willbanks, A., and Sarkar, S. (2015). EMT and tumor metastasis. *Clinical and Translational Medicine* *4*, 6.
- Helsten, T.L., Elkin, S.K., Carter, J., and Kurzrock, R. (2014). The FGFR landscape in cancer: An analysis of 4,869 cases. *J. Clin. Oncol.* *32*:5s.
- Hirsh, V. (2015). Next-Generation Covalent Irreversible Kinase Inhibitors in NSCLC: Focus on Afatinib. *BioDrugs* *29*, 167–183.
- Hojo, S., Koizumi, K., Tsuneyama, K., Arita, Y., Cui, Z., Shinohara, K., Minami, T., Hashimoto, I., Nakayama, T., Sakurai, H., et al. (2007). High-Level Expression of Chemokine CXCL16 by Tumor Cells Correlates with a Good Prognosis and Increased Tumor-Infiltrating Lymphocytes in Colorectal Cancer. *Cancer Research* *67*, 4725–4731.
- Holleczek, B., Stegmaier, C., Radosa, J.C., Solomayer, E.-F., and Brenner, H. (2019). Risk of loco-regional recurrence and distant metastases of patients with invasive breast cancer up to ten years after diagnosis – results from a registry-based study from Germany. *BMC Cancer* *19*, 520.
- Holmström, T.H., Moilanen, A.-M., Ikonen, T., Björkman, M.L., Linnanen, T., Wohlfahrt, G., Karlsson, S., Oksala, R., Korjamo, T., Samajdar, S., et al. (2018). ODM-203 a selective inhibitor of FGFR and VEGFR, shows strong anti-tumor activity, and induces anti-tumor immunity. *Mol. Cancer Ther.*
- Hu, Z., Fan, C., Oh, D.S., Marron, J., He, X., Qaqish, B.F., Livasy, C., Carey, L.A., Reynolds, E., Dressler, L., et al. (2006). The molecular portraits of breast tumors are conserved across microarray platforms. *BMC Genomics* *7*, 96.
- Jin, L., Han, B., Siegel, E., Cui, Y., Giuliano, A., and Cui, X. (2018). Breast cancer lung metastasis: Molecular biology and therapeutic implications. *Cancer Biology & Therapy* *19*, 858–868.

- Johnson, E., Seachrist, D.D., DeLeon-Rodriguez, C.M., Lozada, K.L., Miedler, J., Abdul-Karim, F.W., and Keri, R.A. (2010). HER2/ErbB2-induced Breast Cancer Cell Migration and Invasion Require p120 Catenin Activation of Rac1 and Cdc42. *J Biol Chem* 285, 29491–29501.
- Junttila, T.T., Li, G., Parsons, K., Phillips, G.L., and Sliwkowski, M.X. (2011a). Trastuzumab-DM1 (T-DM1) retains all the mechanisms of action of trastuzumab and efficiently inhibits growth of lapatinib insensitive breast cancer. *Breast Cancer Res. Treat.* 128, 347–356.
- Junttila, T.T., Li, G., Parsons, K., Phillips, G.L., and Sliwkowski, M.X. (2011b). Trastuzumab-DM1 (T-DM1) retains all the mechanisms of action of trastuzumab and efficiently inhibits growth of lapatinib insensitive breast cancer. *Breast Cancer Research and Treatment* 128, 347–356.
- Kalluri, R., and Weinberg, R.A. (2009). The basics of epithelial-mesenchymal transition. *J. Clin. Invest.* 119, 1420–1428.
- Kanai, M., Tashiro, E., Maruki, H., Minato, Y., and Imoto, M. (2009). Transcriptional regulation of human fibroblast growth factor receptor 1 by E2F-1. *Gene* 438, 49–56.
- Kee, J.-Y., Ito, A., Hojo, S., Hashimoto, I., Igarashi, Y., Tsuneyama, K., Tsukada, K., Irimura, T., Shibahara, N., Takasaki, I., et al. (2014). CXCL16 suppresses liver metastasis of colorectal cancer by promoting TNF- $\alpha$ -induced apoptosis by tumor-associated macrophages. *BMC Cancer* 14, 949.
- Keren, L., Bosse, M., Marquez, D., Angoshtari, R., Jain, S., Varma, S., Yang, S.-R., Kurian, A., Valen, D.V., West, R., et al. (2018). A Structured Tumor-Immune Microenvironment in Triple Negative Breast Cancer Revealed by Multiplexed Ion Beam Imaging. *Cell* 174, 1373-1387.e19.
- Kümler, I., Tuxen, M.K., and Nielsen, D.L. (2014). A systematic review of dual targeting in HER2-positive breast cancer. *Cancer Treatment Reviews* 40, 259–270.
- Lee, W., and Naora, H. (2019). Neutrophils fertilize the pre-metastatic niche. *Aging (Albany NY)* 11, 6624–6625.
- Lee, Y.-W., Stachowiak, E.K., Birkaya, B., Terranova, C., Capacchietti, M., Claus, P., Aletta, J.M., and Stachowiak, M.K. (2013). NGF-Induced Cell Differentiation and Gene Activation Is Mediated by Integrative Nuclear FGFR1 Signaling (INFS). *PLOS ONE* 8, e68931.
- Lewis Phillips, G.D., Li, G., Dugger, D.L., Crocker, L.M., Parsons, K.L., Mai, E., Blättler, W.A., Lambert, J.M., Chari, R.V.J., Lutz, R.J., et al. (2008). Targeting HER2-positive breast cancer with trastuzumab-DM1, an antibody-cytotoxic drug conjugate. *Cancer Res.* 68, 9280–9290.
- Li, B., Severson, E., Pignon, J.-C., Zhao, H., Li, T., Novak, J., Jiang, P., Shen, H., Aster, J.C., Rodig, S., et al. (2016). Comprehensive analyses of tumor immunity: implications for cancer immunotherapy. *Genome Biology* 17.

- Lin, Y., Xu, J., and Lan, H. (2019). Tumor-associated macrophages in tumor metastasis: biological roles and clinical therapeutic applications. *Journal of Hematology & Oncology* *12*, 76.
- Liu, Y., and Cao, X. (2016). Characteristics and Significance of the Pre-metastatic Niche. *Cancer Cell* *30*, 668–681.
- Mabe, N.W., Fox, D.B., Lupo, R., Decker, A.E., Phelps, S.N., Thompson, J.W., and Alvarez, J.V. (2018). Epigenetic silencing of tumor suppressor Par-4 promotes chemoresistance in recurrent breast cancer. *J Clin Invest* *128*, 4413–4428.
- Madden, S.F., Clarke, C., Gaule, P., Aherne, S.T., O'Donovan, N., Clynes, M., Crown, J., and Gallagher, W.M. (2013). BreastMark: an integrated approach to mining publicly available transcriptomic datasets relating to breast cancer outcome. *Breast Cancer Res.* *15*, R52.
- Mahnke, Y.D., Schwendemann, J., Beckhove, P., and Schirmmacher, V. (2005). Maintenance of long-term tumour-specific T-cell memory by residual dormant tumour cells. *Immunology* *115*, 325–336.
- Mani, S.A., Guo, W., Liao, M.-J., Eaton, E.N., Ayyanan, A., Zhou, A.Y., Brooks, M., Reinhard, F., Zhang, C.C., Shipitsin, M., et al. (2008). The epithelial-mesenchymal transition generates cells with properties of stem cells. *Cell* *133*, 704–715.
- Mannell, A. (2017). An overview of risk factors for recurrent breast cancer. *S Afr J Surg* *55*, 29–34.
- Mao, P., Cohen, O., Kowalski, K.J., Kusieli, J.G., Buendia-Buendia, J.E., Exman, P., Wander, S.A., Waks, A.G., Chung, J., Miller, V.A., et al. (2019). Acquired FGFR and FGF alterations confer resistance to estrogen receptor (ER) targeted therapy in ER+ metastatic breast cancer. *BioRxiv* 605436.
- Marusyk, A., and Polyak, K. (2010). Tumor heterogeneity: causes and consequences. *Biochimica et Biophysica Acta* *1805*, 105–117.
- Matsumura, S., Wang, B., Kawashima, N., Braunstein, S., Badura, M., Cameron, T.O., Babb, J.S., Schneider, R.J., Formenti, S.C., Dustin, M.L., et al. (2008). Radiation-induced CXCL16 release by breast cancer cells attracts effector T cells. *J Immunol* *181*, 3099–3107.
- McEwen, D.G., and Ornitz, D.M. (1998). Regulation of the fibroblast growth factor receptor 3 promoter and intron I enhancer by Sp1 family transcription factors. *J. Biol. Chem.* *273*, 5349–5357.
- McVeigh, T.P., and Kerin, M.J. (2017). Clinical use of the Oncotype DX genomic test to guide treatment decisions for patients with invasive breast cancer. *Breast Cancer (Dove Med Press)* *9*, 393–400.
- Meacham, C.E., and Morrison, S.J. (2013). Tumour heterogeneity and cancer cell plasticity. *Nature* *501*, 328–337.

- Miller, K.D., Diéras, V., Harbeck, N., Andre, F., Mahtani, R.L., Gianni, L., Albain, K.S., Crivellari, D., Fang, L., Michelson, G., et al. (2014). Phase IIa trial of trastuzumab emtansine with pertuzumab for patients with human epidermal growth factor receptor 2-positive, locally advanced, or metastatic breast cancer. *J. Clin. Oncol.* *32*, 1437–1444.
- Moasser, M.M. (2007). The oncogene HER2: its signaling and transforming functions and its role in human cancer pathogenesis. *Oncogene* *26*, 6469–6487.
- Mohme, M., Riethdorf, S., and Pantel, K. (2017). Circulating and disseminated tumour cells — mechanisms of immune surveillance and escape. *Nat Rev Clin Oncol* *14*, 155–167.
- Montemurro, F., Ellis, P., Anton, A., Wuerstlein, R., Delalogue, S., Bonnetterre, J., Quenel-Tueux, N., Linn, S.C., Irahara, N., Donica, M., et al. (2019). Safety of trastuzumab emtansine (T-DM1) in patients with HER2-positive advanced breast cancer: Primary results from the KAMILLA study cohort 1. *European Journal of Cancer* *109*, 92–102.
- Mori, S., Kodaira, M., Ito, A., Okazaki, M., Kawaguchi, N., Hamada, Y., Takada, Y., and Matsuura, N. (2015). Enhanced Expression of Integrin  $\alpha\beta 3$  Induced by TGF- $\beta$  Is Required for the Enhancing Effect of Fibroblast Growth Factor 1 (FGF1) in TGF- $\beta$ -Induced Epithelial-Mesenchymal Transition (EMT) in Mammary Epithelial Cells. *PLoS ONE* *10*, e0137486.
- Müller, M., Gounari, F., Prifti, S., Hacker, H.J., Schirmacher, V., and Khazaie, K. (1998). EblacZ tumor dormancy in bone marrow and lymph nodes: active control of proliferating tumor cells by CD8+ immune T cells. *Cancer Res.* *58*, 5439–5446.
- Murdoch, C., Muthana, M., Coffelt, S.B., and Lewis, C.E. (2008). The role of myeloid cells in the promotion of tumour angiogenesis. *Nat Rev Cancer* *8*, 618–631.
- Nahta, R. (2012). Molecular Mechanisms of Trastuzumab-Based Treatment in HER2-Overexpressing Breast Cancer. *International Scholarly Research Notices* *2012*, e428062.
- Nair, V.R., and Malladi, S. (2019). Mouse Models to Study Natural Killer Cell-Mediated Immunosurveillance and Metastatic Latency. *Methods Mol. Biol.* *1884*, 141–150.
- Nakaya, Y., and Sheng, G. (2013). EMT in developmental morphogenesis. *Cancer Letters* *341*, 9–15.
- Niikura, N., Liu, J., Hayashi, N., Mittendorf, E.A., Gong, Y., Palla, S.L., Tokuda, Y., Gonzalez-Angulo, A.M., Hortobagyi, G.N., and Ueno, N.T. (2011). Loss of Human Epidermal Growth Factor Receptor 2 (HER2) Expression in Metastatic Sites of HER2-Overexpressing Primary Breast Tumors. *JCO* *JCO.2010.33.8889*.
- Palakurthi, S., Kuraguchi, M., Zacharek, S.J., Zudaire, E., Huang, W., Bonal, D.M., Liu, J., Dhaneshwar, A., DePeaux, K., Gowaski, M.R., et al. (2019). The Combined Effect of FGFR Inhibition and PD-1 Blockade Promotes Tumor-Intrinsic Induction of Antitumor Immunity. *Cancer Immunol Res* *7*, 1457–1471.

- Parker, J.S., Mullins, M., Cheang, M.C.U., Leung, S., Voduc, D., Vickery, T., Davies, S., Fauron, C., He, X., Hu, Z., et al. (2009). Supervised Risk Predictor of Breast Cancer Based on Intrinsic Subtypes. *JCO* 27, 1160–1167.
- Patani, H., Bunney, T.D., Thiyagarajan, N., Norman, R.A., Ogg, D., Breed, J., Ashford, P., Potterton, A., Edwards, M., Williams, S.V., et al. (2016). Landscape of activating cancer mutations in FGFR kinases and their differential responses to inhibitors in clinical use. *Oncotarget* 7, 24252–24268.
- Patel, A., Tiwari, A.K., Chufan, E.E., Sodani, K., Anreddy, N., Singh, S., Ambudkar, S.V., Stephani, R., and Chen, Z.-S. (2013). PD173074, a selective FGFR inhibitor, reverses ABCB1-mediated drug resistance in cancer cells. *Cancer Chemother. Pharmacol.* 72, 189–199.
- Perez, E.A., Romond, E.H., Suman, V.J., Jeong, J.-H., Sledge, G., Geyer, C.E., Martino, S., Rastogi, P., Gralow, J., Swain, S.M., et al. (2014). Trastuzumab Plus Adjuvant Chemotherapy for Human Epidermal Growth Factor Receptor 2-Positive Breast Cancer: Planned Joint Analysis of Overall Survival From NSABP B-31 and NCCTG N9831. *Journal of Clinical Oncology* 32, 3744–3752.
- Perou, C.M., Sørlie, T., Eisen, M.B., van de Rijn, M., Jeffrey, S.S., Rees, C.A., Pollack, J.R., Ross, D.T., Johnsen, H., Akslen, L.A., et al. (2000). Molecular portraits of human breast tumours. *Nature* 406, 747–752.
- Porta, R., Borea, R., Coelho, A., Khan, S., Araújo, A., Reclusa, P., Franchina, T., Steen, N.V.D., Dam, P.V., Ferri, J., et al. (2017). FGFR a promising druggable target in cancer: Molecular biology and new drugs. *Critical Reviews in Oncology / Hematology* 113, 256–267.
- Prior, L., Lim, M., Ward, C., Featherstone, H., Murray, H., D’Arcy, C., Crown, J., and Gullo, G. Metastatic HER2+ Breast Cancer: A Potentially Curable Disease? *Cureus* 9.
- Quesnel, B. (2013). Tumor dormancy: long-term survival in a hostile environment. *Adv. Exp. Med. Biol.* 734, 181–200.
- Rabinovsky, R., Uhr, J.W., Vitetta, E.S., and Yefenof, E. (2007). Cancer dormancy: lessons from a B cell lymphoma and adenocarcinoma of the prostate. *Adv. Cancer Res.* 97, 189–202.
- Rahmoune, H., Chen, H.L., Gallagher, J.T., Rudland, P.S., and Fernig, D.G. (1998). Interaction of heparan sulfate from mammary cells with acidic fibroblast growth factor (FGF) and basic FGF. Regulation of the activity of basic FGF by high and low affinity binding sites in heparan sulfate. *J. Biol. Chem.* 273, 7303–7310.
- Raouf, S., Mulford, I.J., Frisco-Cabanos, H., Nangia, V., Timonina, D., Labrot, E., Hafeez, N., Bilton, S.J., Drier, Y., Ji, F., et al. (2019). Targeting FGFR overcomes EMT-mediated resistance in EGFR mutant non-small cell lung cancer. *Oncogene* 1.
- Research, A.A. for C. (2018). Multiplexed Imaging Characterizes the Tumor–Immune Microenvironment. *Cancer Discov* 8, OF12–OF12.

- Rhim, A.D., Mirek, E.T., Aiello, N.M., Maitra, A., Bailey, J.M., McAllister, F., Reichert, M., Beatty, G.L., Rustgi, A.K., Vonderheide, R.H., et al. (2012). EMT and dissemination precede pancreatic tumor formation. *Cell* *148*, 349–361.
- Röcken, M. (2010). Early tumor dissemination, but late metastasis: insights into tumor dormancy. *J Clin Invest* *120*, 1800–1803.
- Romero, I., Garrido, C., Algarra, I., Collado, A., Garrido, F., and Garcia-Lora, A.M. (2014a). T lymphocytes restrain spontaneous metastases in permanent dormancy. *Cancer Res.* *74*, 1958–1968.
- Romero, I., Garrido, F., and Garcia-Lora, A.M. (2014b). Metastases in Immune-Mediated Dormancy: A New Opportunity for Targeting Cancer. *Cancer Res* *74*, 6750–6757.
- Safarzadeh, E., Orangi, M., Mohammadi, H., Babaie, F., and Baradaran, B. (2018). Myeloid-derived suppressor cells: Important contributors to tumor progression and metastasis. *J Cell Physiol* *233*, 3024–3036.
- Saudemont, A., and Quesnel, B. (2004). In a model of tumor dormancy, long-term persistent leukemic cells have increased B7-H1 and B7.1 expression and resist CTL-mediated lysis. *Blood* *104*, 2124–2133.
- Sharma, S.V., Lee, D.Y., Li, B., Quinlan, M.P., Takahashi, F., Maheswaran, S., McDermott, U., Azizian, N., Zou, L., Fischbach, M.A., et al. (2010). A chromatin-mediated reversible drug-tolerant state in cancer cell subpopulations. *Cell* *141*, 69–80.
- Sharpe, R., Pearson, A., Herrera-Abreu, M.T., Johnson, D., Mackay, A., Welte, J.C., Natrajan, R., Reynolds, A.R., Reis-Filho, J.S., Ashworth, A., et al. (2011). FGFR signaling promotes the growth of triple negative and basal-like breast cancer cell lines both in vitro and in vivo. *Clin Cancer Res* *17*, 5275–5286.
- Shinde, A., Hardy, S.D., Kim, D., Akhand, S.S., Jolly, M.K., Wang, W.-H., Anderson, J.C., Khodadadi, R.B., Brown, W.S., George, J.T., et al. (2019). Spleen tyrosine kinase-mediated autophagy is required for epithelial-mesenchymal plasticity and metastasis in breast cancer. *Cancer Res.*
- Singh, A., and Settleman, J. (2010a). {EMT}, cancer stem cells and drug resistance: an emerging axis of evil in the war on cancer. *Oncogene* *29*, 4741–4751.
- Singh, A., and Settleman, J. (2010b). EMT, cancer stem cells and drug resistance: an emerging axis of evil in the war on cancer. *Oncogene* *29*, 4741–4751.
- Sørlie, T., Perou, C.M., Tibshirani, R., Aas, T., Geisler, S., Johnsen, H., Hastie, T., Eisen, M.B., van de Rijn, M., Jeffrey, S.S., et al. (2001). Gene expression patterns of breast carcinomas distinguish tumor subclasses with clinical implications. *Proc. Natl. Acad. Sci. U.S.A.* *98*, 10869–10874.

- Sotiriou, C., Neo, S.-Y., McShane, L.M., Korn, E.L., Long, P.M., Jazaeri, A., Martiat, P., Fox, S.B., Harris, A.L., and Liu, E.T. (2003). Breast cancer classification and prognosis based on gene expression profiles from a population-based study. *Proc. Natl. Acad. Sci. U.S.A.* *100*, 10393–10398.
- Stachowiak, M.K., and Stachowiak, E.K. (2016). Evidence-Based Theory for Integrated Genome Regulation of Ontogeny—An Unprecedented Role of Nuclear FGFR1 Signaling. *J. Cell. Physiol.* *231*, 1199–1218.
- Swann, J.B., and Smyth, M.J. (2007). Immune surveillance of tumors. *J Clin Invest* *117*, 1137–1146.
- Tan, L., Wang, J., Tanizaki, J., Huang, Z., Aref, A.R., Rusan, M., Zhu, S.-J., Zhang, Y., Ercan, D., Liao, R.G., et al. (2014). Development of covalent inhibitors that can overcome resistance to first-generation FGFR kinase inhibitors. *Proc. Natl. Acad. Sci. U.S.A.* *111*, E4869-4877.
- Tashiro, E., Minato, Y., Maruki, H., Asagiri, M., and Imoto, M. (2003). Regulation of FGF receptor-2 expression by transcription factor E2F-1. *Oncogene* *22*, 5630–5635.
- Trujillo, J.A., Sweis, R.F., Bao, R., and Luke, J.J. (2018). T Cell-Inflamed versus Non-T Cell-Inflamed Tumors: A Conceptual Framework for Cancer Immunotherapy Drug Development and Combination Therapy Selection. *Cancer Immunol Res* *6*, 990–1000.
- Turner, N., Pearson, A., Sharpe, R., Lambros, M., Geyer, F., Lopez-Garcia, M.A., Natrajan, R., Marchio, C., Iorns, E., Mackay, A., et al. (2010). FGFR1 amplification drives endocrine therapy resistance and is a therapeutic target in breast cancer. *Cancer Res.* *70*, 2085–2094.
- Valente, M., Furian, L., and Rigotti, P. (2012). Organ Donors with Small Renal Cancer: Report of 3 Cases. *Transplantation Proceedings* *44*, 1846–1847.
- Wang, H.-F., Wang, S.-S., Huang, M.-C., Liang, X.-H., Tang, Y.-J., and Tang, Y.-L. (2019a). Targeting Immune-Mediated Dormancy: A Promising Treatment of Cancer. *Front Oncol* *9*, 498.
- Wang, M., Zhao, J., Zhang, L., Wei, F., Lian, Y., Wu, Y., Gong, Z., Zhang, S., Zhou, J., Cao, K., et al. (2017). Role of tumor microenvironment in tumorigenesis. *J Cancer* *8*, 761–773.
- Wang, Y., Ding, Y., Guo, N., and Wang, S. (2019b). MDSCs: Key Criminals of Tumor Pre-metastatic Niche Formation. *Front. Immunol.* *10*.
- Warzecha, C.C., Jiang, P., Amirikian, K., Dittmar, K.A., Lu, H., Shen, S., Guo, W., Xing, Y., and Carstens, R.P. (2010). An ESRP-regulated splicing programme is abrogated during the epithelial-mesenchymal transition. *EMBO J.* *29*, 3286–3300.

- Welslau, M., Diéras, V., Sohn, J.-H., Hurvitz, S.A., Lalla, D., Fang, L., Althaus, B., Guardino, E., and Miles, D. (2014). Patient-reported outcomes from EMILIA, a randomized phase 3 study of trastuzumab emtansine (T-DM1) versus capecitabine and lapatinib in human epidermal growth factor receptor 2–positive locally advanced or metastatic breast cancer. *Cancer* *120*, 642–651.
- Welte, T., Kim, I.S., Tian, L., Gao, X., Wang, H., Li, J., Holdman, X.B., Herschkowitz, J.I., Pond, A., Xie, G., et al. (2016). Oncogenic mTOR signaling recruits myeloid-derived suppressor cells to promote tumor initiation. *Nat Cell Biol* *18*, 632–644.
- Wendt, M.K., and Schiemann, W.P. (2009). Therapeutic targeting of the focal adhesion complex prevents oncogenic TGF-beta signaling and metastasis. *Breast Cancer Res.* *11*, R68.
- Wendt, M.K., Smith, J.A., and Schiemann, W.P. (2010). Transforming growth factor- $\beta$ -induced epithelial-mesenchymal transition facilitates epidermal growth factor-dependent breast cancer progression. *Oncogene* *29*, 6485–6498.
- Wendt, M.K., Taylor, M.A., Schiemann, B.J., and Schiemann, W.P. (2011a). Down-regulation of epithelial cadherin is required to initiate metastatic outgrowth of breast cancer. *Mol. Biol. Cell* *22*, 2423–2435.
- Wendt, M.K., Taylor, M.A., Schiemann, B.J., and Schiemann, W.P. (2011b). Down-regulation of epithelial cadherin is required to initiate metastatic outgrowth of breast cancer. *Mol. Biol. Cell* *22*, 2423–2435.
- Wendt, M.K., Tian, M., and Schiemann, W.P. (2012). Deconstructing the mechanisms and consequences of TGF- $\beta$ -induced EMT during cancer progression. *Cell Tissue Res.* *347*, 85–101.
- Wendt, M.K., Schiemann, B.J., Parvani, J.G., Lee, Y.-H., Kang, Y., and Schiemann, W.P. (2013a). TGF- $\beta$  stimulates Pyk2 expression as part of an epithelial-mesenchymal transition program required for metastatic outgrowth of breast cancer. *Oncogene* *32*, 2005–2015.
- Wendt, M.K., Schiemann, B.J., Parvani, J.G., Lee, Y.-H., Kang, Y., and Schiemann, W.P. (2013b). TGF- $\beta$  stimulates Pyk2 expression as part of an epithelial-mesenchymal transition program required for metastatic outgrowth of breast cancer. *Oncogene* *32*, 2005–2015.
- Wendt, M.K., Taylor, M.A., Schiemann, B.J., Sossey-Alaoui, K., and Schiemann, W.P. (2014a). Fibroblast growth factor receptor splice variants are stable markers of oncogenic transforming growth factor  $\beta$ 1 signaling in metastatic breast cancers. *Breast Cancer Res.* *16*, R24.
- Wendt, M.K., Taylor, M.A., Schiemann, B.J., Sossey-Alaoui, K., and Schiemann, W.P. (2014b). Fibroblast growth factor receptor splice variants are stable markers of oncogenic transforming growth factor  $\beta$ 1 signaling in metastatic breast cancers. *Breast Cancer Research* *16*, R24.

- Williams, E.-J., Williams, G., Howell, F.V., Skaper, S.D., Walsh, F.S., and Doherty, P. (2001). Identification of an N-cadherin Motif That Can Interact with the Fibroblast Growth Factor Receptor and Is Required for Axonal Growth. *J. Biol. Chem.* 276, 43879–43886.
- Wu, X., Peng, M., Huang, B., Zhang, H., Wang, H., Huang, B., Xue, Z., Zhang, L., Da, Y., Yang, D., et al. (2013). Immune microenvironment profiles of tumor immune equilibrium and immune escape states of mouse sarcoma. *Cancer Lett.* 340, 124–133.
- Yates, L.R., and Campbell, P.J. (2012). Evolution of the cancer genome. *Nat Rev Genet* 13, 795–806.
- Yates, L.R., Knappskog, S., Wedge, D., Farmery, J.H.R., Gonzalez, S., Martincorena, I., Alexandrov, L.B., Van Loo, P., Haugland, H.K., Lilleng, P.K., et al. (2017). Genomic Evolution of Breast Cancer Metastasis and Relapse. *Cancer Cell* 32, 169-184.e7.
- Ye, T., Wei, X., Yin, T., Xia, Y., Li, D., Shao, B., Song, X., He, S., Luo, M., Gao, X., et al. (2014a). Inhibition of FGFR signaling by PD173074 improves antitumor immunity and impairs breast cancer metastasis. *Breast Cancer Research and Treatment* 143, 435–446.
- Ye, T., Wei, X., Yin, T., Xia, Y., Li, D., Shao, B., Song, X., He, S., Luo, M., Gao, X., et al. (2014b). Inhibition of FGFR signaling by PD173074 improves antitumor immunity and impairs breast cancer metastasis. *Breast Cancer Res. Treat.* 143, 435–446.
- Yu, P., Wilhelm, K., Dubrac, A., Tung, J.K., Alves, T.C., Fang, J.S., Xie, Y., Zhu, J., Chen, Z., De Smet, F., et al. (2017). FGF-dependent metabolic control of vascular development. *Nature* 545, 224–228.
- Zhu, L., Narloch, J.L., Onkar, S., Joy, M., Luedke, C., Hall, A., Kim, R., Pogue-Geile, K., Sammons, S., Nayyar, N., et al. (2019a). Metastatic breast cancers have reduced immune cell recruitment but harbor increased macrophages relative to their matched primary tumors. *BioRxiv* 525071.
- Zhu, L., Narloch, J.L., Onkar, S., Joy, M., Broadwater, G., Luedke, C., Hall, A., Kim, R., Pogue-Geile, K., Sammons, S., et al. (2019b). Metastatic breast cancers have reduced immune cell recruitment but harbor increased macrophages relative to their matched primary tumors. *Journal for ImmunoTherapy of Cancer* 7, 265.
- Zuo, S., Zhu, Z., Liu, Y., Li, H., Song, S., and Yin, S. (2019). CXCL16 Induces the Progression of Pulmonary Fibrosis through Promoting the Phosphorylation of STAT3. *Canadian Respiratory Journal* 2019, 1–8.
- (2013). Trastuzumab Emtansine for HER2-Positive Advanced Breast Cancer. *New England Journal of Medicine* 368, 2442–2442.
- Fibroblast Growth Factor Receptor 3 Interacts with and Activates TGF $\beta$ -Activated Kinase 1 Tyrosine Phosphorylation and NF $\kappa$ B Signaling in Multiple Myeloma and Bladder Cancer.

Following figures were created with BioRender.com: 1.1,1.2,1.3,1.4,5.1,5.2,5.3,and5.4

## APPENDIX A. FGF2/CAR T CELLS

### Background

The adaptive immune system consists of specialized B and T lymphocytes, which provide highly specific immunity against foreign pathogens (Alberts, 2008). They can recognize self vs. non-self-antigens, which leads to the generation of the tailored immune response to inhibit pathogens and pathogen-infected cells (Alberts, 2008). Besides, they create immunological memories via memory B cells and memory T cells so that robust response can be generated in future encounters with the same antigen (Kurtz, 2004). These ‘immunological memories’ are the basis of antibody-mediated therapies like vaccination and more recently developed immune cell-based therapeutics like chimeric antigen receptor expressing T cells (CAR-T cells).

CAR-T cells are genetically modified T cells that are reengineered to target an antigen of interest in tumor cells (Srivastava and Riddell, 2015). Antigen recognition by CAR-T cells is mediated via an extracellular domain, which is either a single-chain antibody or a ligand for a receptor antigen. This extracellular receptor domain is tethered to intracellular signaling domains. Recognition of a tumor-specific antigen leads to the activation of CAR-T cells and a robust subsequent T cell-mediated immune response. CAR-T cell therapies have recently gained enormous research interest as a way to target tumor-associated antigens (Brower, 2015). For example, CD19/CAR-T, where patient-derived primary T cells are engineered to express receptors for CD19, a B-cell specific antigen, have shown tremendous success in clinical trials against chemoresistant B-cell lymphomas (Kochenderfer and Rosenberg, 2013; Kochenderfer et al., 2012). This success with B-cell malignancies inspired researchers to develop CAR-T therapies to treat solid tumors. Initial successes have already been reported in various cancers (Louis et al., 2011; Robbins et al., 2011). Here our goal is to establish a novel CAR-T cell to treat BC metastasis.

In the previous chapters of this dissertation work, we have established FGFR as an emerging target to target to inhibit breast cancer recurrence and metastasis. Here in this chapter, we attempted to develop a cellular CAR T cell therapy to target FGFR1 in metastatic settings (Figure 1).



## Results

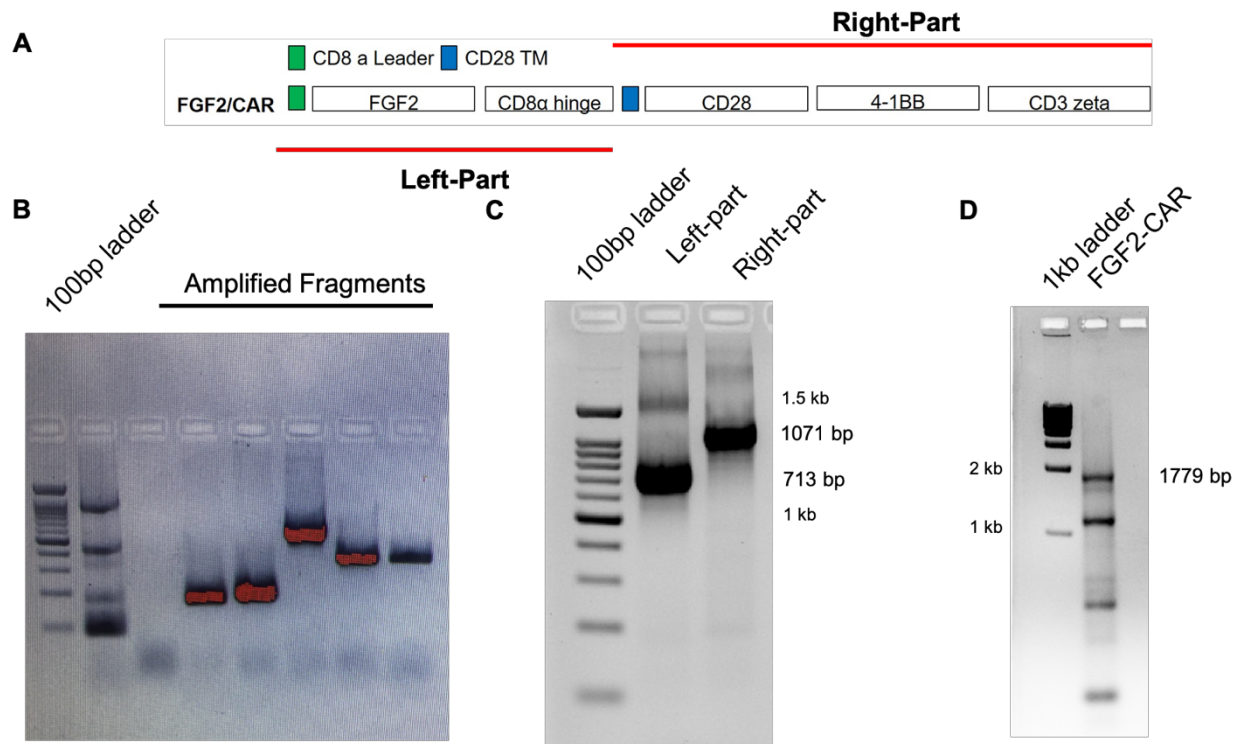


Figure A.2. Construction of FGF2/CAR. A. Schematics of FGF2/CAR design. Left-part fragments contains CD8a leader sequence, FGF2 ligand domain, and CD8a hinge region. Right part contains CD28TM and other intracellular domains such as CD28, 4-1BB, and CD3 zeta domain B. PCR amplifications of different domains of the CAR construct. C. Constructions of the left and the right parts of the CAR were done via overlapping extension PCR(OEPCR) and agarose gel electrophoresis confirmation via band size. D. Full-length FGF2/CAR was also constructed via using both left and right parts, and the correct fragments were identified via agarose gel electrophoresis.

## Discussion

Here we presented a work in progress towards the goal of developing a ligand-based FGFR1 targeting therapy. We have designed and engineered third-generation CARs that target the specific splice variant of FGFR1 that is relevant to breast cancer metastasis. In the future, we need to perform the following experiments to validate this novel therapy:

- i) We will transduce of isolated mouse primary T cells with the FGF2/CARs and verify the expression of FGF2/CAR on the T cell's surface.
- ii) We will use FGFR1 amplified BC cell lines *in vitro* to measure FGF2 mediated T-cell activation and cell death by ELISA and flow cytometry assays.
- iii) We also plan to expand our tests in *in situ* EMT-driven metastatic BC mouse models where we will test the FGF2 mediated inhibition of metastasis *in vivo*.

Successful completion of the current proposal will be a step forward towards developing durable cancer therapeutics against metastatic BC. Finally, we foresee that our proposed FGF2/CAR-T cell therapy has great potential to be translated from pre-clinical mouse models into clinical trials with metastatic BC patients.

## References

- Alberts, B. (2008). The Adaptive Immune System. *The Cell* 1539–1601.
- Brower, V. (2015). The CAR T-Cell Race. *The Scientist* 1–7.
- Kochenderfer, J.N., and Rosenberg, S.A. (2013). Treating B-cell cancer with T cells expressing anti-CD19 chimeric antigen receptors. *Nature Publishing Group* 10, 267–276.
- Kochenderfer, J.N., Dudley, M.E., Feldman, S.A., Wilson, W.H., Spaner, D.E., Maric, I., Stetler-Stevenson, M., Phan, G.Q., Hughes, M.S., Sherry, R.M., et al. (2012). B-cell depletion and remissions of malignancy along with cytokine-associated toxicity in a clinical trial of anti-CD19 chimeric-antigen-receptor-transduced T cells. *Blood* 119, 2709–2720.
- Kurtz, J. (2004). Memory in the innate and adaptive immune systems. *Microbes and Infection* 6, 1410–1417.
- Louis, C.U., Savoldo, B., Dotti, G., Pule, M., Yvon, E., Myers, G.D., Rossig, C., Russell, H. V., Diouf, O., Liu, E., et al. (2011). Antitumor activity and long-term fate of chimeric antigen receptor-positive T cells in patients with neuroblastoma. *Blood* 118, 6050–6056.
- Robbins, P.F., Morgan, R.A., Feldman, S.A., Yang, J.C., Sherry, R.M., Dudley, M.E., Wunderlich, J.R., Nahvi, A. V., Helman, L.J., Mackall, C.L., et al. (2011). Tumor regression in patients with metastatic synovial cell sarcoma and melanoma using genetically engineered lymphocytes reactive with NY-ESO-1. *Journal of Clinical Oncology* 29, 917–924.
- Srivastava, S., and Riddell, S.R. (2015). Engineering CAR-T cells: Design concepts. *Trends in Immunology* 36, 494–502.